8-1999

Depositional and Diagenetic Relationships of the Honaker-Nolichucky Formational Boundary (Middle Cambrian, Conasauga Group), Southern Appalachians

Gary Alan Ottinger
University of Tennessee - Knoxville

To the Graduate Council:

I am submitting herewith a thesis written by Gary Alan Ottinger entitled "Depositional and Diagenetic Relationships of the Honaker-Nolichucky Formational Boundary (Middle Cambrian, Conasauga Group), Southern Appalachians." I have examined the final electronic copy of this thesis for form and content and recommend that it be accepted in partial fulfillment of the requirements for the degree of Master of Science, with a major in Geology.

Kenneth R. Walker, Major Professor

We have read this thesis and recommend its acceptance:

Steve Driese, Claudia Mora

Accepted for the Council:
Carolyn R. Hodges

Vice Provost and Dean of the Graduate School

(Original signatures are on file with official student records.)

To the Graduate Council:

I am submitting herewith a thesis written by Gary Alan Ottinger entitled "Depositional and Diagenetic Relationships of the Honaker-Nolichucky Formational Boundary (Middle Cambrian, Conasauga Group), Southern Appalachians." I have examined the final copy of this thesis for form and content and recommend that it be accepted in partial fulfillment of the requirements for the degree of Master of Science, with a major in Geology.

Kenneth R. Walker, Major Professor

We have read this thesis and
recommend its acceptance:

Accepted for the Council:

Associate Vice Chancellor
and Dean of the Graduate School

DEPOSITIONAL AND DIAGENETIC RELATIONSHIPS OF THE HONAKER-NOLICHUCKY FORMATIONAL BOUNDARY (MIDDLE CAMBRIAN, CONASAUGA GROUP), SOUTHERN APPALACHIANS

A Thesis

Presented for the

Master of Science

Degree

The University of Tennessee, Knoxville

Gary Alan Ottinger

August 1999

DEDICATION

This thesis is dedicated to my mother,

Mary Lou Ottinger,

who constantly supported endeavors I wanted to undertake, who always encouraged me to do my best, and whose infinite love molded me into the person I am today.

ACKNOWLEDGMENTS

I can honestly say that reaching a milestone of this magnitude would not have been possible, had it not been for the help, guidance, and support of many people along the way. Foremost, I want to thank Dr. Kenneth R. Walker, Carden Professor of Geology and Associate Vice Chancellor of Research for the University of Tennessee, who served as my advisor during my graduate career. His personable, friendly disposition and vast knowledge of carbonate sedimentary geology sparked my interest in carbonates as an undergraduate, and made the grueling task of completing this thesis less difficult. He, along with other faculty at the University of Tennessee, were a major reason for my return to graduate school at the University of Tennessee.

My research committee members, Dr. Steve Driese and Dr. Claudia Mora, are also acknowledged for their assistance with "quick questions" from time to time. Their input and critical reviews have made this thesis a much better manuscript. Specifically, I am grateful to Dr. Driese for assisting me with cathodoluminescence microscopy and teaching me field methods; I thank Dr. Mora for her time and patience in the stable isotope laboratory. Working with these professors, both in and out of the classroom, has been a rewarding experience for me. They are not only great geoscientists, but they are also great people. I also want to express my appreciation to the Discretionary Funds Committee and the Mobil Carbonate Fund for their monetary support.

Past "bankers" of the Carbonate Research Group, Dr. Bosiljka Glumac and Dr. Stan Dunagan, are recognized for their knowledge of carbonate geology, especially of

eastern Tennessee, and their friendship. In a way, I think of these two individuals as additional members of my research committee.

I also appreciate Amelia Robinson, Dee Dee Haun, Elizabeth Humbert, Peter Nester, Janna Peevler, Dave King, Heather Gastineau, and Dana Miller for making me realize that college can be some of the best times of one's life. My friendship with them has made graduate school fun(?) in many ways. Extra kudos go out to Amelia Robinson for believing in me and fixing computer glitches when I felt like throwing the PC out the window! Amy, you are a very special person with an abundance of talent. I don't think that I could ever convey how thankful I am for all the things you have done for me.

Last, but certainly not least, I want to thank my family (especially my mother) for their love, support, and guidance these past 27 years. I learned from them very early that an education is important and that "homework comes before play". Although I did not always implement the latter(!), I feel these notions, as well as others, helped to focus me in the right direction.

Most of all, I want to thank the Lord for blessing me in so many ways and guiding me through another chapter of my life.

ABSTRACT

The upper Honaker and lower Nolichucky Formations (Middle Cambrian, Conasauga Group) in northeastern Tennessee comprise part of a thick pericratonic Cambro-Ordovician passive margin sequence along the eastern edge of North America. Throughout the Cambrian, the interplay of autocyclic controls, including sediment supply, tectonism and accompanying subsidence, and eustasy, resulted in various sedimentary architectures, including the Conasauga platform and intrashelf basin adjacent to the craton. To date, the Middle Cambrian westerly carbonate sections adjacent to and within the intrashelf basin (near Knoxville) have been studied in considerable detail. Particularly, these studies have proposed a third-order sequence boundary near Knoxville as well as a Middle Cambrian Conasauga platform development model . Yet, the thick time-equivalent dolostones further on-platform (near Johnson City) and their relationship to overlying units, as well as the deposits further west, have only been examined in the broadest sense. These relationships are the focus for this study.

Field and stratigraphic relationships and petrographic observations reveal four depositional packages that comprise the upper Honaker and lower Nolichucky Formations, in ascending order: 1) peritidal; 2) ooid shoal; 3) transitional; and 4) basinal shale. The first three packages make up the upper Honaker and the fourth package comprises the lower Nolichucky Formation. The progression of these packages represents the same deepening trend that initiates a new phase of genetically-

related rock units further to the west during the Middle Cambrian (Srinivasan, 1993; Rankey, 1993). The change from peritidal facies to ooid shoal facies is the first indication of the drowning event, and this allows the third-order sequence boundary to be extended and placed between these shallow water facies. Hence, the extension of the sequence boundary further to the east expands the Middle Cambrian Conasauga platform development model.

The upper Honaker depositional setting consisted of subtidal thrombolite and intertidal shoal facies that created a semi-closed lagoon with hypersaline conditions further on-platform. In addition, rare evaporite molds and the abundance of penecontemporaneous dolomite imply a semi-arid climate. As the deepening event ensued and, consequently, shifted the carbonate environments towards the east, restricted areas of the platform became open to fresh seawater. Salinity levels decreased to a range more suitable for invertebrate organisms as a result of mixing during the latter part of the Middle Cambrian, as suggested by the transitional depositional package. The craton-derived basinal shale package of the lower Nolichucky Formation in more easterly areas (Johnson City, Tennessee) suggests the intrashelf basin filled, and allowed mature passive margin sedimentation to begin in the Late Cambrian (Maynardville Formation). Furthermore, the Maryville-Nolichucky (sequence boundary) contact in the west is slightly older than the upper Honaker-Nolichucky formational contact of this study, based on platform architecture ($<1^{\circ}$ slope) and direction of flooding, even though the carbonate units are stratigraphically equivalent to one another.

Marine, meteoric, and/or burial diagenetic calcite and dolomite phases are present in varying amounts within the upper Honaker and lower Nolichucky. Plane light microscopy, cathodoluminescence, and stable isotope compositions constrained the timing and origin of these diagenetic components. Both early and late phases of dolomite are present in this study. Evidence for early dolomite is based on its relationship to early marine components such as evaporites and fenestrae. Later replacive and authigenic dolomite phases are inferred from cross-cutting relationships and stable isotope compositions. These phases are a result of elevated temperatures and burial diagenesis associated with the Taconic Orogeny during the Middle Paleozoic that reset the $\delta^{18}O$ isotopic signal in these rocks (average -9 ‰ PDB). Meteoric calcite (average $\delta^{13}C$ is -8 ‰ PDB) likely precipitated late in tectonic-induced fractures related to uplift during the Late Paleozoic, based on cross-cutting relationships. Furthermore, estimated fluid compositions for the calcite ($\delta^{18}O$ of -7 ‰ SMOW) seem to also support a late meteoric source.

This study shows that the integration of various geologic disciplines (e.g., stratigraphic relationships, petrography, and stable isotopes) is necessary in order to gain a better understanding of depositional and diagenetic relationships, as well as to constrain the timing and origin of diagenetic phases. In addition, and most importantly, this research reveals that third-order sequence boundaries are not always represented as pronounced changes in lithology (e.g., carbonate-shale). As such, sequence stratigraphy proponents may need to reconsider their longstanding concepts, particularly those related to flooding events in mixed carbonate-clastic systems.

TABLE OF CONTENTS

LIST OF TABLES

Table **Page**

LIST OF FIGURES

Figure **Page**

CHAPTER 1

INTRODUCTION

The Conasauga Group in eastern Tennessee (Figure 1.1) is a sedimentary package consisting of six alternating carbonate and shale formations that was deposited during Middle and Late Cambrian time. It comprises part of a thick pericratonic Cambro-Ordovician passive margin sequence along the eastern edge of the North American continent (Srinivasan, 1993). The passive margin setting for these strata formed as a result of extensional breakup of Rodinia during the Late Proterozoic. Various sedimentary architectures (ramps, platforms, and basins) were created through the interplay of autocyclic controls, including sediment supply, tectonism and accompanying subsidence, and eustasy, which occurred throughout the Cambrian (Rankey, 1993). According to Rodgers (1953), three distinct phases of sedimentation occurred during the Middle and Late Cambrian: (1) a phase dominated by carbonate lithologies to the east and southeast, (2) a western and northwestern phase dominated by shale, and (3) a central phase comprised of interbedded carbonate and shale units. This research is focused near the boundary between the eastern and central phases of Rogers (1953) (Figure 1.2).

Outcrop belts of the Conasauga Group in eastern Tennessee occur in a northeasterly trend and are exposed in a series of southeasterly dipping thrust sheets in the Valley and Ridge physiographic province. They are underlain by shaly, silty, and sandy siliciclastic deposits (Early Cambrian Rome Formation) which serve as the

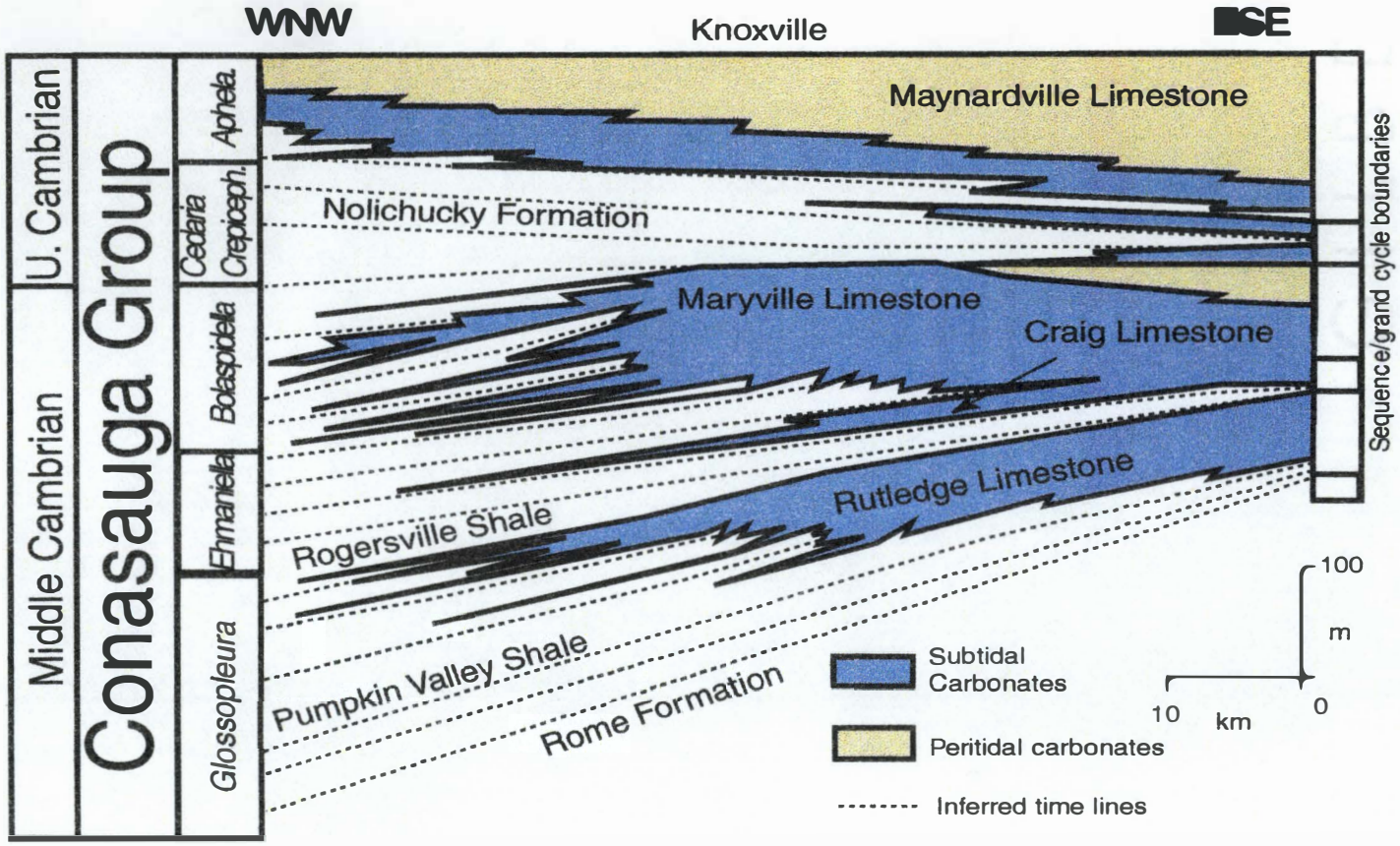

Figure 1.1 - The Conasauga Group in eastern Tennessee showing stratigraphic relationships of the six major units (Pumpkin Valley Shale, Rutledge Limestone, Rogersville Shale, Maryville Limestone, Nolichucky Formation, Maynardville Limestone) (after Walker et al., 1990). Carbonate lithologies are shaded and siliciclastics are not. Modified from Srinivasan and Walker, 1993.

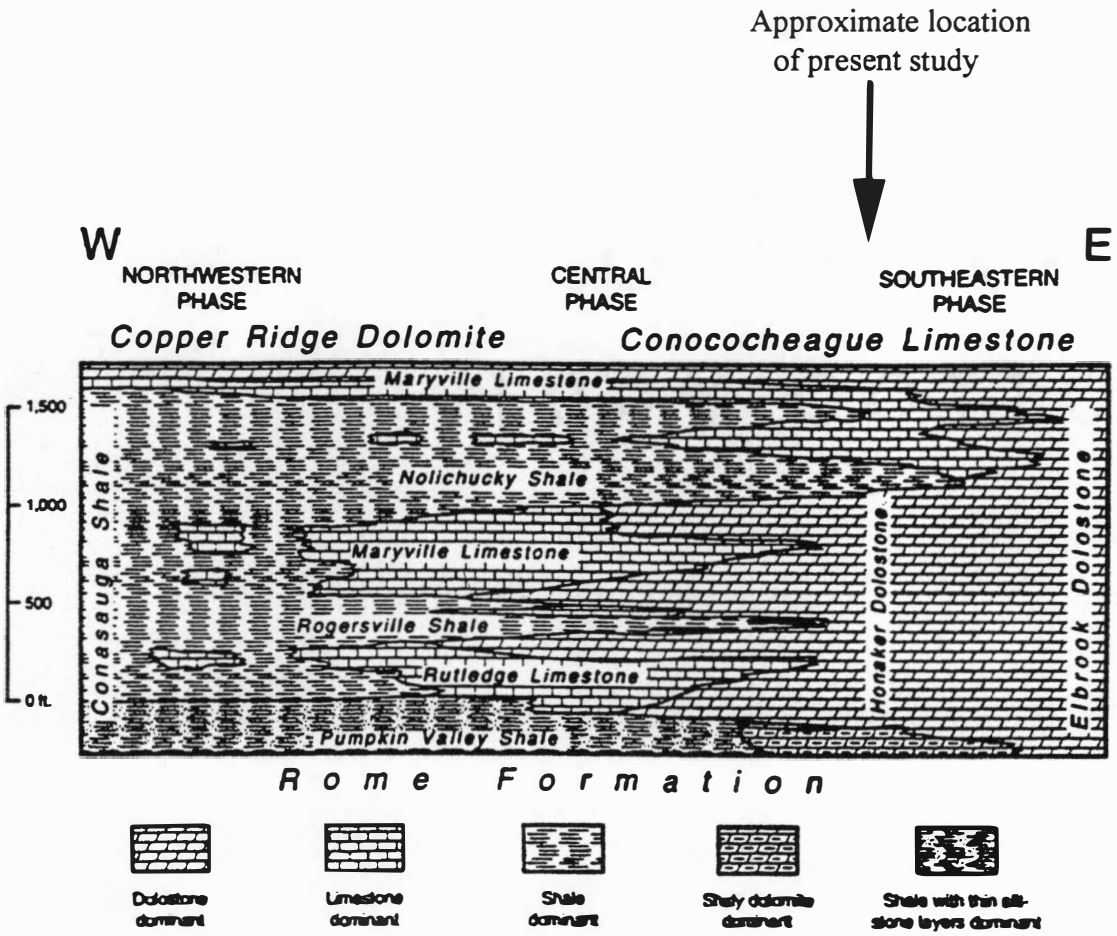

Figure 1.2 - Generalized facies relationships of the Conasauga Group in eastern Tennessee and southwestern Virginia showing the major sedimentation phases of Rodgers (1953). Large arrow shows the approximate location for this study. Modified from Rodgers (1953).

decollement surface for most of the thrust sheets. The Conasauga Group is overlain conformably by the Upper Cambrian Knox Group which is dominated by carbonate lithologies. The Conasauga Group in eastern Tennessee varies in thickness from 350 m to 700 m with carbonate units thickening to the east (Srinivasan, 1993). One of the thick, easterly carbonate units (Honaker Dolomite) and its apparently conformable relationship with the overlying Nolichucky Formation are the foci for this study.

The thickness of the Honaker Dolomite in the study area varies as a result of structural deformation. From field data it is estimated that only the upper 100 m to 200 m of the Formation crops out in eastern Tennessee (Byerly, 1966). According to Milici (1973), the thickness of the Nolichucky Formation ranges from 140 m to 180 m. Exposures of both units are limited due to weathering and structural complications. Yet, in eastern Tennessee, the upper Honaker Dolomite and lower Nolichucky Formation are exposed in a few localities between the Pulaski-Stanton and Holston Mountain thrust sheets in steeply dipping, northeasterly trending outcrop belts (Figure 1.3a). The southernmost upper Honaker exposure for this study is near Greeneville, Tennessee along the Nolichucky River at Greeneville Dam. The other outcrop localities are near Johnson City, Tennessee. One is situated adjacent to I-81 just southwest of the I-181 and I-81 interchange. The other exposure for this study is further to the northeast at the Blountville exit off I-81. Although this study is focused solely on the Tennessee area, Honaker rocks do extend into southwestern Virginia. This thesis contributes to previous Conasauga Group research projects in eastern

Figure 1.3 - **A)** Simplified location map showing the occurrences of the Conasauga Group (shaded) in northeastern Tennessee, along with major thrust faults and outcrops for this study. **B)** Sketch showing the Middle Cambrian palinspastically restored paleogeographic setting and likely extent of the Conasauga platform, as well as its location relative to the craton. Shaded rectangle represents the study area. Modified from Hasson and Haase (1988), Srinivasan and Walker (1993), and Rankey (1993).

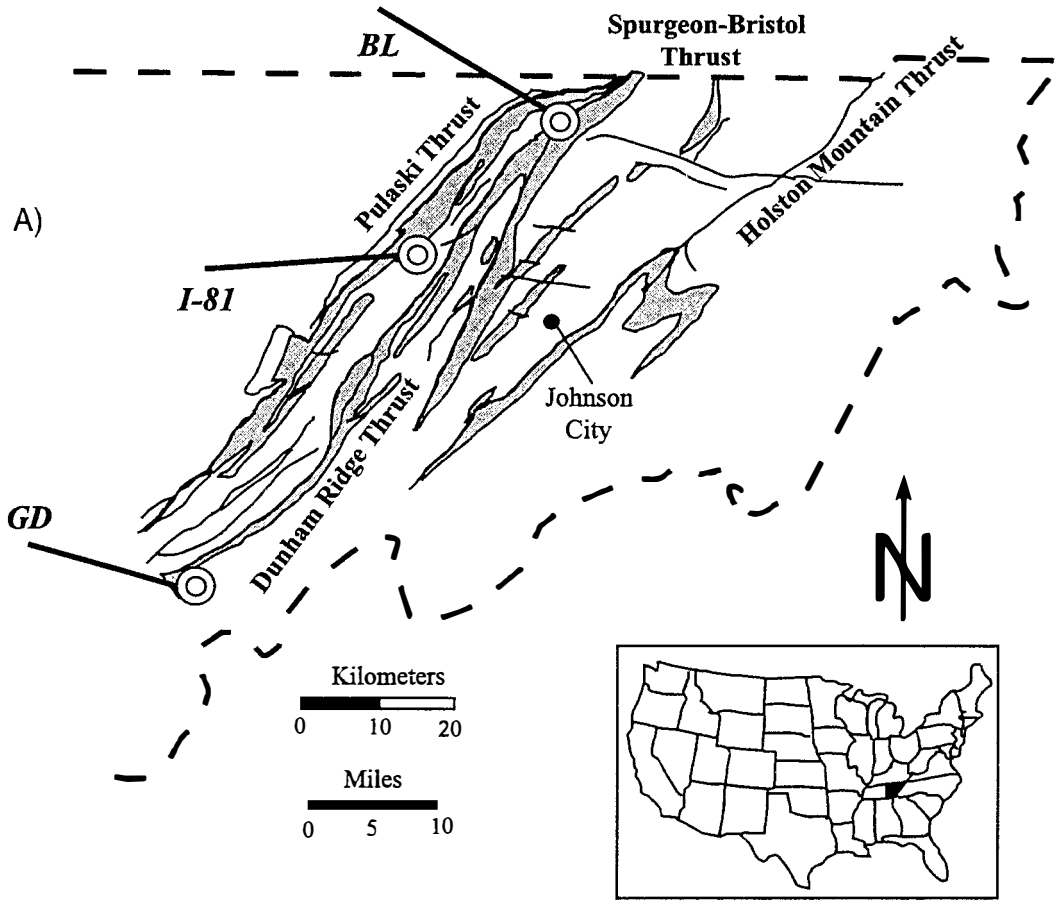
A)
BL
Spurgeon-Bristol Thrust
Pulaski Thrust
Holston Mountain Thrust
I-81
Johnson City
GD
Dunham Ridge Thrust
N
Kilometers
0 10 20
Miles
0 5 10

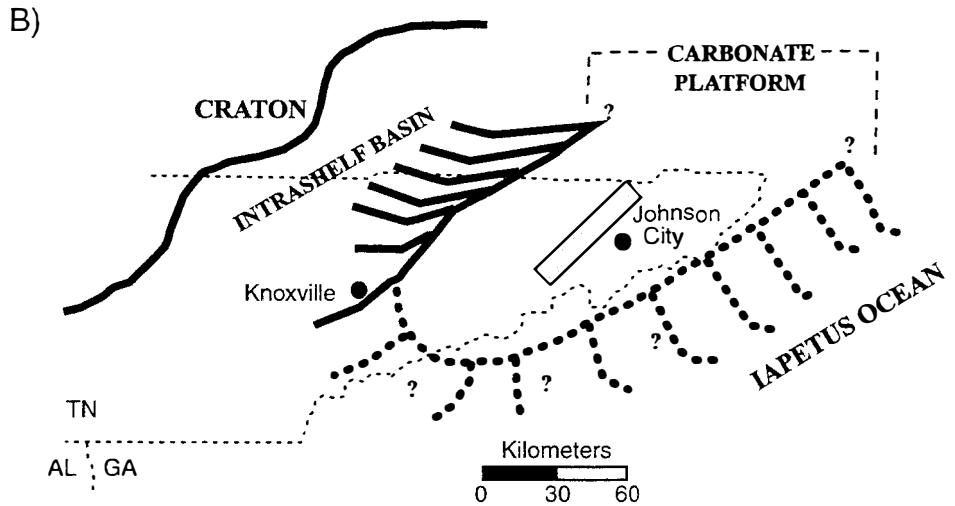
B)
CRATON
CARBONATE PLATFORM
INTRASHELF BASIN
Johnson City
Knoxville
IAPETUS OCEAN
TN
AL
GA
Kilometers
0 30 60

Tennessee carried out by the Carbonate Research Group at the University of Tennessee.

Previous Research

Like many other lithologic units in this region, the Honaker Dolomite and Nolichucky Formation were first described by Safford (1856, 1869), who named these units the Knox Shale. Later investigations into the Conasauga Group helped to resolve distinctions within the Knox Shale. Early biostratigraphic studies in the Conasauga Group focused on faunal diversities within various formations. Butts (1940) concentrated on Rutledge, Rogersville, and Maryville units in Virginia whereas Woodward (1949) dealt with Rutledge, Rogersville, and Nolichucky strata in Tennessee. More recent studies by Derby (1965) and Rasetti (1965) improved the biostratigraphic temporal resolution of the Honaker-Maryville and Nolichucky contact. The broad lithostratigraphic and structural aspects of the Honaker have been described by various researchers in eastern Tennessee: Rodgers (1953), King and Ferguson (1960), Pugh (1966), Little (1969), Wilson (1979), Erwin (1981), and Hasson and Haase (1988). Lithofacies and platform relationships between the uppermost Honaker and overlying Nolichucky Formation were described by Markello and Read (1981,1982) in southwestern Virginia. Diagenesis for the coeval Honaker and Maryville formations in Tennessee and Virginia was addressed by Cook (1983).

The most recent, and extensive, research on the Conasauga Group was carried out by the Carbonate Research Group at the University of Tennessee. Simmons (1984)

and Kozar (1986) studied depositional environments and stratigraphy of the Middle Cambrian Maryville Limestone at two locations in eastern Tennessee. Weber (1988) documented numerous lithofacies and addressed depositional settings as well as the degree of cyclicity within the Nolichucky Formation. Foreman (1991) studied the depositional components of the Nolichucky Formation as well as the post-depositional alteration of these rocks using geochemical techniques. Srinivasan (1993) and Rankey (1993) addressed sequence stratigraphic relationships, diagenesis, and depositional history for the Maryville Limestone. More importantly, they documented a third order sequence boundary for the Middle Cambrian in eastern Tennessee. Stefaniak (1996) examined the Rutledge Limestone documenting its stratigraphy and depositional history. Glumac (1997) concentrated on the youngest carbonate unit within the Conasauga Group (the Maynardville Limestone) assessing the change from immature passive margin sedimentation to a mature passive margin setting based on the termination of Grand Cycles. Because of their studies, a great deal more has been learned about the stratigraphy and diagenesis of the carbonate units within the Conasauga, especially near Knoxville, Tennessee (Maryville Limestone); thus a reexamination of the stratigraphy and diagenesis of the coeval carbonates in the Honaker/Nolichucky interval near Johnson City, Tennessee seems appropriate. The most important aspect of the reexamination is to define the Maryville-Nolichucky sequence boundary in a different geographic setting and hopefully expand the Middle Cambrian Conasauga model further on-platform.

Although the Conasauga carbonates have been studied rather extensively, a concise, universally accepted model for controls governing deposition and stacking patterns has not been achieved, especially for the Maryville (contrast Kozar et al., 1990 with Koerschner and Read, 1990). Milankovitch-driven eustatic fluctuations, tectonism, autocyclic processes, and a combination thereof have been proposed by many researchers in recent years. Rankey (1993) addressed this issue and put forth a plausible hypothesis for the Middle Cambrian Conasauga depositional controls. He suggested that the controls on sedimentation patterns during Maryville deposition were numerous and temporally and spatially variable. Sediment loading, tectonism associated with regional extension, thermal subsidence, irregular eustatic sea level fluctuations, and autogenic processes all exerted an influence on stacking patterns. The absolute input of each of these factors is probably unresolvable from the stratigraphic record.

Purpose/Significance

This research marks the first in-depth study of the upper Honaker Dolomite and lower Nolichucky Formation by a UTK worker in recent years. It will help determine whether the depositional processes and mechanisms which occurred in westerly carbonates near Knoxville, Tennessee (Maryville Limestone - Conasauga Group) are also evidenced further on-platform in coeval deposits near Johnson City, Tennessee (Upper Honaker Dolomite - Conasauga Group). More importantly, it will explore a

platform-interior region for the major sequence boundary recently documented further off-platform by Srinivasan (1993) and Rankey (1993). The results generated from this study will reveal that the conspicuous carbonate-shale sequence boundary discovered previously near the platform margin in the Maryville Limestone is represented by a subtle, gradational change in carbonate lithofacies further to the east/northeast. In addition, this study will relate how depositional setting and style(s) of diagenesis are linked, as well as show the importance of using various methodologies such as field and stratigraphic relationships, petrographic observations, cathodoluminescence, and stable isotopes in depositional and diagenetic studies. The information generated from this study will not only provide more insight into the upper Honaker Dolomite and lower Nolichucky Formation, it will also convey a better understanding of the regional Conasauga platform development during the Middle Cambrian.

CHAPTER 2

STRATIGRAPHY AND DEPOSITIONAL SETTINGS

Introduction

This chapter focuses on stratigraphic and paleoenvironmental interpretations of the upper Honaker - lower Nolichucky interval in northeastern Tennessee near Johnson City, Tennessee. There are three main objectives for this chapter: first, to describe the major lithofacies of the two formations; second, to characterize the depositional settings; and third, to relate the results to the Middle Cambrian Conasauga depositional model for eastern Tennessee and define the sequence boundary evidenced in coeval deposits in a different region (Rankey, 1993; Srinivasan, 1993).

The Middle Cambrian Conasauga depositional model for eastern Tennessee results from a synthesis of various integrated studies. Most of these Conasauga studies focused in east Tennessee near Knoxville. The distal (and coeval) Honaker sediments located further to the northeast near Johnson City, Tennessee have only been studied in a broad sense. The last known in-depth studies of these rocks were by Erwin (1981) and Cook (1983). The Nolichucky Formation has recently been examined by various workers (Markello and Read, 1982; Weber, 1988; Foreman, 1991). The present work provides even more information concerning Middle Cambrian depositional controls and environments as well as sequence stratigraphic relationships.

Stratigraphy and Stratigraphic Relationships

Three well-exposed outcrops of the upper Honaker and lower Nolichucky Formations were measured and sampled for this study (Figure 2.1). Appendix A contains detailed stratigraphic columns coupled with field and petrographic descriptions. The stratigraphic sections are between the Pulaski and Spurgeon-Bristol thrust faults in northeastern Tennessee (Figure 1.3a) along a roughly northeast transect within steep southeasterly dipping beds. The Greeneville Dam outcrop (GD) and Blountville outcrop (BL) were compared and correlated to the intermediate I-81 section, which was recently investigated in considerable detail (Ottinger et al., 1997).

Collectively, all three sections represent shallow water peritidal carbonate deposition (upper Honaker) followed by a relative rise in sea level which, ultimately, inundated and terminated carbonate production and deposited prograding siliciclastics on top of the carbonate platform (lower Nolichucky). This progression is evidenced by cyclic peritidal facies (subtidal, intertidal, and supratidal) overlain by dark-colored shaly facies. The upper Honaker is characterized by mudstones, algal boundstones, and packstones with varying amounts of peloids, intraclasts, ooids, and skeletal allochems typical of modern carbonate environments like the Trucial Coast of the Arabian Gulf. The lower portions of the upper Honaker contain classic examples of tidal flat sedimentary features: desiccation structures, evaporite vugs, fenestrae, detrital quartz, algal and mechanically-generated laminae as well as burrows (Hardie, 1977; Flugel, 1982). The middle portions of the upper Honaker contain active and marginal shoal deposits, whereas the uppermost portions contain rare echinoderm, trilobite, and

Figure 2.1 - Stratigraphic columns of the upper Honaker and lower Nolichucky Formations. See text for description of major lithofacies. Lithologic key: Sh, shale; M/W, mudstone/wackestone; P, packstone; G, grainstone; B, boundstone; Dashed horizontal line near the top of the sections is the Honaker/Nolichucky contact. Faint, stippled lines near the top of the sections correspond to tie-lines based on facies variations. Key to distance between outcrops: present day/reconstructed distance.

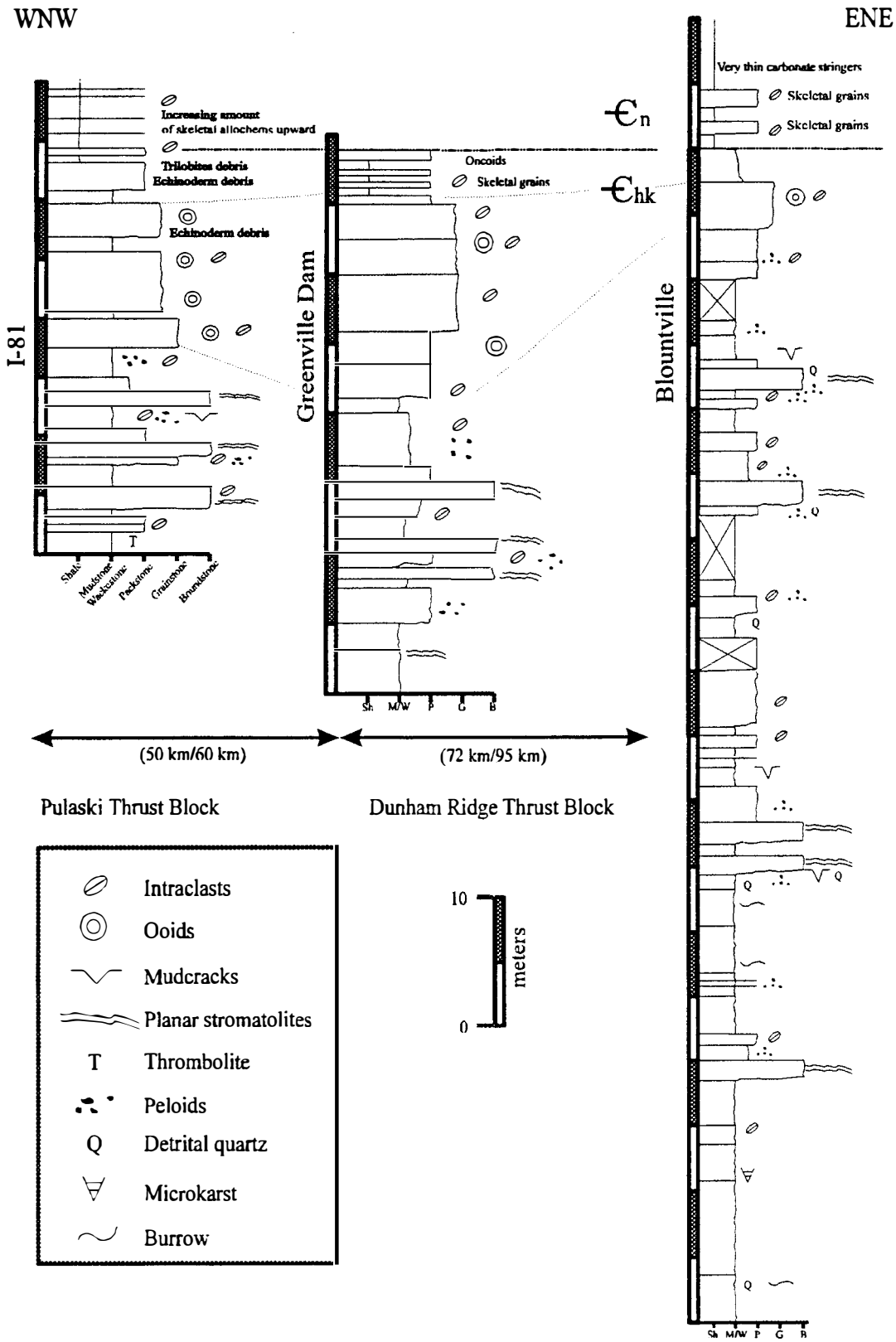
WNW
ENE
Increasing amount of skeletal allochems upward
Trilobites debris
Echinoderm debris
Echinoderm debris
Oncoids
Skeletal grains
Very thin carbonate stringers
Skeletal grains
Skeletal grains
ϵ_n
ϵ_{hk}
I-81
Greenville Dam
Blountville
T
Q
Shale
Mudstone/ Wackestone
Packstone
Grainstone
Boundstone
Sh
M/W
P
G
B
(50 km/60 km)
(72 km/95 km)
Pulaski Thrust Block
Dunham Ridge Thrust Block
Intraclasts
Ooids
Mudcracks
Planar stromatolites
T Thrombolite
Peloids
Q Detrital quartz
Microkarst
Burrow
10
0
meters

brachiopod detritus. The lower Nolichucky Formation is characterized by interbedded paper-laminated shales and carbonate stringers composed of flat-pebble conglomerates interpreted as storm deposits (Sepkoski, 1982; Weber, 1988). Because these exposures are regionally correlative and represent different locations on the vast Conasauga platform, a closer inspection of each outcrop conveys more detailed information about depositional settings/controls during the Middle Cambrian.

For example, the I-81 section (in the Pulaski thrust sheet) and the GD section (in the Dunham Ridge thrust sheet) are quite similar with the exception of shoal facies and transitional facies (carbonate-shale interbeds) near the Honaker-Nolichucky formational boundary. The shoal deposits are not as prominent at the GD section as they are at the I-81 stop. Both active shoal and drowned shoal deposits occur at the I-81 exposure (Ottinger et al., 1997), yet only shoal margin facies are represented at the GD section. The transitional facies at the GD section also contain thicker carbonate beds interbedded with shale. These subtle differences are important as they show specific paleoenvironmental characteristics, which are necessary in order to develop a more precise depositional interpretation.

The BL section (in the Spurgeon-Bristol thrust sheet) shows significant differences compared to the other two locales. These differences are probably the result of the more on-platform location of this section; BL is located one thrust belt further eastward than the GD section and two thrust belts relative to the I-81 section. BL is characterized by having more microbial laminated beds, more detrital quartz grains, increased number of desiccation episodes, and more evaporitic vugs. The

increased percentage of detrital quartz further on-platform likely suggests wind-driven sediment from the westerly craton (Dalrymple et al., 1985). Supratidal characteristics such as these imply longer periods of exposure on the tidal flat environment (Flugel, 1982; Hardie, 1977; Tucker and Wright, 1990). In addition, BL lacks significant oolite facies. Those that occur are interpreted as shoal margin deposits rather than scattered ooids brought in from adjacent subenvironments. The BL section also lacks a transitional facies at the Nolichucky contact. Carbonate beds of the upper Honaker give way abruptly to the shaly deposits of the overlying lower Nolichucky. The lack of carbonate-shale interbeds, coupled with the long-exposed supratidal environment and lag time, imply relatively rapid inundation at this location on the Conasauga platform; this is discussed below.

Description of Major Lithofacies

Below are the major lithofacies found within the upper Honaker and lower Nolichucky Formations. As is customary with peritidal systems, other facies combinations do occur, but they are rare.

Subtidal

Ribbon rocks --- Subtidal ribbon rocks (Demicco, 1983; Chow and James, 1992) occur in the upper Honaker near the base of the BL exposure. Lenticular beds of limestone comprised of darker mudstone layers and lighter peloid-rich layers characterize this lithofacies (Figure 2.2b). These deposits grade upward into mudstones and microbial laminates of the peritidal facies. Glumac (1997) observed

Figure 2.2 - Subtidal lithofacies of the upper Honaker and lower Nolichucky Formation in northeastern Tennessee. [Abbreviation/decimal] correspond to sample locality and cumulative thickness. See Chapter 1 or Appendix A for more information concerning the measured sections. All photomicrographs are plane-polarized images. **A**. Dolomitized ooid (o) intraclast (i) packstone representing drowned shoal depositional conditions [I-81/26.2]. **B**. Ribbon rocks consisting of alternating light and dark-colored bands of peloid and carbonate mud-rich layers, respectively [BL/1.0]. **C**. "Clotted" texture of algal-rich thrombolite (t) facies [I-81/H1-0.72]. **D**. Mechanically-induced laminations within a dolomitized mudstone ("couplets"). Note cross-laminations [BL/30]. **E**. Echinoderm fragments (e) and intraclasts (i) of mud-rich packstone lithologies [BL/94.4] near the Honaker-Nolichucky contact. **F.** Honaker-Nolichucky contact at the Blountville section. Note change in bedding thickness at the contact. Jacob's staff (1m) for scale.

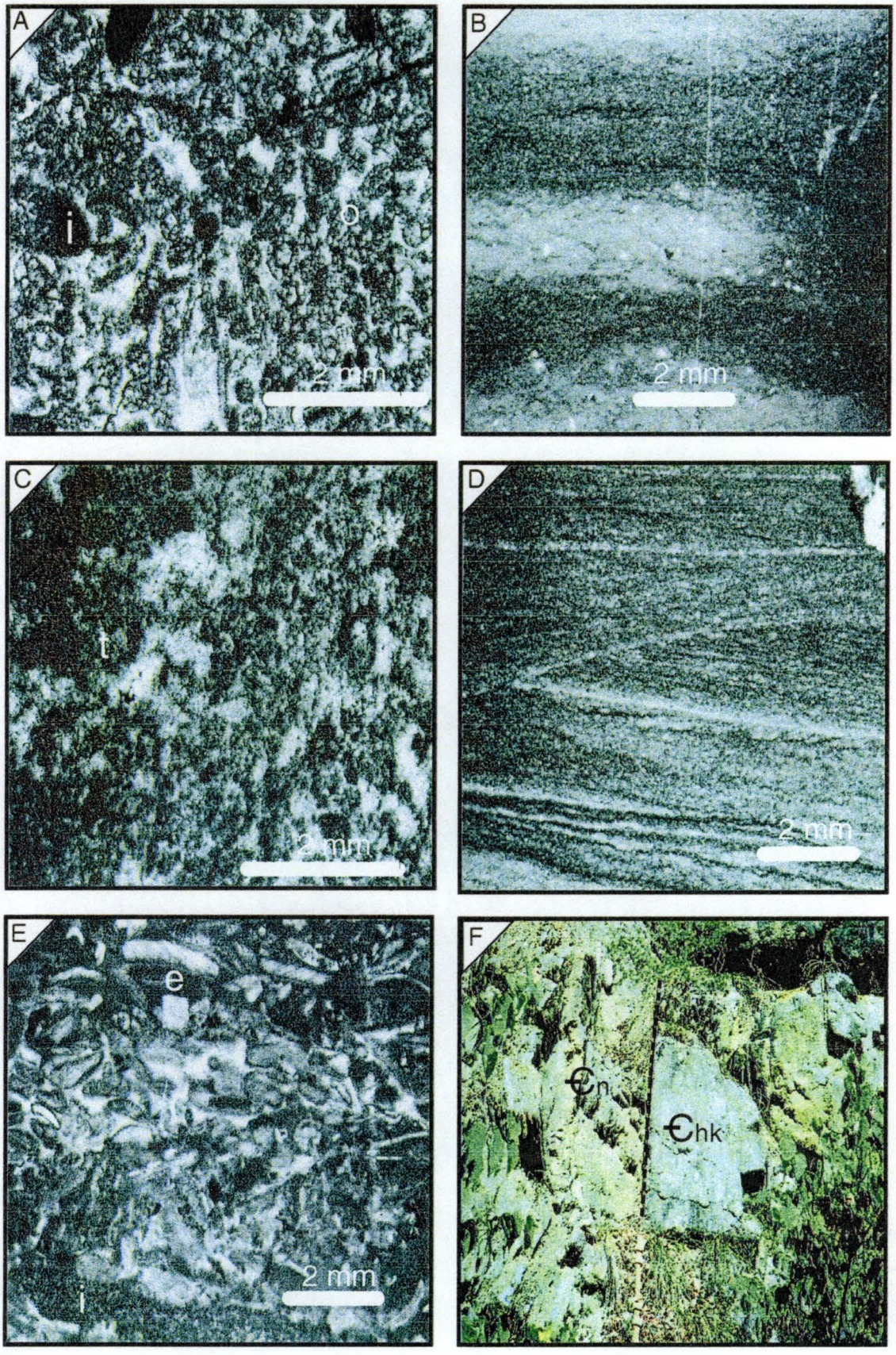
A
i
b
2 mm
B
2 mm
C
t
2 mm
D
2 mm
E
e
2 mm
i
F
ε_n
ε_{hk}

similar ribbon rocks in lower portions of the Upper Cambrian Maynardville Limestone and they are characteristic of the Middle Cambrian Rutledge Limestone (Stefaniak, 1996) as well. The layering of mudstone and peloids indicates a relatively calm water setting with episodic storm events. The subtidal ribbon rocks within the Honaker are unique in that they have not been dolomitized like the other lithofacies. This can be explained by the distal location of this depositional environment from the syndepositional dolomite forming areas (e.g., tidal flats); diagenesis will be discussed in the next chapter.

Ooid intraclast packstone --- This lithofacies occurs at the I-81 and GD sections above the peritidal package in the upper Honaker. Intraclasts within these deposits range from mud chips to algal-derived to multigenerational. They vary in size from < 1millimeter up to a few centimeters. Intraclast textural features, such as changes in dolomite crystal size and crystal color, imply early (marine) alteration based on their relationship to later diagenetic fabrics. Ooids, which are less than 1 millimeter in diameter, have been micritized as well as dolomitized (Figure 2.2a). The degree of alteration of both types of allochem varies considerably depending on host lithology, environments of formation, and diagenetic fluids. The mixture of these allochems suggests shoal margin deposition in slightly deeper water where water turbulence was low to moderate. The dolomitized intraclasts were derived from tidal flat portions of the platform. This is supported by reddish, rounded clasts in some samples.

Mudstone --- Dolomitized mudstones are prominent in all three stratigraphic sections. Samples commonly contain rare peloids and intraclasts, which generally

occur in zones rather than dispersed throughout, typical of low tidal energies and storm-induced activity. Some mudstones may be classified as wackestone lithologies. They sometimes also contain current-generated laminations, or couplets, from sporadic agitation (Figure 2.2d). The peloids that occur likely originated from mud clasts, micritized grains, or algae (Tucker and Wright, 1990). Derivation from fecal matter (Tucker and Wright, 1990) is discredited due to the interpreted stressful conditions for eukaryotic life forms in tidal flat settings such as the upper Honaker (see below). Most dolomitized mudstones have fenestral porosity occluded with dolomite.

Thrombolite --- Non-laminated and highly porous (dolomitized) *Renalcis* bioherms are found at the I-81 section (Figure 2.2c). The lack of thrombolites at the other two locations can be explained by the limited areal extent of such facies. These samples likely represent shallow subtidal patch reefs, which inhibited water circulation and establishment of higher energy conditions further on-platform.

Skeletal intraclast wackestone/packstone --- Grains such as fragments of echinoderms, trilobites, and brachiopods, in addition to intraclasts, make up this lithofacies. Samples are composed of iron-rich calcite and dolomite. Skeletal intraclast wackestone/packstone are typically found in lower parts of the Nolichucky Formation (Figure 2.2e). Fossil assemblages with the aforementioned signify non-fluctuating salinity and water temperatures (Boggs, 1987; Flugel, 1982; Gall, 1983).

Shale --- Calcareous silty shale is represented at all three stratigraphic sections. Intervals of this lithology are interbedded with intraclast packstone beds and flat pebble conglomerate stringers at the I-81 and GD sections. This lithofacies is associated with

the "transitional" package of Ottinger et al. (1997). These siliciclastic deposits are very thinly laminated and dark green to brown in color. The first prominent shale bed near the top of each stratigraphic section marks the Nolichucky contact (Figure 2.2f).

Intertidal

Ooid packstone/grainstone --- The presence of these deposits is limited stratigraphically at all three locations (Figure 2.1). Collectively, all three stratigraphic sections contain about 30 meters of this lithofacies, with the Greeneville Dam outcrop comprising approximately one-half (13 meters). The ooids are micritized to varying degrees, with some being indistinguishable from highly rounded mud intraclasts derived further on-platform (Figure 2.3a,b). They have been dolomitized to the extent that identification of microfabrics is difficult. This lithology represents active shoal deposition followed by drowned shoal subtidal deposits (re-mobilized ooid intraclast packstone) mentioned above.

Supratidal

Stromatolitic boundstone --- Stromatolites are present at all three sections. This lithofacies can be divided into two subfacies: stratiform stromatolites (or microbial laminates) and laterally linked hemispheroids (LLH) (Figure 2.4b,d, and c, respectively). Both are indicative of decreased wave energy in the peritidal setting (Logan et al., 1964; Aitken, 1967; Chafetz, 1973). They both contain fenestrae, desiccation features (Figure 2.4a), detrital quartz and some evaporitic vugs.

Figure 2.3 - Common intertidal facies within the upper Honaker Dolomite in northeastern Tennessee. All images are captured in plane-polarized light. **A.** Dolomitized ooid grainstone with micritized and compressed ooids (co) along stylolites. 'Box' conveys difficulty in distinguishing rounded mud clasts and micritized ooids [I-81/25.23]. **B.** Dolomitized ooids (do) with selectively micritized ooids (mo) [I-81/23.4]. **C.** Dolomitized intraclast ooid grainstone. Large, convolute-shaped ooid intraclasts (oi) imply relatively minimal transport and early diagenesis [I-81/24.5].

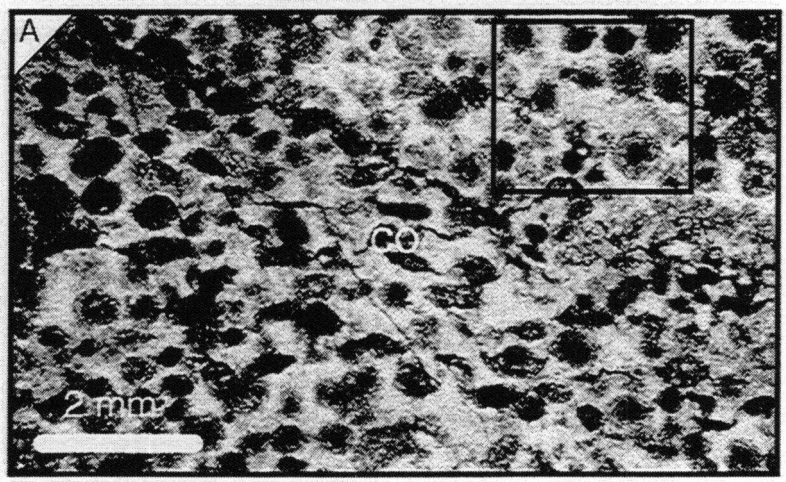
A
2 mm

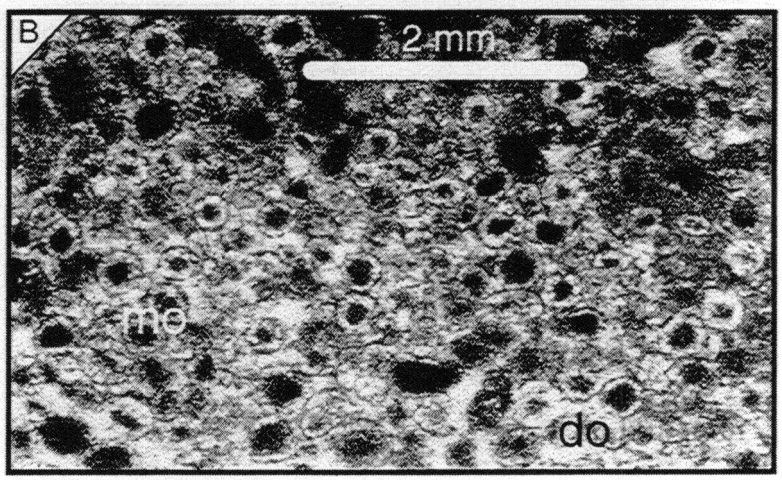
B
2 mm
mo
do

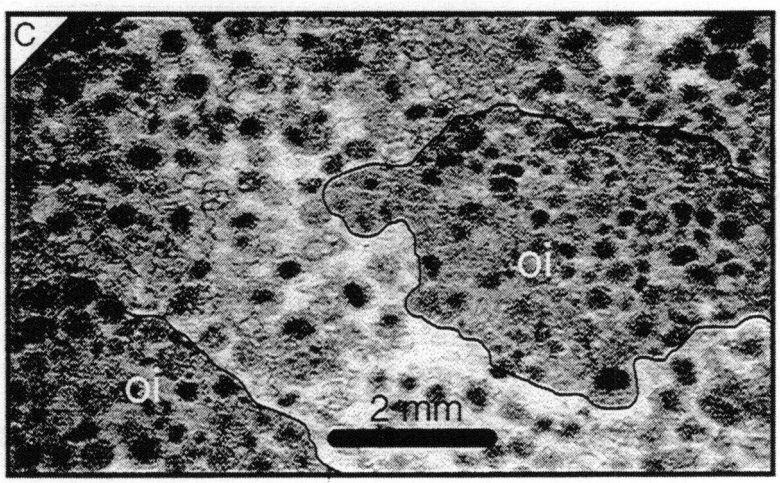
C
oi
oi
2 mm

Figure 2.4 - Supratidal facies of the upper Honaker Dolomite. All photomicrographs are plane-polarized images. **A.** Pervasive desiccation of peritidal rocks [BL/42.9]. **B.** Microbial laminate showing interlaminar fenestrae filled with dolomite [I-81/H7-8.65] and **C.** laterally-linked hemispheroids (LLH) [BL/18.8] of the upper Honaker Dolomite with spalling of laminae from desiccation shown in upper center. Note the change in relief of biogenic layering between B and C. B reflects slightly lower depositional energy conditions compared to C. **D.** Microbial laminated rock showing zones of brecciation (b) on a bedding plane [GD/?]. Also note the "butcher-block" weathering pattern - common for dolostones. 'Sharpie' pen for scale.

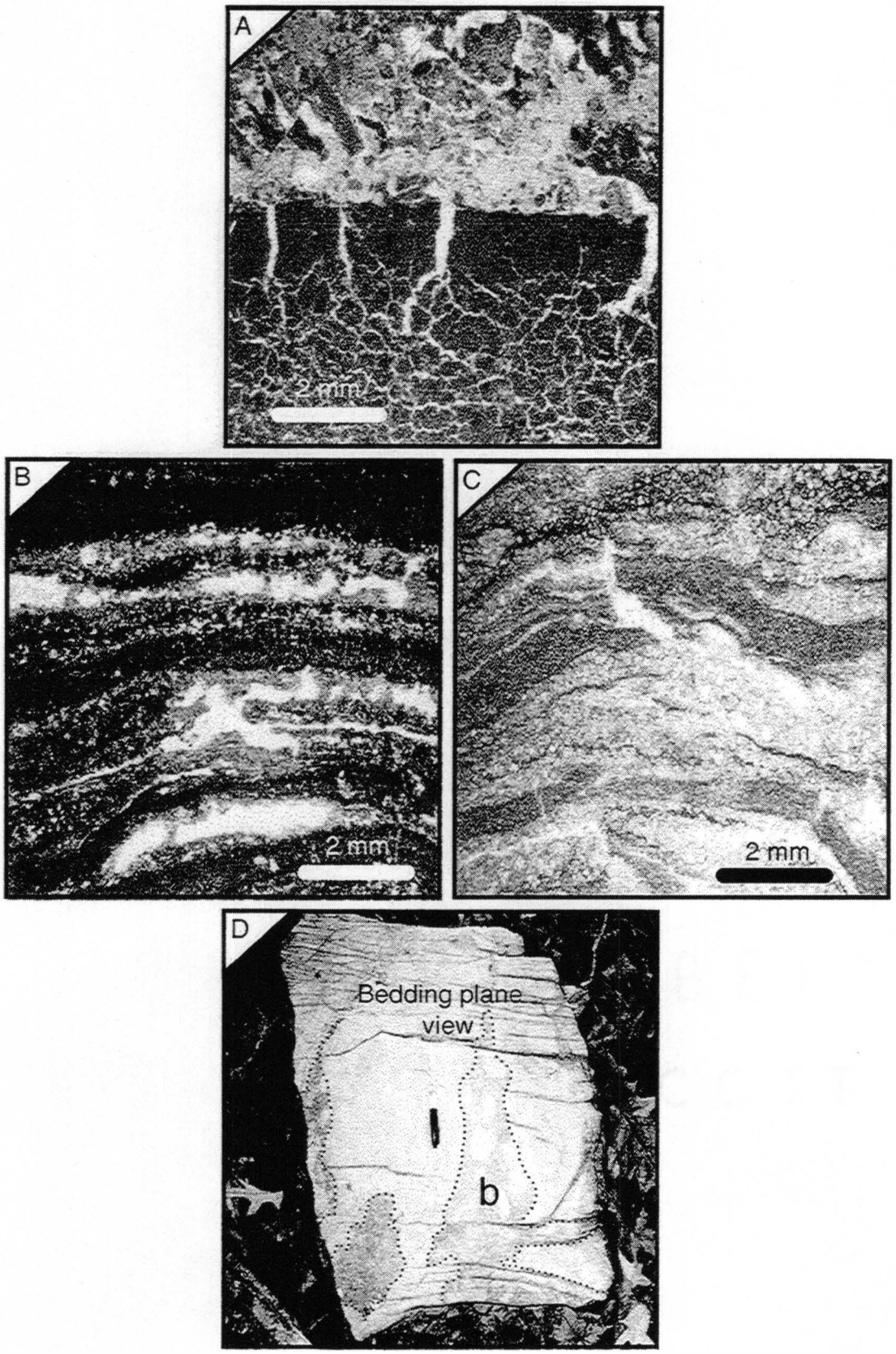
A
2 mm
B
2 mm
C
2 mm
D
Bedding plane
view
b

Synthesis of Major Lithofacies and Depositional Environments

In general, stratigraphic relationships of the upper Honaker-lower Nolichucky lithofacies convey a deepening upwards trend, from peritidal facies grading into mixed carbonate-shale facies. Closer examination reveals four depositional packages: 1) a "peritidal" package, 2) a shoal package, 3) a transitional package that is limited to the Greeneville Dam and I-81 sections, and 4) a basinal shale package. The increase in accommodation space, especially in peritidal settings, typically creates a mosaic of shallow water depositional environments dependent on their location relative to sea level. Thus, the Honaker is interpreted as a peritidal "complex" rather than a single environment. The "complex" nomenclature is justified by the lithologic variability and facies relationships in the sections due to small relative sea level fluctuations or progradation and retrogradation of subenvironments. The upper Honaker peritidal depositional environments shown in Figure 2.5 are similar to other ancient peritidal depositional environments (Glumac, 1997) in many respects (Table 2.1). There are many modern analogs as well such as Andros Island, the Trucial Coast, and the Florida Keys that possess similar peritidal characteristics (Hardie and Shinn, 1986; Tucker and Wright, 1990; many others).

Subtidal *Renalcis* thrombolite bioherms formed patch reefs that inhibited water circulation further on-platform. Intertidal ooid shoals also contributed to this semi-closed setting. The restricted lagoonal environment caused increased salinity levels and low energy conditions further on-platform, as evidenced by no fauna and abundant micrite, respectively. The limited occurrence of evaporite pseudomorphs also suggests

UPPER HONAKER
DEPOSITIONAL ENVIRONMENTS

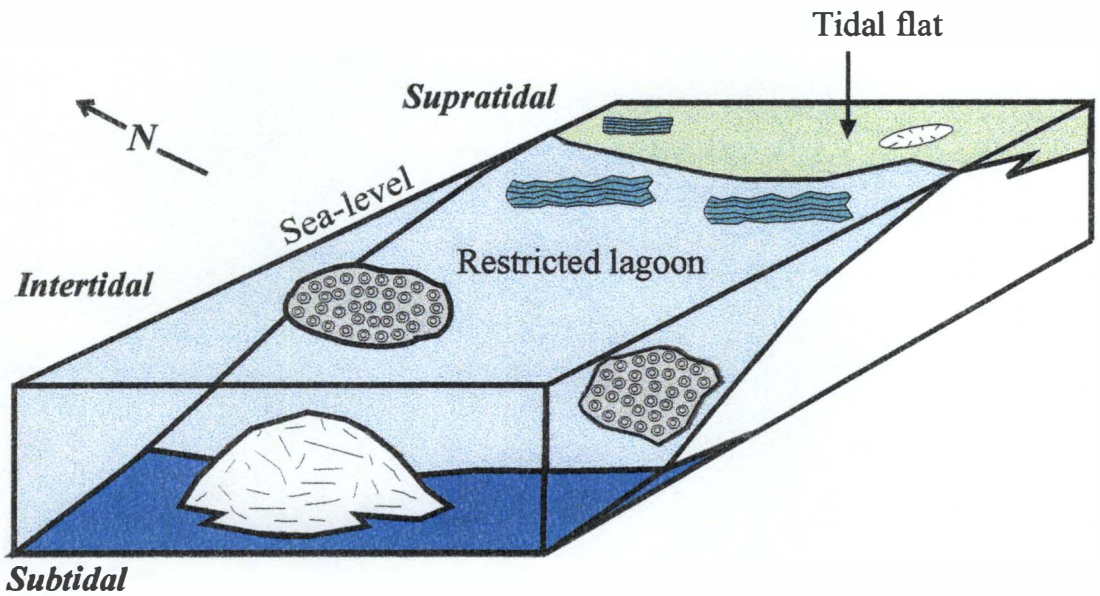

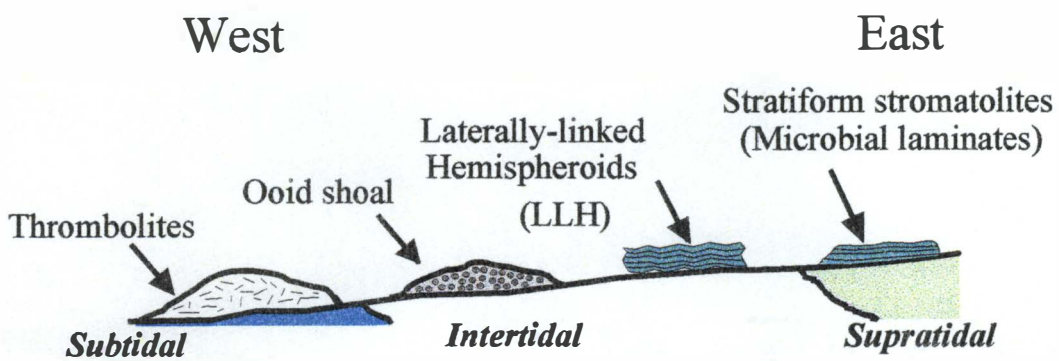

Figure 2.5 - Generalized depositional setting for the upper Honaker Formation in northeastern Tennessee showing relative position of major lithofacies with respect to sea level fluctuations. Note paleo-north arrow. Not to scale.

Table 2.1 - Comparison of ancient peritidal environments during the Middle and Late Cambrian in Tennessee. Although they involve the same geologic Period, the Middle and Late Cambrian in eastern Tennessee represent two different tectono-stratigraphic settings. The Middle Cambrian peritidal facies flank an intrashelf basin to the east, whereas the Late Cambrian peritidal deposits comprise the initial stages of a passive margin setting after the intrashelf basin filled. Late Cambrian information from Glumac (1997).

Honaker Dolomite (Middle Cambrian)	**Maynardville Formation (Late Cambrian)**
1. Stratiform and LLH stromatolites	**1.** Stratiform, LLH, SH, Columnar, and Digitate stromatolites
2. Pervasively dolomitized deposits	**2.** Selectively dolomitized deposits
3. Ribbon rocks & thrombolites (subtidal facies)	**3.** Ribbon rocks & thrombolites (subtidal facies)
4. Semi-arid climate (rare evaporite molds)	**4.** Semi-arid climate (rare evaporite molds)
5. "Couplets" common	**5.** "Couplets" predominant lithofacies
6. Detrital quartz silt and sand	**6.** Detrital quartz sand
7. Sequence boundary (result of deepening)	**7.** Sequence boundary (result of shallowing)

a semi-arid climate (Glumac, 1997). According to modern analogs, salinity levels during the Middle Cambrian may have exceeded 40‰ based on the paucity of skeletal producing organisms and semi-arid climate (Flugel, 1982). Based on the random occurrence of intraclasts and the interpreted paleoclimate, periodic storms were likely present and contributed to Middle Cambrian depositional controls. As the relative rise in sea level occurred, the barrier portions of the peritidal complex were inundated and the once restricted lagoonal setting became open. This inundation lowered salinity levels by mixing fresh seawater with the restricted environment, which then allowed subtidal faunal elements such as echinoderms, trilobites, and brachiopods to thrive. The occurrence of inarticulate brachiopods and echinoderms suggests that salinity and water temperatures decreased to a relatively constant level. Stenohaline, stenothermal organisms yield a great deal of information regarding paleoclimate and depositional setting provided minimal transport has taken place. The skeletal fragments found within this setting are likely the result of migratory, open-water facies backstepping above peritidal facies. The deepening eventually halted carbonate production and craton-derived siliciclastics prograding from the west ultimately buried the carbonate platform.

Another potential mechanism for lowering salinity is freshwater percolation in karst regions. The upper Honaker shows some evidence of dissolution and brecciation, especially in subaerially exposed supratidal portions of the platform (Figure 2.4d). Cement types usually indicate if meteoric processes have acted on exposed carbonate rocks. More often than not, the fluids precipitate clear, meteoric calcite cements in

pore spaces. Cement morphologies are usually meniscus or pendant-shaped in the vadose zone indicating non-saturation (Roberson, 1989). However, overprinting by dolomitization has made these cement morphologies essentially unidentifiable. Although the degree and extent of freshwater percolation is indeterminable, it still must be included as a viable mechanism that lowers salinity in restricted, shallow water environments.

The upper Honaker portion of the platform had a slight inclination (<1°) to flat-topped architecture, based on the work by Srinivasan (1993). The I-81 and Greeneville Dam sections have a transitional package of carbonate-shale interbeds near the top of the sections. The Blountville section lacks these interbeds, and it is the most easterly section for this study (furthest on-platform). The two westerly sections (I-81 and GD) were located on the slightly inclined portion of the platform and the BL section was situated on the flat-topped area. As the relative rise in sea level occurred, the westerly sections were flooded at a relatively slower rate than the easterly section based simply on platform morphology. As sea level reached the exposed, flat-topped easterly section, sea level rapidly extended across the platform. The lag time necessary to initiate carbonate sedimentation, in conjunction with the relatively quick rise in sea level, terminated carbonate production. The exact cause of this sea level rise is still being debated.

A relative rise in sea level was interpreted by Srinivasan (1993) and Rankey (1993) as due to a combination of eustasy, tectonism, and other regional controls. Osleger and Montanez (1996) and others, on the other hand, argue that depositional

controls were influenced solely by eustasy during the Middle Cambrian. Two main lines of evidence suggest that eustasy was less important than local controls in the studied sections: 1) lack of biostratigraphic correlation of this cycle boundary from the Conasauga basin to the Great Basin region where Osleger and Montanez did their work; and 2) lack of correlative cycles across wide areas. Rankey (1993) addressed this issue and showed that Conasauga facies are not extensive, but instead represent a facies "mosaic" that was segmented due to differential sediment loading, tectonism, and other autocyclic processes along the trend of the platform. Moreover, if eustasy was the sole mechanism which governed sea level rise, extensive third order sequence boundaries for this part of the Middle Cambrian should be found around the world. To date, the writer has not discovered any such documented studies. However, a consensus on this issue is not foreseen in the near future.

What is not argued is the existence of a sequence boundary for this part of the Middle Cambrian. Srinivasan (1993) identified a drowning unconformity near Knoxville, Tennessee. The distinct boundary separates subtidal Maryville carbonate deposits from overlying silty clay Nolichucky deposits. Northeast of Knoxville, Rankey (1993) discovered a backstepping platform facies within the Maryville above the sequence boundary, which was also overlain by Nolichucky rocks.

The creation of accommodation space at Srinivasan's subtidal exposure/drowning unconformity, in addition to lag time necessary to initiate carbonate production again, allowed craton-derived siliciclastics to accumulate directly on top of subtidal carbonates. Further on-platform where Maryville subtidal/peritidal facies

dominated and exposure was limited, the increase in accommodation space allowed carbonate sediments to accumulate and retrograde (or backstep) with sea level. This lasted until deepening waters shut down the carbonate factory and allowed the Nolichucky deposits to encroach even further on-platform (Honaker).

Because the upper Honaker is synchronous with the Maryville and because Nolichucky deposits also overly the Honaker, the third-order sequence boundary should be evidenced further on-platform, provided that subaerial exposure has not erased its signature in the rock record.

Figure 2.6 shows the relationship of this study to the regional Middle Cambrian Conasauga depositional model. The peritidal package is equivalent in both Maryville and upper Honaker rocks. The third-order sequence boundary at the base of the Maryville backstepping platform is correlative with the peritidal/shoal package contact in the Honaker. The flooding which established this boundary created accommodation space on top of the upper Honaker peritidal package and allowed seawater to extend further on-platform and shift high energy shoal-type facies on top of peritidal deposits. The prograding siliciclastics (Nolichucky) encroaching from the west eventually filled the intrashelf basin, buried the Maryville and Honaker portions of the Conasauga platform, and established a mature passive margin setting during the earliest Late Cambrian. Thus, the Honaker-Nolichucky formational boundary in the study area is considerably younger than the Maryville-Nolichucky formational/sequence boundary further to the west. Therefore, the main grand cycle boundary (sequence boundary) actually occurs within carbonate beds of the upper Honaker, specifically between

Figure 2.6 - Time-sequential block diagrams showing stratigraphic relationships for the Middle Cambrian in eastern Tennessee. Blocks A and B show coeval Maryville deposition and block C extends further to the east/northeast (Honaker Dolomite). Maryville facies relationships prior to the deepening event are shown in **A**. As a relative rise in sea level occurred, basinal deposits (Nolichucky Formation) onlapped the subtidal and peritidal facies of the Maryville (**B**), creating a backstepping platform/shelf in shallower regions. The deepening trend was interpreted by Srinivasan (1993) and Rankey (1993) as a third-order sequence boundary. This sequence boundary is evidenced in the coeval upper Honaker by peritidal facies overlain by shoal facies (**C**). As the relative rise in sea level persisted, basinal deposits (Nolichucky Formation) eventually migrated further to the east and buried the Honaker portions of the Conasauga platform during the early Late Cambrian.

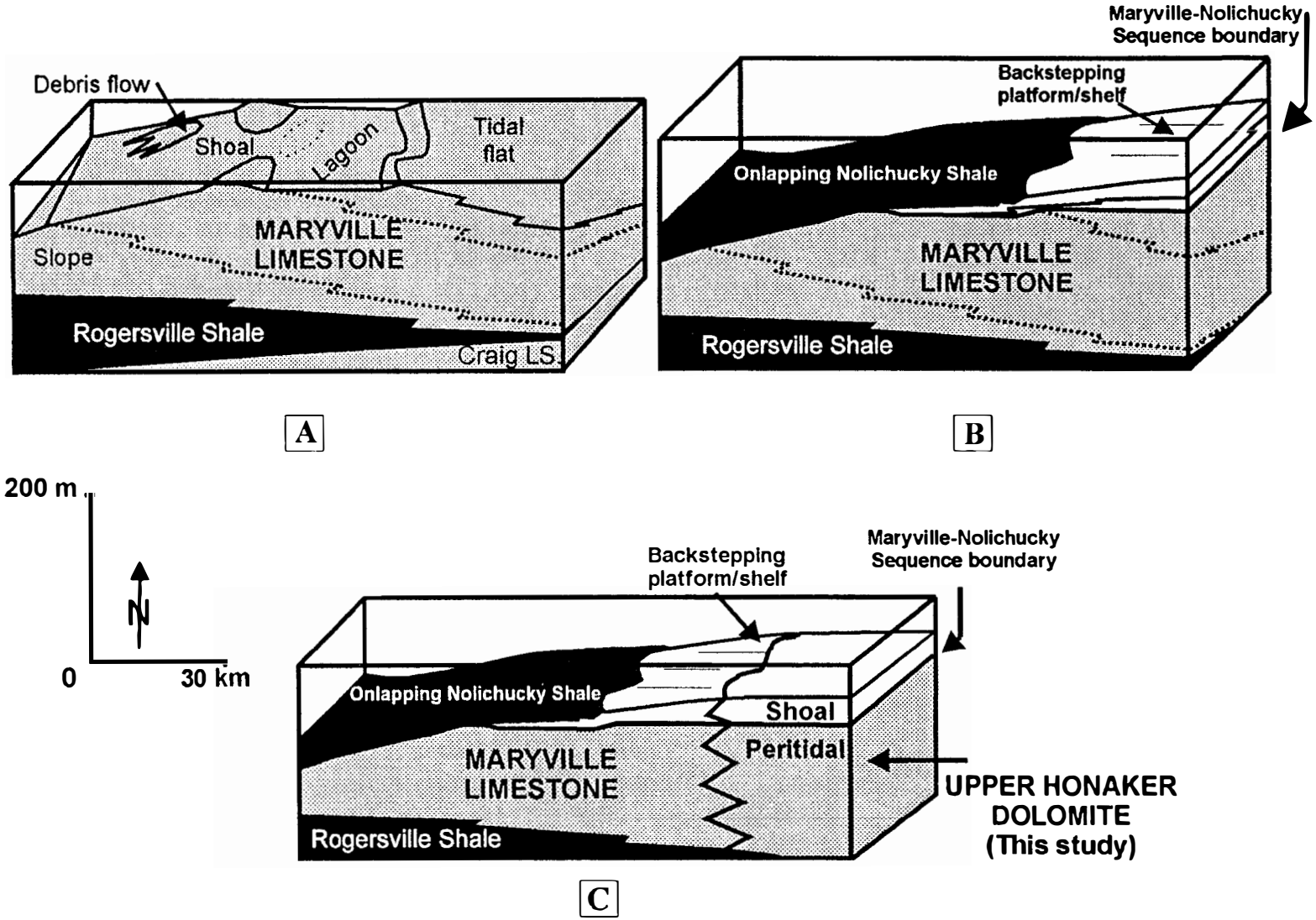
Debris flow
Shoal
Lagoon
Tidal flat
MARYVILLE LIMESTONE
Slope
Rogersville Shale
Craig LS
A
Maryville-Nolichucky Sequence boundary
Backstepping platform/shelf
Onlapping Nolichucky Shale
MARYVILLE LIMESTONE
Rogersville Shale
B
200 m
N
0
30 km
Backstepping platform/shelf
Maryville-Nolichucky Sequence boundary
Onlapping Nolichucky Shale
Shoal
Peritidal
MARYVILLE LIMESTONE
Rogersville Shale
UPPER HONAKER DOLOMITE (This study)
C

peritidal and ooid shoal deposits. This subtle facies change is the first sign of deepening further on-platform within the upper Honaker. Thus, the notion that sequence boundaries are most often represented in the geologic record as drastic changes in lithology (such as carbonate-shale), usually associated with an unconformity, may need to be re-examined, especially in mixed carbonate-clastic areas. Further to the west near the Conasauga platform margin, this prominent lithologic change is evident. However, in the platform-interior regions, it is recorded simply as a subtle change in carbonate facies.

CHAPTER 3

THE RELATIONSHIP BETWEEN DEPOSITIONAL SETTINGS AND DIAGENESIS: AN EXAMPLE FROM THE MIDDLE CAMBRIAN CONASAUGA GROUP, NORTHEASTERN TENNESSEE

Introduction

Although this chapter is not the primary focus of this research, it does highlight the post-depositional processes that have altered the sediments of the Middle Cambrian upper Honaker and lower Nolichucky in northeastern Tennessee. Piecing together diagenetic histories for sedimentary units is usually quite tedious; however, implementation of a multi-disciplinary approach using petrography, cathodoluminescence, and stable isotopes, in conjunction with the interpreted depositional setting (Chapter 2) help to constrain the timing and location of certain diagenetic events. Diagenesis usually occurs in three main environments: the marine, the meteoric, and the burial. Following deposition, sediments usually follow a time-sequential series of events, with the expected sequence depending on the initial site of sediment deposition (Walker, 1989). Hence, the depositional setting plays a crucial role in diagenetic interpretations.

As a result of exhaustive work related to carbonate diagenesis, much has been learned about the sediment-rock transformation. These studies have revealed diagnostic characteristics of marine, meteoric, and burial settings, such as cement morphologies, isotopic signatures, and trace element compositions just to name a few.

Marine diagenesis is typically characterized by micritization, nucleation of cement phases consisting of calcite and aragonite (fibrous, bladed, syntaxial,

botryoidal), some early dolomite, inclusions, iron minerals, and (minor) neomorphic growth of preexisting depositional and diagenetic components (James and Choquette, 1983; Longman, 1980). Isotopic research by Lohmann and Walker (1989) yielded a $\delta^{18}O$ value of -5 ‰ PDB and a $\delta^{13}C$ value of -0.5 ‰ PDB for Cambrian marine calcite.

Meteoric systems can be divided into three subzones (vadose zone, phreatic zone, and marine-meteoric mixing zone), each of which have specific physical and chemical characteristics. In general, meteoric calcite is characterized by oxygen isotope compositions that are depleted in ^{18}O relative to contemporary seawater values. During burial, an increase in temperature also yields a similar depletion in $\delta^{18}O$ values. Post-Silurian carbonate units that have been subjected to meteoric diagenesis may exhibit considerable depletion in ^{13}C. Depletion of ^{13}C values caused by input of soil-derived light carbon, is much less prevalent in pre-Silurian rocks. This results from the absence of land plants prior to Silurian time (Tobin and Walker, 1994).

The vadose zone, which lies above the water table, is characterized by oxidizing conditions, gravity-driven flow, varying temperatures, and unsaturated pore space, just to name a few. Karst dissolution, meniscus/pendant cement morphologies, and the precipitation of inclusion-free equant calcite are also typical for this zone (Roberson, 1989). Cements derived from vadose fluids are usually depleted with respect to iron and have poor crystal terminations (James and Choquette, 1984). The saturated phreatic zone below the water table is characterized mainly by relatively clear, isopachous cement fringes around allochems or drusy mosaic fabrics in pores, provided

that the pore fluids themselves are saturated with respect to $CaCO_3$. The third subzone of the meteoric diagenetic system represents the mixing of meteoric and brackish fluids with seawater. The most likely precipitate to evolve in this subzone is dolomite. Dolomite may arise by fresh groundwater impinging on hypersaline supratidal areas (Scoffin, 1987). According to Badiozamani (1973), mixing of 10% seawater and 90% freshwater can form a solution slightly undersaturated with calcite and oversaturated with dolomite. Land (1973), implementing stable isotopes and trace elements, deduced a similar conclusion (Longman, 1980).

Diagenetic conditions within the burial setting are characterized by increased temperatures and pressures, reducing pore fluids, ferroan calcite/dolomite phases, dull luminescence and depleted ^{18}O and ^{13}C isotopic signatures. $\delta^{13}C$ values decline only slightly, whereas $\delta^{18}O$ compositions decrease sharply (Choquette and James, 1987). This trend is a result of temperature affecting $\delta^{18}O$ fractionation more than $\delta^{13}C$ fractionation and the likely effect of low amounts of carbon in most diagenetic fluids. Dolomite crystal structures may even warp if temperatures exceed 80°C, according to Radke and Mathis (1980). Non-fabric selective neomorphic alteration and dissolution of preexisting carbonate phases may also occur (Hardie, 1987; Choquette and James, 1987). Cements generated under these conditions are usually pore central as well.

Methods

A total of 137 thin sections prepared from over 150 hand samples from three localities between the Spurgeon-Bristol and Pulaski thrust sheets in northeastern Tennessee were examined in detail. All thin sections were stained with Alizarin Red S and a mixed stain of Alizarin Red S and Potassium Ferricyanide, according to Dickson (1965), to differentiate calcite and dolomite and to identify ferroan phases. Selected polished thin sections were analyzed for cathodoluminescence using a Citl Cold Cathode Luminescence 8200 mk3 microscope. Operating conditions were as follows: voltage: 10-12 kV, beam current: 150-170 mA, chamber pressure: 180-200 millitorr.

Samples for stable isotope analyses were drilled from selected thin section billets using a microscope mounted dental drill. A total of 21 samples were analyzed for carbon and oxygen isotopes at the stable isotope laboratory at the University of Tennessee, Knoxville. Samples were roasted at 375°C for 2 hours to remove volatile organic material and then reacted with phosphoric acid at 25°C for 24 hours (calcite) and 48 hours (dolomite) to liberate CO_2 gas. Following extraction, the CO_2 gas was analyzed on a Finnigan MAT Delta Plus mass spectrometer. All compositions are reported in standard delta permil notation (‰) relative to the PDB standard (Appendix B).

Description of major diagenetic components

Replacive Fabrics

Micritization

Micritized grains are very common in marine settings, especially low energy shallow waters. The most common micritized grains in this study are ooids and intraclasts. Carbonate grains such as these are bound by endolithic microorganisms (algae and cyanobacteria) that bioerode the outer perimeter of the allochem, leaving a veneer for microcrystalline calcite to accumulate (Tucker and Wright, 1990). The intraclasts in the Upper Honaker typically possess a dark micritic rim and were later dolomitized (Figure 2.2a). Ooids, on the other hand, are significantly micritized with rare observable concentric laminae, causing some ooids to appear as rounded mud clasts (Figure 2.3a). The ooids were later dolomitized and deformed with burial (Figure 2.3b).

Dolomicrite

This fabric is common in mud-rich lithologies: mudstones, fine-grained mechanical laminates ('couplets') (Figure 2.2d), and between stratiform and LLH stromatolite laminae (Figure 2.4b,c). It postdates the micritization phase previously discussed. Dolomicrite crystals (<30 μm) are planar to nonplanar and may be anhedral to euhedral. The dolomite is typically non-ferroan to weakly ferroan and exhibits dull to non-luminescence. It is one of the most common fabrics, especially in the upper

Honaker rocks. Dolomicrite is depleted in ^{18}O relative to Cambrian calcite isotopic values (-8.2 ‰ PDB versus -5 ‰ PDB) (Lohmann and Walker, 1989) but is similar with respect to carbon isotopic values (-0.8 ‰ PDB versus -0.5 ‰ PDB). Part of this may be due to $\Delta_{calc\text{-}dol}$. Framboidal pyrite is a common accessory mineral to this fabric and is influenced by microbial activity.

Dolomicrospar

This replacive fabric is very similar to dolomicrite, but coarser (30-70 μm). It usually occurs between bedding parallel stylolites and in coarser portions of 'couplets' and clay seams. Some intraclasts have this texture as well. This dolomite is non-ferroan to weakly ferroan and emits dull to non-luminescent patterns containing patchy areas of bright luminescence.

Coarse Crystalline Dolomite

Larger dolomite crystals (70-400 μm) are commonly found in coarser-grained lithologies. They replace intraclasts, peloids, ooids, echinoderm fragments, stromatolites, and less stable calcite cements (Figure 3.1a). The crystals are usually anhedral to subhedral and may possess a cloudy center and clear outer rim commonly referred to as "CCCR dolomite" (Sibley, 1982). Cook (1983) estimated this fabric to account for over 1/3 of completely dolomitized rocks within the Honaker Formation. It may obliterate original fabrics, but ghost structures are quite common (Figure 2.3b, 3.1b,c). Stylolitization predates and postdates this altering texture. Coarser crystalline dolomite is typically non-luminescent with occasional dull-bright banding and is non-ferroan to weakly ferroan. Oxygen isotopic values are more negative relative to

Figure 3.1 - Common replacive fabrics of the upper Honaker and lower Nolichucky captured in plane-polarized light. **A** shows non-ferroan calcite (nfc) that has been replaced by planar dolomite (do) within a coarse-crystalline dolomitized mudstone. [I-81/20.6] **B.** Dolomite overprinting can lead to ghost structures as evidenced by the trilobite grain (t) [I-81/29.2]. Intraclasts (I), as well as many other allochems within the upper Honaker, possess an isopachous rim of dolomite implying early dolomitization. **C.** Baroque dolomite (bq) is a later replacive fabric indicative of increased temperatures (>80°C). Coarse replacive dolomite (crd) as well as baroque dolomite typically obliterates host fabrics. [BL/16.8] **(D)** Ooids are another common ghost structure within the dolomitized rocks of the upper Honaker [I-81/29.2].

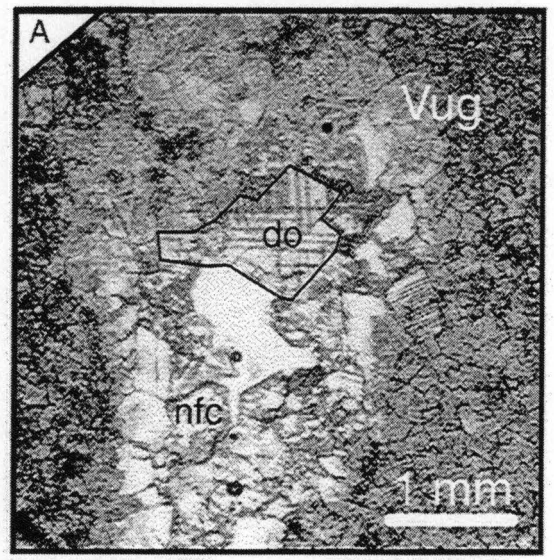
A
Vug
do
nfc
1 mm

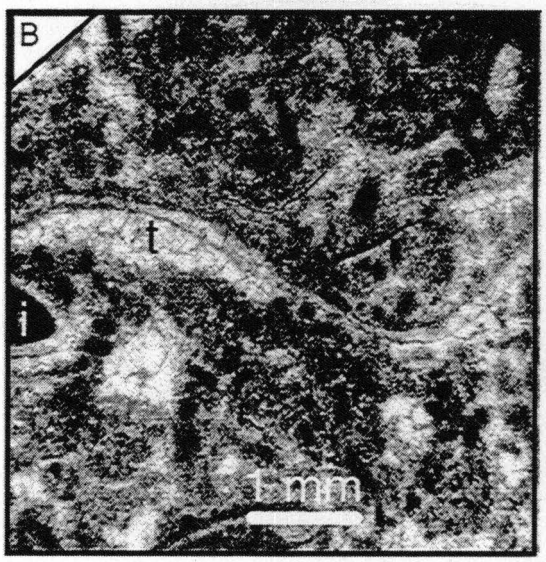
B
t
i
1 mm

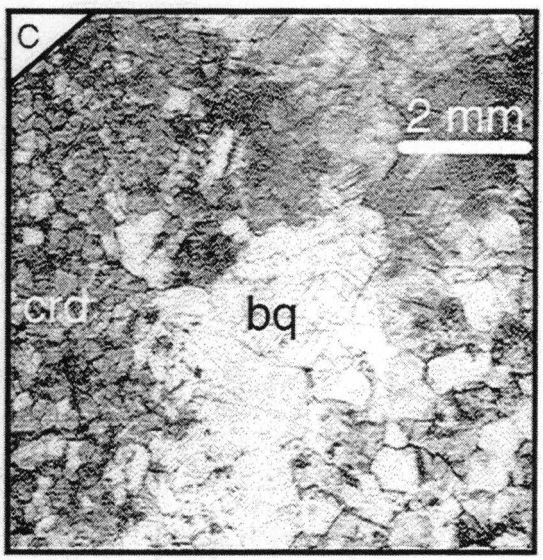
C
2 mm
bq

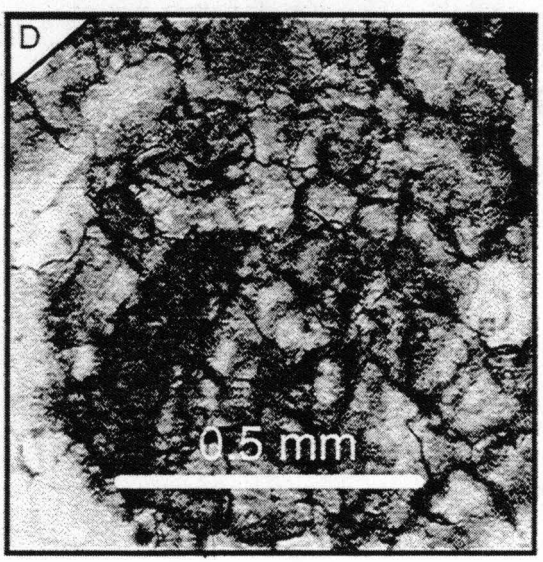
D
0.5 mm

dolomicrite or Cambrian marine calcite; carbon isotope compositions show minimal change.

Non-planar Replacive Dolomite

Commonly referred to as "saddle" or "baroque" dolomite (Radke and Mathis, 1980), non-planar replacive dolomite is coarse (up to 1-2 mm) and somewhat turbid, with well developed crystal faces that are characterized by sweeping extinction in cross-polarized light. Host fabrics are obliterated (Figure 3.1c) by this fabric and it is volumetrically the least abundant replacive phase in this study. Trace elemental composition inferred from staining varies from non-ferroan to ferroan. Saddle dolomite is non-luminescent under CL and isotopic compositions for $\delta^{18}O$ and $\delta^{13}C$ are -8.8‰ PDB and -1.7‰ PDB, respectively.

Neomorphic Fabrics

Ferroan Calcite

This mineral is commonly associated with skeletal packstones, matrix material, and fractures of the lower Nolichucky Formation (Figure 2.2e). Although crystal size and shape of the host fabric appear unchanged as a result of diagenesis, diagenetic fluids have likely altered the trace element composition based on staining and cathodoluminescence. This calcite has dull orange luminescence.

Authigenic Cements

Fibrous/bladed Cements

Fibrous/bladed cements, indicative of marine diagenetic settings, are rare in most rocks of this study with the exception of skeletal packstones in the lower Nolichucky Formation. These cements are weakly ferroan to ferroan and have a dull orange luminescence under CL. Fibrous/bladed cements typically grade into equant drusy mosaic fabrics.

Syntaxial Cements

This cement type is also associated with marine diagenesis and lower Nolichucky rocks, similar to the fibrous/bladed cements. It is present in packstone deposits as syntaxial overgrowths precipitated as individual crystals sharing crystallographic orientation with host echinoderm fragments. Syntaxial cements are usually turbid and may be either non-ferroan or ferroan. The CL pattern of these cements is a dull orange luminescence. The lack of fibrous/bladed and syntaxial cement morphologies in the upper Honaker is likely a function of depositional setting and subsequent conditions (tidal flat and syndepositional dolomitization), later dolomite overprinting, and/or combination thereof.

Crystalline Dolomite

Dolomite is common in the upper Honaker, but determining authigenic or replacive phases is sometimes questionable. Dolomite occludes a variety of pore types (Figure 3.2): fenestral, fracture, vuggy, moldic and intergranular. Detailed microscopy

Figure 3.2 - Authigenic precipitates in the upper Honaker and lower Nolichucky. All photomicrographs were captured in plane-polarized light. **A.** Dolomitized mudstones contain well preserved marine features such as evaporitic molds (ev) occluded with dolomite, thereby implying early precipitation. Moldic porosity (m) from allochems such as this sponge spicule are typically rare due to the stressful environmental setting. [BL/63.8] **B.** Tectonic-induced fractures related to uplift are filled with baroque dolomite (bq) and other burial cements. Sample also shows moldic porosity (m) filled with dolomitized matrix material as well as coarse crystalline dolomite. [BL/92.7] **C.** Framboidal pyrite is relatively common in both formations. Its association with dolomicrite implies early precipitation. [BL/74.6]

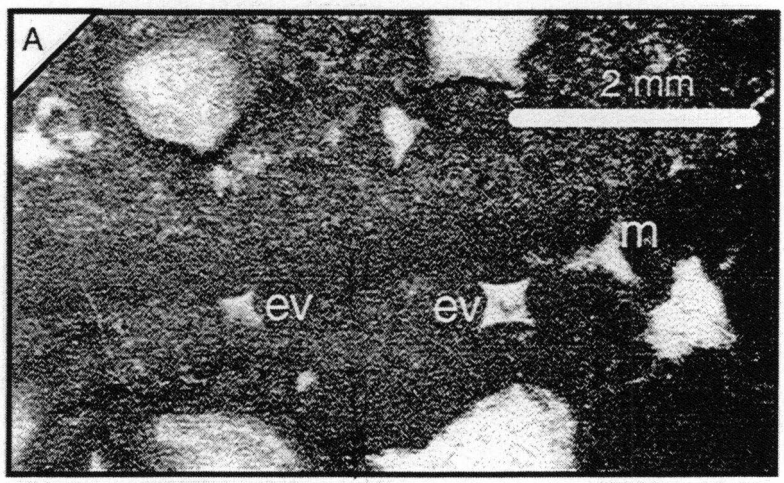
A
2 mm
m
ev
ev

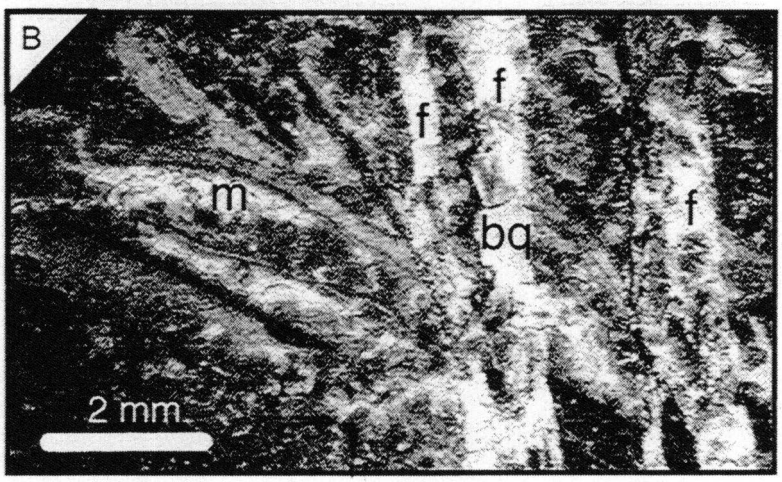
B
f
f
f
m
bq
2 mm

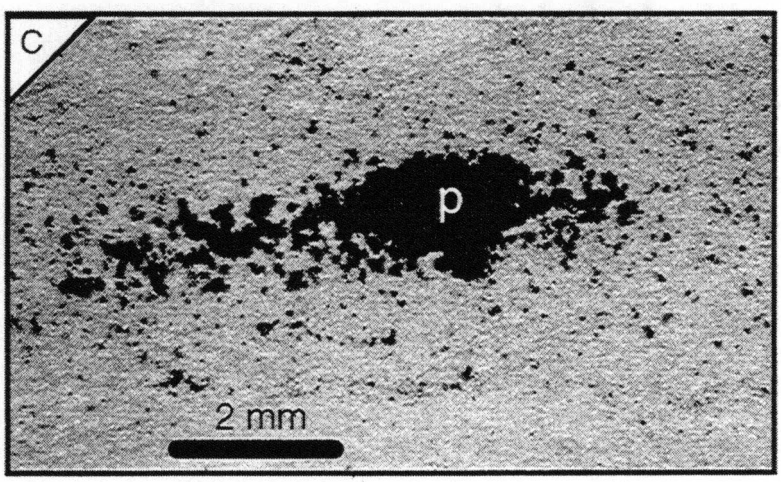
C
p
2 mm

has revealed certain features that help constrain the relative timing of dolomitization within the upper Honaker. For example, intraclasts in wackestone/packstone lithologies possess an isopachous fringe of dolomite, which implies early dolomitization. Most of the lithologies have been overprinted with dolomicrite or dolomicrospar (both relatively early diagenetic events), which hinder their recognition. Also, the association of early diagenetic components such as evaporitic vugs (Figure 3.2a), fenestrae (Figure 2.4b), and framboidal pyrite (Figure 3.2c) with dolomite suggest early marine precipitation. Isotopic compositions of dolomicrite and dolomite-filled fenestrae have very similar carbon values near -0.9 ‰ PDB but slightly different oxygen values (-8.5 ‰ PDB and -10.6 ‰ PDB, respectively). The oxygen compositions do not reflect marine values; the more negative values may be the result of alteration by later burial fluids. Yet, the most striking evidence for marine dolomite is its relationship to some syntaxial calcite; sparse dolomite rhombs are engulfed by syntaxial cements. They occur higher in the stratigraphic sections, near the Nolichucky contact. Marine dolomite crystals vary in size from 60 to 300 μm and possess irregular crystal boundaries. They are non-ferroan and dully luminescent under CL.

Baroque Dolomite

Non-planar dolomite not only replaces previous fabrics but it can also precipitate very late in fractures (Figure 3.2b). The temperatures (>80°C) usually necessary for baroque dolomite to precipitate imply burial diagenetic conditions. Baroque dolomite cement occludes tectonic-related fractures within the upper Honaker dolostones and postdates reduced iron-rich calcite phases of the lower Nolichucky

Formation. The curved crystals are non-luminescent and vary in size, but are typically 1-2 mm; the crystal centers are also turbid.

MVT Mineralization

Mississippi Valley-Type mineralization is found in the upper Honaker. Mineralization is characterized by clear to slightly turbid tabular crystals with low to moderate birefringence (2nd order blue). It occurs in a few samples throughout the entire stratigraphic sections as a later cement phase associated with calcite-filled fractures. Crystal size varies, but is commonly 500 μm to 1mm. Under CL, it is non-luminescent. This mineral is likely a member of the Barite Group (either barite or celestite) (O.C. Kopp, personal communication).

Equant Calcite

Non-ferroan equant calcite is predominantly located in late fractures and intergranular pores of the upper Honaker. It is associated with dedolomitization, MVT mineralization, and other late diagenetic events. Any early equant calcite precipitates have likely been overprinted by dolomite. Cathodoluminescence produces microbands of bright orange and non to dull luminescent patterns. Crystals can be very large and blocky (up to 4 mm). Average $\delta^{13}C$ is -9 ‰ PDB and $\delta^{18}O$ is -10 ‰ PDB.

Other diagenetic features

Fractures

Various generations of tectonically-induced fractures are present in the rocks of this study, especially the thick bedded dolostones of the upper Honaker. Structural deformation related to compression and uplift have created at least 3 generations of fractures based on cross-cutting relationships. The fractures are filled with turbid saddle dolomite, coarse planar dolomite, equant calcite, and/or pyrite. Carbonate precipitates may be ferroan to non-ferroan. Most fracture-fillings emit dull orange luminescence under CL with the exception of pyrite, which is non-luminescent.

Stylolitization

Both bedding parallel and bedding normal stylolites are evidenced in the upper Honaker and lower Nolichucky Formations. The amplitude of the stylolites is a function of the clay content in the host lithology. Stylolites, as well as clay seams, contain coarse crystals of dolomite, dolomicrospar, quartz, or other insoluble materials. They are usually ferroan and dully luminescent with bluish purple specks. Stylolite formation occurred prior to, during, and following fracturing.

Geochemistry

Stable Isotopes

Stable isotope compositions provide important clues concerning the properties of different diagenetic environments. Compositions of phases precipitated in various

environments are a function of kinetic effects (i.e., temperature, biological controls, unidirectional processes such as photosynthesis, etc.) and equilibrium effects (i.e., bond energy differences) (Hoefs, 1997). The stable isotope composition of all the depositional and diagenetic phases are summarized in Appendix B.

Figure 3.3 is a crossplot of $\delta^{18}O$ and $\delta^{13}C$ values showing two distinct dolomite and calcite zones that roughly possess the inverted J-shaped curve of Lohmann (1982). The more negative $\delta^{18}O$ values for the dolomites convey 'reset' isotopic signals due to recrystallization at the higher temperatures of burial diagenesis. For example, dolomicrite and fenestral dolomite are well documented and common microfacies in early marine diagenetic settings, yet their oxygen isotopic compositions are similar to saddle dolomite, which can only form in the presence of sulfate-rich marine fluids or warm (>80°C) burial fluids. The temperature range for the saddle dolomite formation can be estimated from measured $\delta^{18}O$ values of the dolomite and assumed $\delta^{18}O$ compositions of burial fluids. Using a range of $\delta^{18}O$ compositions for modern formation waters in sedimentary basins of 0 to 5 ‰ SMOW (Kharaka and Thordsen, 1992) and -9 ‰ PDB for the saddle dolomite yields a temperature range of 95°C to 150°C for saddle dolomite precipitation (equations after Land, 1985). Thus, the timing of saddle dolomite precipitation, in conjunction with the estimated temperature range, reduce the likelihood of sulfate-rich marine fluids precipitating these non-planar dolomite phases.

Figure 3.3 - Crossplot of stable isotopic values for the diagenetic components of the upper Honaker and lower Nolichucky interval. Note the isolated fields for dolomite and calcite. The 'box' represents a common isotopic range for most Early Paleozoic meteoric calcites in the southern Appalachians based on the literature. Note the variance between calcites of this work relative to calcites from other Early Paleozoic studies. Lohmann and Walker's (1989) Cambrian marine calcite composition is also plotted.

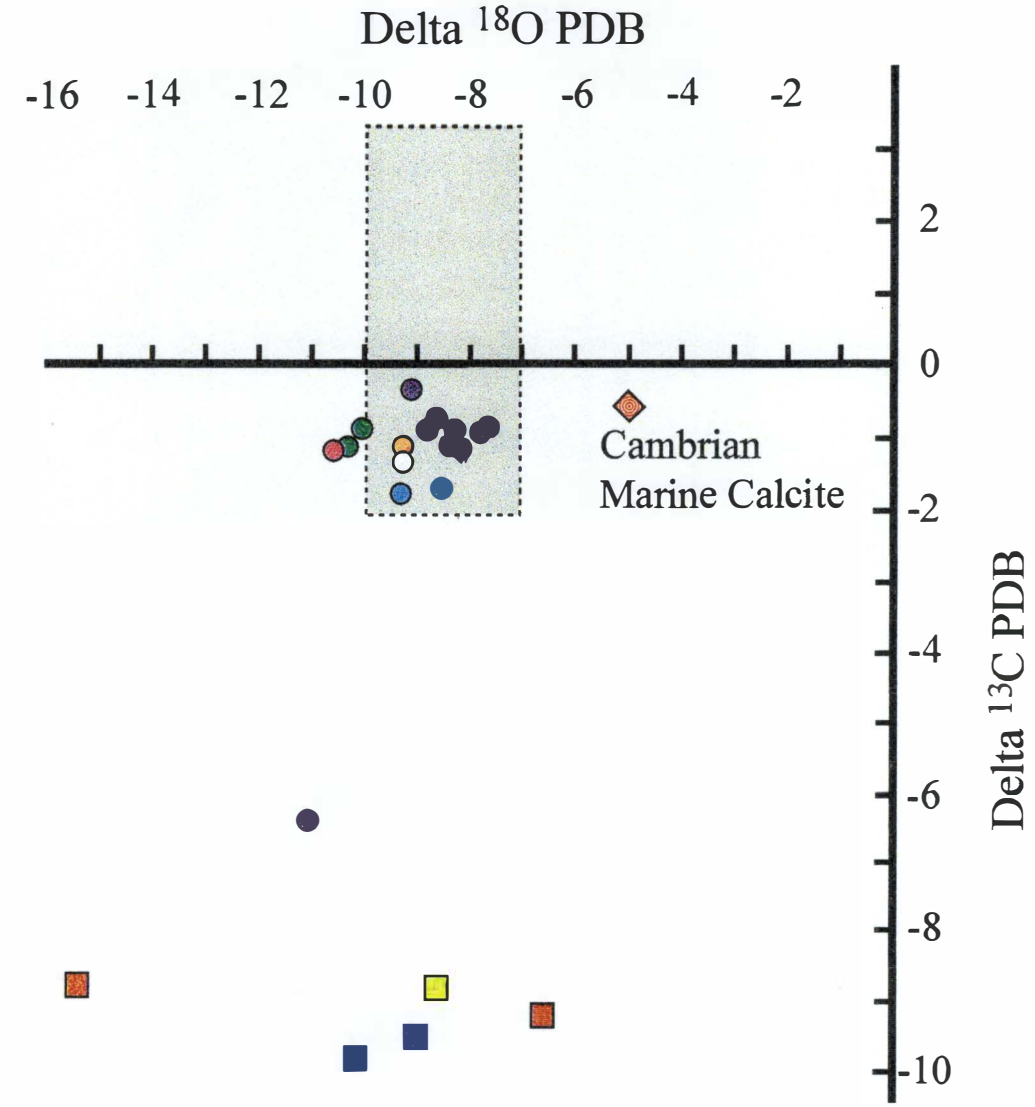

DOLOMITES

- Dolomicrite
- Planar dolomite - Vuggy
- Planar dolomite - Fenestral
- Dolomite - Non-descriptive
- Replacive Dolomite
- Non-planar dolomite

CALCITES

- Intergranular
- Vuggy
- Fracture
- Cambrian marine calcite

The ^{18}O-depleted calcite compositions, which are also significantly lighter in ^{13}C compared to most Early Paleozoic calcite values, could possibly be a function of various diagenetic mechanisms, including oxidation of organic matter in suboxic diagenetic settings, initiation of methanogenesis under anoxic conditions, introduction of light carbon into the subsurface by land plants, or simply alteration by modern ^{13}C-depleted meteoric fluids (Hoefs, 1997). This range of possibilities can be constrained by inferring fluid compositions for the calcite, which are estimated by integrating likely temperatures and measured $\delta^{18}O$ values of the carbonate samples into the following equation: $1000\ln\alpha_{(calc\text{-}water)} = 2.78(10^6T^{-2}) - 2.89$ (Friedman and O'neil, 1977). By assuming temperature conditions of early and late diagenesis (approximately 30°C to 70°C), and using an average $\delta^{18}O$ value for the calcite (-10 ‰ PDB), the calculations suggest fluid compositions were comparable to either modified seawater at higher temperatures (-1 to -2 ‰ SMOW) or meteoric water at lower temperatures (-7 ‰ SMOW). However, because much of the calcite is associated with dolomite dissolution and fracture porosity, and because calcite appears to be one of the last precipitated phases based on cross-cutting relationships, calcite probably occurred as the formations rose from deep burial diagenetic settings into the shallow meteoric realm by way of tectonic uplift and unroofing during the Late Paleozoic Alleghanian Orogeny. Land plants during this time could have depleted the $\delta^{13}C$ signal by incorporating light carbon into the subsurface. Likewise, the influence of present-day meteoric fluids on these rocks could also be a viable mechanism, considering ^{13}C in modern fresh waters can be depleted by as much as -20 ‰ PDB if biological CO_2

predominates in a system (Hoefs, 1997). The author, however, suggests that a more extensive isotopic study be carried out to ascertain the exact cause(s) of this anomalous range of $\delta^{13}C$ calcites since most Early Paleozoic compositions are more positive (Figure 3.3).

It is important to note that petrographic observations of diagenetic components (previous section) reveal that much of the dolomite precipitated during both marine and burial diagenetic conditions. In addition, stable isotopic compositions of the calcite imply two different fluid compositions that are both capable of yielding the same isotopic signature. The discrepancies within petrographic observations and stable isotopic data alone are overcome by collectively integrating the two disciplines to confine the range of possibilities (i.e., timing and origin of diagenesis). Hence, omitting one of these methods would result in ambiguous and potentially inaccurate interpretations.

Cathodoluminescence

Cathodoluminescence (such as bright, dull, and non-luminescent) in carbonate lithologies are a function of multiple factors including the presence of activators (such as Mn^{2+} and Pb^{2+}), quenchers (such as $Fe^{2+,3+}$, Co^{2+},and Ni^{2+}), and the relative concentrations of rare earth elements (REE's) in diagenetic fluids (Machel et al., 1991). Non-chemically-dependant factors such as, but not limited to, temperature, salinity, and crystal surface structure may also influence cathodoluminescence (Machel and Burton, 1991). From luminescence patterns, broad inferences can be made about fluid

chemistry during crystallization of cements. Cathodoluminescence also allows for better recognition of cement phases that are not visible with plane light microscopy. For example, many early calcite-filled fractures within the upper Honaker were overprinted and hidden by the more stable dolomite crystals (Figure 3.4c). Cathodoluminescence revealed these areas as bright orange-red fractures (calcite) in a non-luminescent groundmass (dolomite) (Figure 3.4d).

The cements and depositional components of the Honaker/Nolichucky interval reveal various luminescent patterns. The abundant dolomite of the upper Honaker is dull to non-luminescent, suggesting high temperatures and/or increased amounts of reduced iron, typical of burial diagenetic conditions. It may occasionally be zoned. Calcite, on the contrary, is bright to dully luminescent and may possess microbands. Cross-cutting relationships and stable isotopic compositions suggest that calcite in the upper Honaker likely precipitated late from meteoric fluids. It is evidenced by calcite microbanding on brecciated, dolomitized clasts (Figures 3.4 a,b) and more negative ^{13}C values (Figure 3.3). Calcite in the Nolichucky Formation, however, has dull to moderately bright orange luminescence. This has been interpreted to indicate low concentrations of dissolved Fe^{2+} in marine fluids during deposition and stabilization of subtidal facies. Sparse siliciclastic deposits of the upper Honaker, mainly detrital quartz, have bright bluish purple luminescence. The difference in luminescence patterns between the two formations is an artifact of depositional setting and subsequent diagenetic alteration(s).

Figure 3.4 - Paired plane-polarized light and cathodoluminescence photomicrographs. **A,B** show intergranular calcite with microbands and dissolved dolomite breccia clasts. [I-81/3.4] **C,D** show the utility of cathodoluminescence. Plane-polarized light microscopy reveals only one generation of fractures in the dolomicrospar lithology while cathodoluminescence conveys more than one generation. [I-81/30]

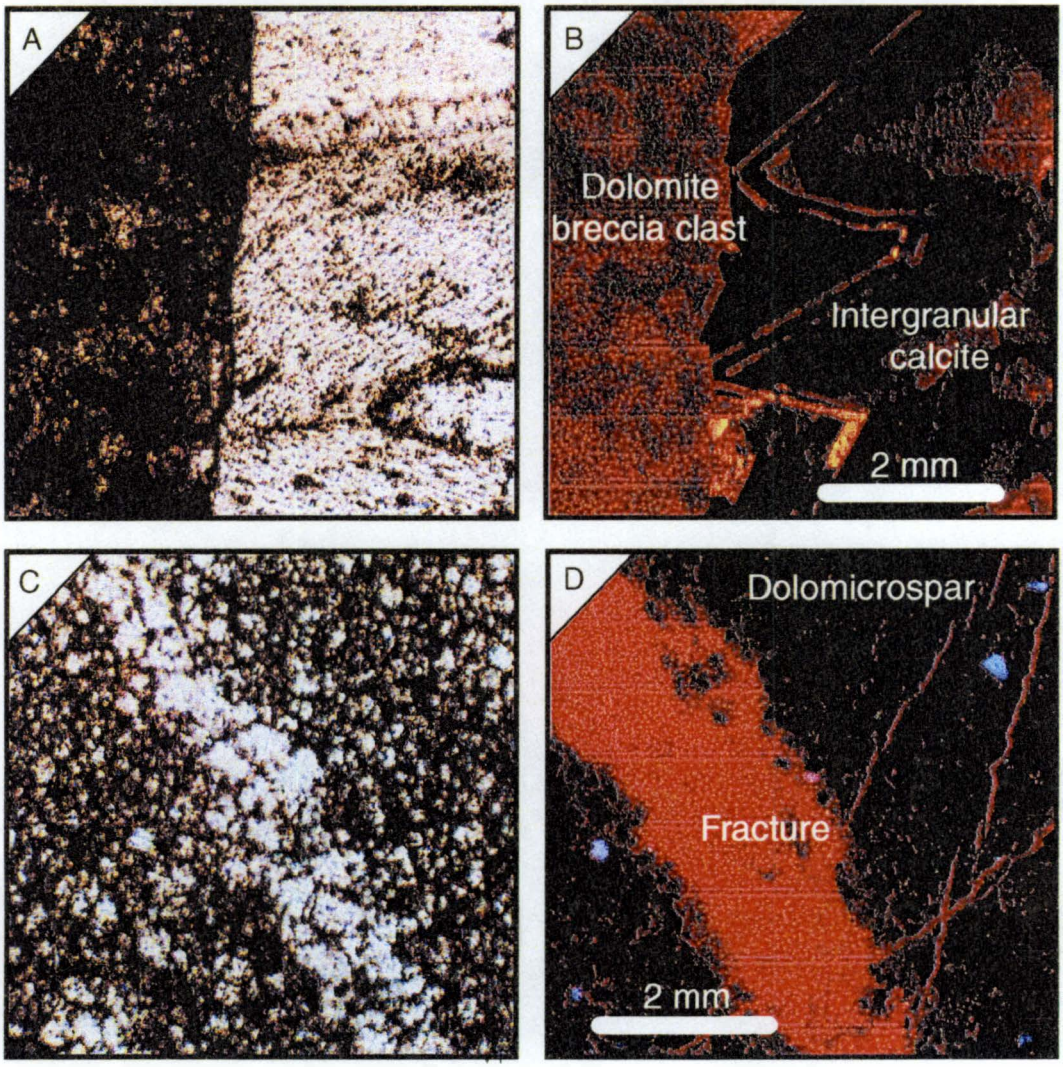
A
B
Dolomite
breccia clast
Intergranular
calcite
2 mm
C
D
Dolomicrospar
Fracture
2 mm

Discussion of Stabilization Processes

Marine Diagenetic Environment

The bulk of marine carbonates begin to undergo diagenesis very early in the marine setting. Early marine cements may be calcitic, aragonitic, or dolomitic depending on a number of factors including, but not limited to, water depths (shallow versus deep marine), geologic time (Sandberg,1983), and depositional setting and subenvironments. Because water depths were relatively constant during deposition of the rocks studied here (supratidal to subtidal range), and because the formations examined are similar in age, depositional environments become the main factor regarding diagenesis of the upper Honaker and lower Nolichucky.

Marine dolomite is a common diagenetic component, especially in the upper Honaker. Many models for surface dolomitization have been proposed: Dorag mixing, sabkha with evaporative reflux, Kohout convection, seepage-reflux, shallow-subtidal (Machel and Mountjoy, 1986; Tucker and Wright, 1990), as well as others. Many of these are modifications of previous models.

Dolomite will precipitate provided enough Mg^{2+} and CO_3^{2-} are in a system, fluids are mobile, and kinetic inhibitors such as hydration spheres (which preferentially incorporate Mg^{2+} before Ca^{2+}), dissolved sulfates, and organic material are overcome (Machel and Mountjoy, 1986). The early marine dolomite of the upper Honaker could have formed in a variety of ways: reflux of slightly hypersaline lagoon waters, tidal pumping, freshwater/seawater mixing (Tucker and Wright, 1990), and/or some

combination of these. Each possibility is addressed below. The difficulty of discerning which is most correct for this study reflects what little is understood about dolomite forming processes. Carbonate sedimentologists must look at all aspects of a depositional/diagenetic system to arrive at the most likely mechanism(s).

The reflux of slightly hypersaline lagoon waters is a plausible mechanism for early dolomitization. Subtidal thrombolite and intertidal facies may have acted in concert to limit seawater mixing in interior portions of the platform and, consequently, raise salinity levels. The "semi-closed" lagoon setting would have allowed hypersaline waters to seep and reflux in the underlying peritidal sediments. Evaporation usually accompanies this process, especially in modern, arid systems like the Trucial Coast of the Persian Gulf (Bush, 1973). More humid regions, like the Bahama Bank carbonates, contain minimal evaporites (Hardie and Shinn, 1986). The upper Honaker likely represents a combination of the two modern analogs (semi-arid climate), because although it contains some evaporite molds in carbonate mud-rich lithologies (Figure 3.2a), the Conasauga paleolatitude during the Middle Cambrian was similar to that of the present day Bahama Bank (Torsvik et al., 1991).

Tidal pumping is also a potential mechanism, but not as likely as the aforementioned, due to the calm lagoon setting further on-platform. However, because this environment was located in the tidal zone, fluctuations in tidal regime could have contributed to some of the early dolomite. Spring high-stands could have introduced Mg^{2+} into the sediments from fresh unaltered seawater.

The tidal zone location also implies freshwater-seawater mixing as another mechanism for dolomite precipitation. Exposed portions of the carbonate platform (supratidal and intertidal facies) could have been areas of dissolution and, thus, conduits for freshwater percolation. Topographic-driven flow through the platform would mix meteoric and marine fluids. Based on the shallow (to exposed) carbonate setting and climatic conditions, karstification would have likely occurred as well. However, only rare episodes of dissolution are recorded in the upper Honaker rocks (Figure 2.4d). This suggests that: 1) later dolomite overprinting has erased most of the karstification evidence and/or, 2) karstification was not significant during this time; petrographic observations seem to support the former as some vugs contain an early phase of calcite followed by a later replacive form of dolomite (Figure 3.1a).

All three mechanisms, collectively, could have exerted controls on dolomite precipitation as well. The interpreted depositional setting for the upper Honaker possesses all the criteria necessary to promote early dolomitization (evaporation, Mg^{2+} supply, fluid migration, etc.). Any combination of dolomite models is plausible, provided they truly reflect the geology.

Basinward of syndepositional dolomite areas are intertidal ooid shoal facies and subtidal facies, respectively. Early dolomitization may have taken place in these settings, however later dolomite overprinting nullifies its recognition in these rocks. Early cementation is suggested by the shape and size of ooid-intraclasts (Figure 2.3c). The irregular, non-streamline morphology of the clasts implies minimal transport and early (marine) diagenesis of the packstone and grainstone lithologies. Calcite likely

precipitated in the intergranular pores but was later converted to a more stable dolomitic phase during burial diagenesis. Deeper subtidal deposits such as skeletal-rich packstone facies also suggest early marine calcite. Syntaxial overgrowths on echinoderm debris, microcrystalline calcite, fibrous/bladed crystals along skeletal grain boundaries, and framboidal pyrite are classic examples of subtidal marine features. The majority of these rocks were later selectively dolomitized with the exception of carbonate beds within the shale-rich lower Nolichucky Formation. The non-alteration of these subtidal carbonate beds is likely a result of shale interbeds inhibiting fluid percolation. Late diagenetic alteration is discussed in the next section.

Much of the micrite in both formations has been dolomitized. Distinguishing marine dolomite and burial dolomite is sometimes difficult, however, stable isotopic data usually allows for better distinction of dolomite origin and timing. Even though fine-grained carbonate sediment has the potential to be isotopically altered during dolomitization, it has been demonstrated that most finely-crystalline dolomites usually retain their carbon isotopic composition from the precursor $CaCO_3$ for the following reasons: 1) the dominant source of carbon is the precursor carbonate mineral phase; 2) the formation of dolomicrite is usually a very early diagenetic process; and 3) pore space occlusion during penecontemporaneous cementation can usually isolate dolostones from later diagenetic fluids (Glumac, 1997; Narbonne et al., 1994; Kaufman and Knoll, 1995). Dolomicrite isotopic values plot the closest to Cambrian seawater values compared to any other diagenetic phase (Figure 3.3). However, the 3‰ difference between the Cambrian marine calcite and dolomicrite is significantly higher

than that of Glumac's (1997) 1‰ difference for similar age, shallow water deposits in the southern Appalachians. Thus, different diagenetic histories were likely imposed on the two Cambrian peritidal complexes.

Burial and Late Meteoric Diagenetic Environments

Burial diagenesis is a later event that is typical of many ancient lithologies, especially Early Paleozoic rocks of Tennessee. Tectonism, thermal and non-thermal subsidence, weathering, eustasy, and other controls during the Paleozoic have created vast amounts of accommodation space and sedimentary fill in the southern Appalachian region. A burial curve (Figure 3.5) based on overburden thickness from Srinivasan (1993) suggests that Maryville-Honaker deposits were buried more than 4.5 km and were exposed to temperatures slightly greater than 150°C by the Late Paleozoic. The temperatures and pressures associated with these conditions would have led to various processes including physical and chemical compaction, dissolution, cementation, burial dolomitization (neomorphism), mineral reactions, and organic maturation (Choquette and James, 1987). Most of these processes are evidenced within the upper Honaker and lower Nolichucky Formations.

Following the last relative rise in sea level which inundated the Conasauga platform and deposited deeper water deposits (Nolichucky) on top of peritidal carbonates (Honaker), shallow burial conditions were exerted on the lithologies. The upper Honaker contains replacive fabrics such as dolomicrospar and zoned dolomite.

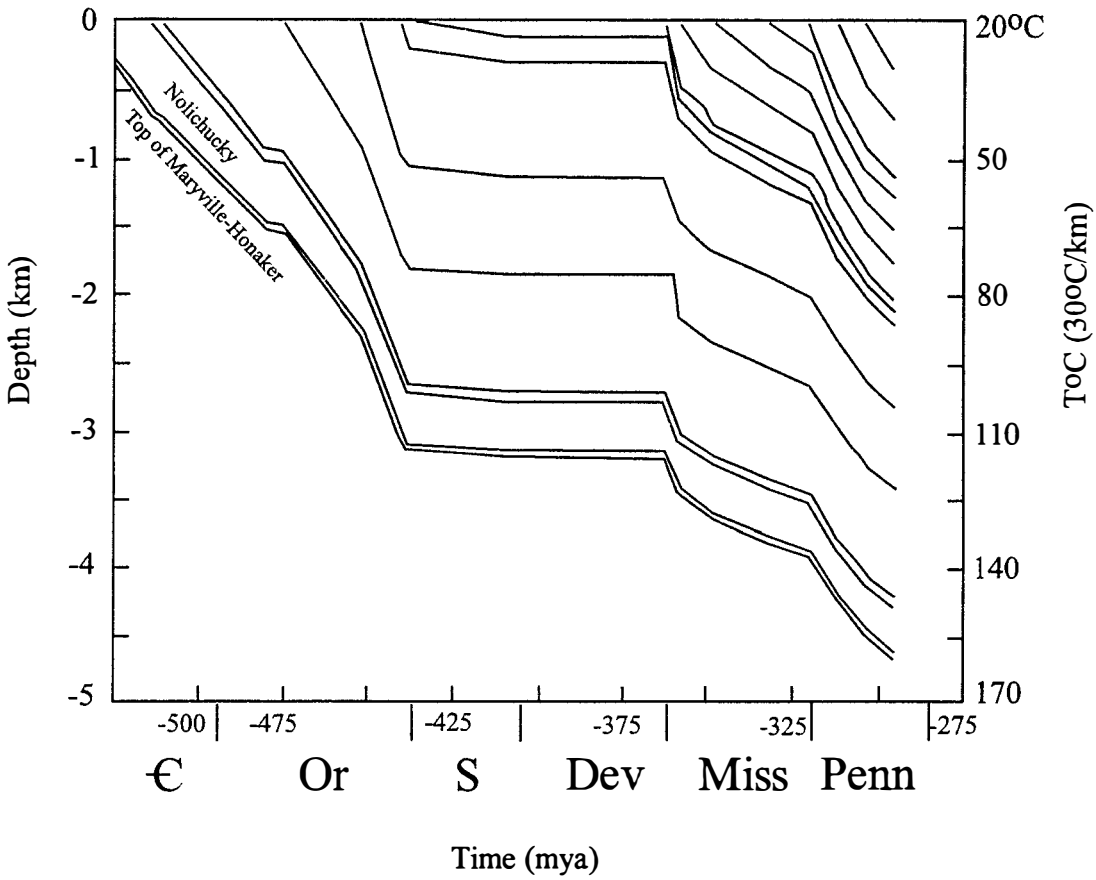

Figure 3.5 - Burial history plot based on overburden thickness for the Maryville Limestone and overlying strata in eastern Tennessee. Maryville rocks are time-eqivalent and proximal to the rocks of this study (Honaker Dolomite), thus overburden thickness should have been similar. Note that surface temperature is assumed to be 20°C and geothermal gradient is assumed to be 30°C per kilometer. Modified from Srinivasan (1993).

Dolomicrospar likely evolved from a dolomicrite precursor whereas the zoned dolomite probably implies replacement of early, marine dolomite or low-Mg calcite (Cook, 1983). Zoned dolomites are comprised of a turbid crystal center and a translucent outer rim. The cloudy center is a result of ion impurities (Mn^{2+}, Fe^{2+}, etc.) contained in seawater that were incorporated into the crystal lattice; the translucent perimeter suggests a change in fluid composition through time, probably mixed marine-meteoric fluids.

The presence of vuggy porosity, which is especially evident with the aid of cathodoluminescent microscopy, suggests dissolution by meteoric fluids. Cathodoluminescence reveals patchy zones of bright luminescent calcite pre-dating dull to non-luminescent replacive dolomite in the upper Honaker. The exact timing of dissolution events is somewhat questionable due to the limited occurrence of these calcite/dolomite-occluded pores.

Intermediate and deep burial diagenetic conditions have left more recent signatures that are more easily identified. Relative depleted isotopic values, reduced-iron cement phases, compaction, stylolitization, fracturing, MVT mineralization, and baroque dolomite are quite common in the Middle Cambrian strata. Their individual time frames may be questionable however, as most events were more or less contemporary. Based on the burial curve from Srinivasan (1993) (Figure 3.5), baroque dolomite formation and other deep burial events probably began during the Late Ordovician following the Taconic Orogeny (~450 mya). This assumption is based on

an 80°C minimum limit for baroque dolomite (Radke and Mathis, 1980; Choquette and James, 1987).

The increase in temperature related to burial led to a decrease in $\delta^{18}O$ values. Oxygen values of deep burial phases are depleted relative to Middle Cambrian marine settings by as much as 6 ‰ PDB (Figure 3.3). Overburden stresses associated with the Taconic Orogeny led to lower porosity due to physical and chemical compaction. Chemical compaction, or pressure solution, produced bedding parallel and bedding normal stylolites in most of the thick bedded dolomitized mudstone and wackestone lithologies. The amplitude of the suture pattern is a function of the clay content and grain size; the orientation of the stylolite aligns normal to the dominant stress field. Hence, the bedding parallel stylolites were produced by overburden stresses, whereas the bedding normal stylolites formed as a result of compression due to thrusting. The stylolites (and clay seams) usually contain dolomite crystals and other insoluble materials.

Tectonic activity resulted in 3 (possibly more) episodes of brittle deformation in these rocks, based on cross-cutting relationships. Most fractures are occluded with planar and non-planar forms of dolomite. The planar dolomite probably stemmed from meteoric water percolating down through the rocks following tectonism. As tectonism and subsequent sediment deposition continued into the middle Paleozoic, increased temperatures linked to burial produced baroque dolomite in the fractures. Ferroan calcites/dolomites neomorphosed in the carbonate beds that were located proximal to Nolichucky shale layers as well. The iron-rich phases and high temperatures likely

produced the pyrite that coats most of the lithologies and occurs later in fractures. Stylolitization also occurred contemporaneously with these other events.

As burial-induced temperatures elevated even more, MVT minerals (barite?) derived from basinal sources were precipitated pore-centrally in some of the fractures. These fractures are somewhat rare but do occur throughout the entire stratigraphic interval.

The Alleghanian Orogeny during the Late Paleozoic uplifted these formations to their present orientation in the Valley and Ridge physiographic province. During the Mesozoic Era, unroofing of younger sedimentary material allowed leaching and dolomite dissolution (dedolomitization) to occur, which still continue today (Cook, 1983). The dedolomitizing event is evidenced by non-ferroan equant calcite between brecciated dolomitized clasts (Figure 3.4 a,b) that probably formed close to the surface. Temperatures were approximately 25-30°C based on the oxygen isotopic compositions and calculated results of the calcite-water fractionation relationship (Friedman and O'Neil, 1977). Depleted carbon isotopic values of the equant calcite seem to reflect a meteoric signal as well (Figure 3.3).

Paragenetic Sequence

Integrating plane-polarized light and cathodoluminescent microscopy, stable isotopes, and examples from other carbonate studies permits relative time frames to be placed on the diagenetic phases or events in this study. Figure 3.6 is a proposed paragenetic sequence for the Middle Cambrian upper Honaker and lower Nolichucky

Figure 3.6 - Paragenetic sequence for the upper Honaker and lower Nolichucky Formations. Note superscripts for diagenetic phases/events that are limited to subtidal and peritidal facies, respectively. The paragenetic sequence is arranged from early marine and evaporitic conditions to deep burial conditions. There is an additional meteoric phase of non-ferroan equant calcite following deep burial. See text for discussion.

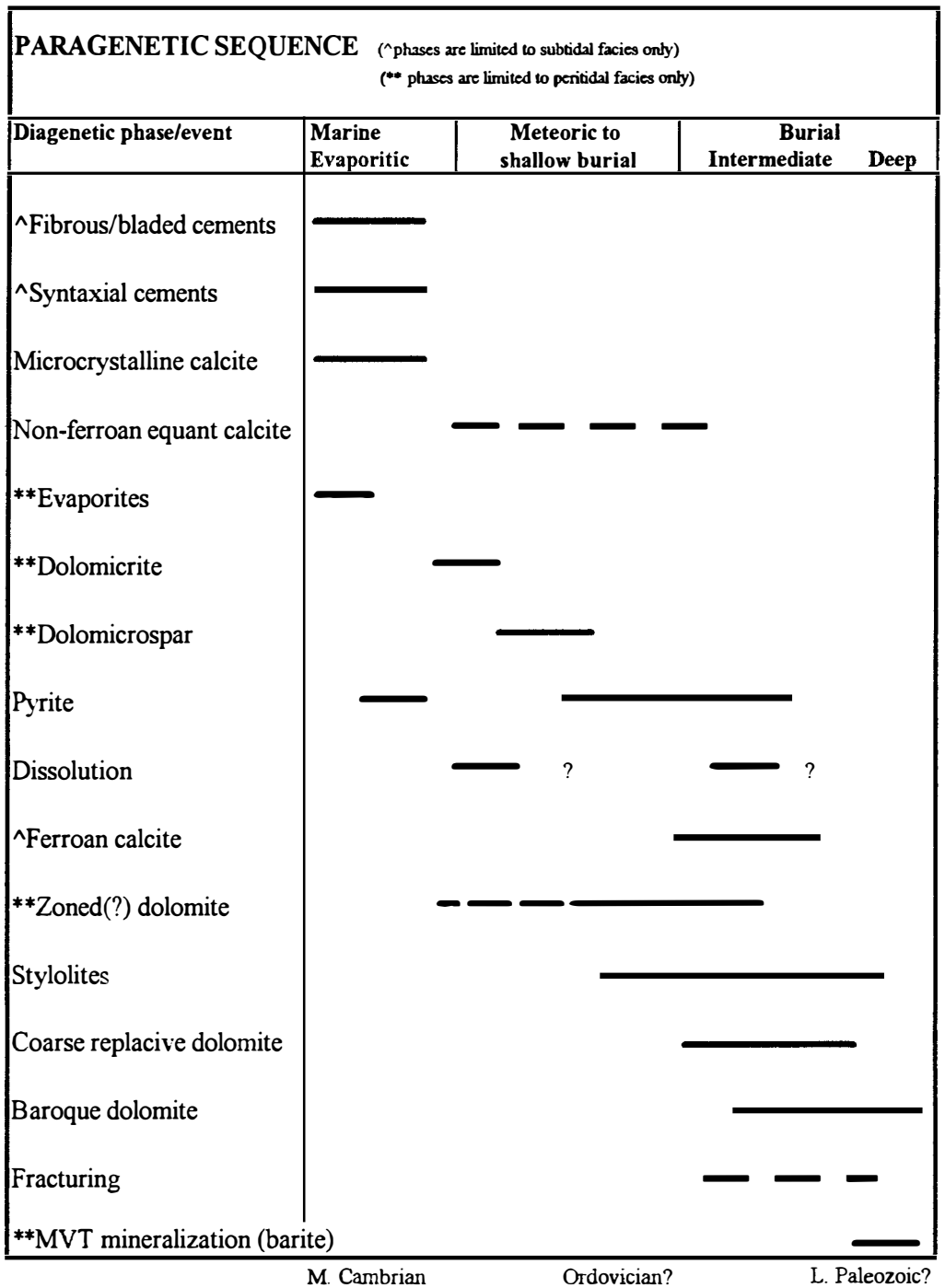
PARAGENETIC SEQUENCE
(^phases are limited to subtidal facies only)
(** phases are limited to peritidal facies only)
Diagenetic phase/event
Marine Evaporitic
Meteoric to shallow burial
Burial Intermediate
Deep
^Fibrous/bladed cements
^Syntaxial cements
Microcrystalline calcite
Non-ferroan equant calcite
**Evaporites
**Dolomicrite
**Dolomicrospar
Pyrite
Dissolution
?
?
^Ferroan calcite
**Zoned(?) dolomite
Stylolites
Coarse replacive dolomite
Baroque dolomite
Fracturing
**MVT mineralization (barite)
M. Cambrian
Ordovician?
L. Paleozoic?

formational boundary.

The information presented in this chapter should convey that diagenetic phases are a function of many factors, with initial depositional site being one of the most important. The time-sequential series of diagenetic events that comprise the paragenetic sequence are similar to depositional facies in general - they are not laterally extensive. Thus, superscript symbols represent phases that are limited to peritidal and subtidal facies of the Honaker and Nolichucky formations. It should also convey the importance of combining various geologic disciplines when trying to interpret diagenetic histories.

CHAPTER 4

CONCLUSIONS

1. The coeval (Middle Cambrian) Maryville and upper Honaker rocks in eastern Tennessee span a large geographic region. The results of this study relate well to the depositional model previously proposed by Maryville researchers and, thus, expand the Middle Cambrian Conasauga depositional model farther to the east/northeast. The results also allow for a better understanding of depositional and diagenetic controls for this portion of the Cambrian Conasauga Group.
2. The third order sequence boundary found in more westerly carbonates (top of Maryville Limestone, Srinivasan, 1993; or in the upper Maryville, Rankey, 1993) is also present further eastward within the upper Honaker Dolomite, where it is manifested by shoal facies overlying peritidal deposits. The backstepping platform/shelf of the Maryville (Rankey, 1993) is correlative with the ooid shoal facies of the upper Honaker, based on field and stratigraphic relationships. The subtle facies change that marks the sequence boundary within the upper Honaker is unique and, therefore, should influence sequence stratigraphy proponents to reconsider their longstanding concepts.
3. The basinal onlapping shale facies of the Nolichucky Formation in more easterly areas (Johnson City, Tennessee) suggest the intrashelf basin filled completely. This allowed for passive margin sedimentation to initiate during the Late Cambrian (Maynardville Limestone). It also means that the carbonate/shale contact near

Knoxville is older than the facies-similar carbonate/shale contact near Johnson City, based on platform architecture and direction of flooding.

4. This study is another example of how depositional settings and subsequent diagenetic alterations are linked. Marine, meteoric, and burial conditions have all imparted their signatures on the Middle Cambrian Honaker-Nolichucky formational boundary in northeastern Tennessee.
5. Subtidal thrombolite and intertidal shoal facies acted as barriers for the more interior portions of the Conasauga platform during the Middle Cambrian. This restricted marine setting allowed salinity levels to rise considerably based on the paucity of skeletal organisms and likely contributed to much of the penecontemporaneous dolomite found in the upper Honaker.
6. Rare evaporite molds and the abundance of penecontemporaneous dolomite imply a semi-arid climate for this part of the platform during the Middle Cambrian. Moreover, the paleolatitude for Honaker/Nolichucky deposition was similar to present day Bahamas - a typical analog for shallow marine carbonates.
7. Following the relative rise in sea level, which initiated a new phase of genetically-related carbonates (sequence boundary), restricted areas of the platform became open to fresh seawater. Salinity decreased to a range more suitable for invertebrate organisms as a result of the mixing waters during the latter part of the Middle Cambrian.
8. Petrographic observations, cathodoluminescence, and stable isotope geochemistry have revealed marine, meteoric, and burial diagenetic calcite and dolomite phases.

Petrographically, much of the dolomite formed early based on its relationship to early marine components such as evaporites and fenestrae. However, stable isotope compositions of these same samples reveal very negative $\delta^{18}O$ values. The discrepancy between petrographic observations and isotopic data indicates recrystallization and exchange with warm burial fluids.

9. Stable isotopic values form 2 generalized fields: low $\delta^{18}O$ dolomites and low $\delta^{13}C$ calcites. Dolomite compositions result from high temperatures related to burial following the Taconic Orogeny (Middle Ordovician) and calcite compositions likely result from meteoric fluids following uplift (Late Paleozoic).
10. This study shows the importance of synthesizing multi-disciplines (stratigraphic and field relationships, petrographic observations, cathodoluminescence, and stable isotopes) to better understand depositional and diagenetic relationships.

LIST OF REFERENCES

Aitken, J.D., 1967, Classification and environmental significance of cryptalgal limestones and dolomites, with illustrations from the Cambrian and Ordovician of southwestern Alberta: Journal of Sedimentary Petrology, v. 37, p. 1163-1178.

Badiozamani, K., 1973, The Dorag dolomitization model - application to the Middle Ordovician of Wisconsin: Journal of Sedimentary Petrology, v. 43, p. 965-984.

Boggs, S., Jr., 1987, Principles of Sedimentology and Stratigraphy: Merril Publishing Company, Columbus, Ohio, 784 p.

Bush, P., 1973, Some aspects of the diagenetic history of the sabkha in Abu Dhabi, Persian Gulf, p. 395-408, *in* Purser, B.H., ed., The Persian Gulf: Springer Verlag, Berlin, New York, 471 p.

Butts, C., 1940, Geology of the Appalachian Valley in Virginia, Part I: Virginia Geological Survey Bulletin, v. 52, pt. 1, 568 p.

Byerly, D.W., 1966, Structural geology along a segment of the Pulaski fault, Greene County, Tennessee: unpublished Ph.D. dissertation, University of Tennessee, 94 p.

Chafetz, H.S., 1973, Morphological evolution of Cambrian algal mounds in response to a change in depositional environment: Journal of Sedimentary Petrology, v. 43, p. 435-446.

Choquette, P.W., and James, N.P., 1987, Diagenesis in limestones - 3. The deep burial environment: Geoscience Canada, v. 14, p.3-35.

Chow, N. and James, N.P., 1992, Synsedimentary diagenesis of Cambrian peritidal carbonates: evidence from hardgrounds and surface paleokarst in the Port au Port Group, western Newfoundland: Bulletin of Canadian Petroleum Geology, v. 40, p. 115-127.

Cook, A.H.O, 1983, Diagenesis of the Maryville and upper Honaker Formations (Cambrian), Tennessee and Virginia: with emphasis on dolomitization and silicification: unpublished M.S. thesis, Duke University, Durham, 164 p.

Dalrymple, R.W., Narbonne, G.M., and Smith, L., 1985, Eolian action and the distribution of shales in North America: Geology, v. 13, p. 607-610.

Demicco, R.V., 1983, Wavy and lenticular-bedded carbonate ribbon rocks of the Upper Cambrian Conococheague Limestone, central Appalachians: Journal of Sedimentary Petrology, v. 53, p. 1121-1132.

Derby, J.R., 1965, Paleontology and stratigraphy of the Nolichucky Formation in southwest Virginia and northeast Tennessee: unpublished Ph.D. dissertation, Virginia Polytechnic Institute, 468 p.

Dickson, K.A.D., 1965, Modified staining technique for carbonates in thin section: Nature, v. 4971, p. 587.

Erwin, P.N., 1981, Stratigraphy, depositional environments, and dolomitization of the Maryville and the upper Honaker formations (Cambrian), Tennessee and Virginia: unpublished M.S. thesis, Duke University, Durham, 232 p.

Flugel, E., 1982, Microfacies Analysis of Limestones: Springer-Verlag (Berlin), 630 p.

Foreman, J.L., 1991, Petrologic and geochemical evidence for water-rock interaction in the mixed carbonate-siliciclastic Nolichucky Shale (Upper Cambrian) in east Tennessee: Unpublished Ph.D. dissertation, University of Tennessee, Knoxville, 228 p.

Friedman, I., and O'Neil, J.R., 1977, Compilation of stable isotope fractionation factors of geochemical interest: United States Geological Survey Professional Paper 440-KK, p. 1-12.

Gall, 1983, Ancient sedimentary environments and the habitats of living organisms: introduction to paleoecology: Springer-Verlag, Berlin, 219 p.

Glumac, B., 1997, Cessation of Grand Cycle deposition in the framework of passive margin evolution: controlling mechanisms and effects on carbonate deposition and diagenesis, Cambrian Maynardville Formation, southern Appalachians: unpublished Ph.D. dissertation, University of Tennessee, Knoxville, 380 p.

Hardie, L.A., 1977, Sedimentation on the Modern Carbonate Tidal Flats of Northwest Andros Island, Bahamas: The Johns Hopkins University Press, Studies in Geology No. 22. p. 178-183.

Hardie, L.A., 1987, Dolomitization: a critical review of some current views: Journal of Sedimentary Petrology, v. 57, p. 166-183.

Hardie, L.A., and Shinn, E.A., 1986, Carbonate depositional environments modern and ancient, part III: tidal flats: Colorado School of Mines Quarterly, v. 81, no. 1, 73 p.

Hasson, K.O. and Haase, C.S., 1988, Lithofacies and paleogeography of the

Conasauga Group, (Middle and Late Cambrian) in the Valley and Ridge province of east Tennessee: GSA Bulletin, v.100, no. 2, p. 234-246.

Hoefs, J.H., 1997, Stable isotope geochemistry, 4the ed.: Springer, 201 p.

James, N.P. and Choquette, P.W., 1983, Diagenesis 6. Limestones - The seafloor diagenetic environment: Geoscience Canada, v. 10, p. 162-179.

James, N.P. and Choquette, P.W., 1984, Diagenesis 9. Limestones - The meteoric diagenetic environment: Geoscience Canada, v. 11, p. 161-194.

Jernigan, D.R. and Walker, K.R., 1989, Carbonate cementation environments and products: an overview, *in* Walker, K.R., ed., The fabric of cements in Paleozoic limestones: University of Tennessee Studies in Geology Number 20, p. 11-18.

Kaufman, A.J., and Knoll, A.H., 1995, Neoproterozoic variations in the C-isotopic composition of seawater: stratigraphic and biogeochemical implications: Precambrian Research, v. 73, p. 27-49.

Kharaka, Y.K., and Thordsen, J.J., 1992, Stable isotope geochemistry and origin of waters in sedimentary basin, *in* Clauer, N., and Chaudhuri, S., eds., Isotopic Signatures and Sedimentary Records: Springer-Verlag, New York, p. 411-466.

King, P.B. and Ferguson, H.W., 1960, Geology of northeastern-most Tennessee: USGS Professional Paper 311, 136 p.

Koerschner, W.F., and Read, J.F., 1990, Field and modeling studies of Cambrian carbonate cycles, Virginia Appalachians - Reply. Journal of Sedimentary Petrology, v. 60, no. 5, p. 795-796.

Kozar, M.G., 1986, The stratigraphy, petrology, and depositional environments of the Maryville Limestone (Middle Cambrian) in the vicinity of Powell and Oak Ridge, Tennessee: Unpublished M.S. thesis, Univ. of Tennessee, Knoxville. 242 p.

Kozar, M.G., Weber, L.J., and Walker, K.R., 1990, Field and modeling studies of Cambrian carbonate cycles, Virginia Appalachians - Discussion: Journal of Sedimentary Petrology, v. 60, no. 5, p. 790-794.

Land, L.S., 1973, Holocene meteoric dolomitization of Pleistocene limestones, north Jamaica, *in* Longman, M.W., 1980, Carbonate diagenetic textures from near-surface diagenetic environments: American Association of Petroleum Geologists, v. 64, p. 461-487.

Land, L.S., 1985, The origin of massive dolomites: Journal of Geological Education, v. 33, p. 112-125.

Land, L.S., Salem, M.R.I., and Morrow, D.W., 1975, Paleohydrology of ancient dolomites: geochemical evidence: AAPG Bulletin, v. 59, p. 1602-1625.

Little, R.L., 1969, Lithostratigraphy and structural geology of a portion of the Dunham Ridge thrust block, Greene and Washington Counties, Tennessee: unpublished Ph.D. dissertation, University of Tennessee, Knoxville, 130 p.

Logan, B.W., Rezak, R., and Ginsburg, R.N., 1964, Classification and environmental significance of algal stromatolites: Journal of Geology, v. 72, p. 68-83.

Lohmann, K.C., 1982, Inverted J carbon and oxygen isotopic trends - criteria for shallow meteoric phreatic diagenesis: Geological Society of America Annual Meeting, Abstracts with Programs, p. 548.

Lohmann, K.C, and Walker, J.C.G., 1989, The $\delta^{18}O$ record of Phanerozoic abiotic marine calcite cements: Geophysical Research Letters, v. 16, p. 319-322.

Longman, M.W., 1980, Carbonate diagenetic textures from near-surface diagenetic environments: American Association of Petroleum Geologists, v. 64, p. 461-487.

Machel, H.G., and Burton, E.A., 1991, Factors governing cathodoluminescence in calcite and dolomite, and their implications for studies of carbonate diagenesis, *in* Barker, C.E., and Kopp, O.C., eds., Luminescence microscopy and spectroscopy: quantitative and qualitative aspects: SEPM short course 25, Dallas, Texas, p. 37-57.

Machel, H.G., Mason, R.A., Mariano, A.N., and Mucci, A., 1991, Causes and emission of luminescence in calcite and dolomite, *in* Barker, C.E., and Kopp, O.C., eds., Luminescence microscopy and spectroscopy: quantitative and qualitative aspects: SEPM short course 25, Dallas, Texas, p. 9-25.

Machel, H.G., and Mountjoy, E.W., 1986, Chemistry and environments of dolomitization - a reappraisal: Earth Science Reviews, v. 23, p. 175-222.

Markello, J.R., and Read, J.F., 1981, Carbonate ramp-to-deeper shale shelf transition of an Upper Cambrian intrashelf basin, Nolichucky Formation, southwest Virginia Appalachians: Sedimentology, v. 28, p.573-597.

Markello, J.R., and Read, J.F., 1982, Upper Cambrian intrashelf basin, Nolichucky

Formation, southwest Virginia Appalachians: AAPG Bulletin, v. 66, no. 7, p. 860-878.

Milici, R.C., 1973, The stratigraphy of Knox County, Tennessee: Tennessee Division of Geology Bulletin, v. 70, p. 9-24.

Narbonne, G.M., Kaufman, A.J., and Knoll, A.H., 1994, Integrated chemostratigraphy and biostratigraphy of the upper Windermere Supergroup (Neoproterozoic), Mackenzie Mountains, northwestern Canada: Geological Society of America Bulletin, v. 106, p. 1281-1291.

Oslegar, D.A. and Montanez, I.P., 1996, Cross-platform architecture of a sequence boundary in mixed siliciclastic-carbonate lithofacies, Middle Cambrian, southern Great Basin, USA: Sedimentology, v. 43, p. 197-217.

Ottinger, G.A., Dunagan, S.P., Foster, C.J., Glumac, B., and Walker, K.R., 1997, Depositional packages of the uppermost Honaker Dolomite and lower Nolichucky Formation (Middle Cambrian, Conasauga Group): Evolving carbonate sedimentation in a platformal to deep water setting. SE GSA, Geological Society of America Abstracts with Programs, v. 29, no. 3, p. 61.

Pugh, L.E., 1966, Geology along a portion of the Cross Mountain fault near Blountville, Sullivan County, Tennessee: unpublished M.S. thesis, University of Tennessee, Knoxville, 66 p.

Radke, B.M., and Mathis, R.L., 1980, On the formation and occurrence of saddle dolomite: Journal of Sedimentary Petrology, v. 50, p. 1149-1168.

Rankey, E.C., 1993, Carbonate platform response to tectonism and eustasy: the Middle Cambrian carbonates of the lower and middle Conasauga Group, east Tennessee: unpublished M.S. thesis, University of Tennessee, Knoxville, 191 p.

Rankey, E.C., Walker, K.R., and Srinivasan, K., 1994, Gradual establishment of Iapetan "passive" margin sedimentation: stratigraphic consequences of Cambrian episodic tectonism and eustasy, southern Appalachians: Journal of Sedimentary Research, v. 64, no. 4, p. 298-310.

Rasetti, F., 1965, Upper Cambrian trilobite faunas of northeastern Tennessee: Smithsonian Miscellaneous Collections, v. 148, 127 p.

Read, J.F., 1989, Controls on evolution of Cambrian-Ordovician passive margin, U.S. Appalachians: *in* Crevello, P.D., Wilson, J.L., Sarg, J.F., Read, J.F., eds., Controls on carbonate platform and basin development: SEPM Special Publication No. 44, p. 147-165.

Roberson, K.E., 1989, Meteoric cements, *in* Walker, K.R., ed., The fabric of cements in Paleozoic limestones: Studies in Geology 20, p. 54-65.

Rodgers, J., 1953, Geologic map of east Tennessee with explanatory text: Tennessee Division of Geology Bulletin, v. 58, 168 p.

Safford, J.M., 1856, A geological reconnaissance of the state of Tennessee: Nashville, State of Tennessee, 164 p.

Safford, J.M., 1869, Geology of Tennessee: Nashville, State of Tennessee, 550 p.

Sandberg, P.A., 1983, An oscillating trend in Phanerozoic non-skeletal carbonate mineralogy: Nature, v. 305, p. 19-22.

Scoffin, T.P., 1987, An introduction to carbonate sediments and rocks: Blackie, London, 274 p.

Sepkoski, J.J., 1982, Flat-pebble conglomerates, storm deposits, and the Cambrian bottom fauna, *in* Einsele, G., and Seilacher, A., eds., Cyclic and Event Stratification: Springer-Verlag, New York, p. 371-385.

Sibley, D.F., 1982, The origin of common dolomite fabrics: clues from the Pliocene: Journal of Sedimentary Petrology, v. 52, p. 1087-1100.

Simmons, W.A., 1984, Stratigraphy and depositional environments of the Middle Cambrian Maryville Limestone (Conasauga Group) near Thorn Hill, Tennessee: unpublished M.S. thesis, University of Tennessee, Knoxville, 275 p.

Srinivasan, K., 1993, Depositional history, sequence stratigraphy and diagenesis of Maryville Limestone (Middle Cambrian), southern Appalachians: unpublished Ph.D. dissertation University of Tennessee, Knoxville, 166 p.

Srinivasan, K., Walker, K.R., and Goldberg, S.A., 1994, Determining fluid source and possible pathways during burial dolomitization of Maryville Limestone (Cambrian), southern Appalachians, USA: Sedimentology, v. 41, p. 243-308.

Srinivasan, K. and Walker, K.R., 1993, Sequence stratigraphy of an intrashelf basin carbonate ramp to rimmed platform transition: Maryville Limestone (Middle Cambrian), southern Appalachians: GSA Bulletin, v. 105, p. 883-896.

Stefaniak, A., 1996, The stratigraphy and depositional history of the Middle Cambrian Rutledge Limestone, east Tennessee: Unpublished M.S. thesis, Univ. of Tennessee, Knoxville. 181 p.

Tobin, K.J., and Walker, K.R., 1994, Meteoric diagenesis below a submerged platform: implications for $\delta^{13}C$ compositions prior to pre-vascular plant evolution, Middle Ordovician, Alabama, U.S.A.: Sedimentary Geology, v. 90, p. 95-111.

Torsvik, T.H., Ryan, P.D., Trench, A., and Harper, D.A.T., 1991, Cambrian-Ordovician paleogeography of Baltica: Geology, v. 19, no. 1, p. 7-10.

Tucker, M.E., and Wright, P.V., 1990, Carbonate sedimentology: Blackwell Scientific Publications (Oxford), 482 p.

Walker, K.R., 1989, The fabric of cements in Paleozoic limestones: Ch. 1, Introduction. K.R. Walker, ed., University of Tennessee Studies in Geology Number 20. p. 1-3.

Walker, K.R., Foreman, J.L., and Srinivasan, K., 1990, The Cambrian Conasauga Group of eastern Tennessee: A preliminary general stratigraphic model with a more detailed test for the Nolichucky Formation: Morgantown, West Virginia, Appalachian Basin Industrial Associates, v. 17, p. 184-189.

Weber, L.J., 1988, Paleoenvironmental analysis and test of stratigraphic cyclicity in the Nolichucky Shale and Maynardville Limestone (Upper Cambrian) in central east Tennessee: Unpublished Ph.D. dissertation, University of Tennessee, Knoxville, 389 p.

Wentworth, C.K., 1922, A scale of grade and class terms for clastic sediments: Journal of Geology, v. 30, p. 377-392.

Wilson, S.M., 1979, Geology of the Fall Branch, Tennessee area: unpublished M.S. thesis, University of Tennessee, Knoxville, 80 p.

Woodward, H.P., 1949, Cambrian system of West Virginia: West Virginia Geological Survey Bulletin, v. 20, 317 p.

APPENDICES

Appendix A

Description of Measured Sections

Sample descriptions [column 3] are listed from the base to the top of the measured interval. The sample numbers [column 2] indicate the cumulative stratigraphic thickness above the datum. Multiple samples from a unit are designated by letters (i.e., 5a, 5b, 5c,...) [column 1]. This subdivision allows for better unit characterization as the samples change stratigraphically upwards. The datum is typically the base of the outcrop, but not always. A significant portion of the upper Honaker at the GD section is submerged. The datum here represents the first measurable carbonate bed stratigraphically above the submerged portion. The base of the Honaker Dolomite (Rome Formation contact) does not occur at any of the measured localities. Three outcrops were measured and sampled for this project:

I-81.....Interstate 81 near Johnson City, TN

GD.....Greeneville Dam

BL.....Blountville exit

Measurement Conventions

Bedding thickness

Thick bedded.....30-100 cm
Medium bedded.....10-30 cm
Thin bedded.....3-10 cm
Very thin bedded.....up to 3 cm

**Grain size* *(from Wentworth, 1922)*

Coarse-grained.....visible to the naked eye
Medium-grained.....identifiable only with a hand lens
Fine-grained.....identifiable with hand lens but difficult
Very fine-grained....grains indistinguishable even with hand lens

* Field descriptions have been supplemented with petrographic observations due to the fine-grained texture and pervasive dolomitization of the sediments.

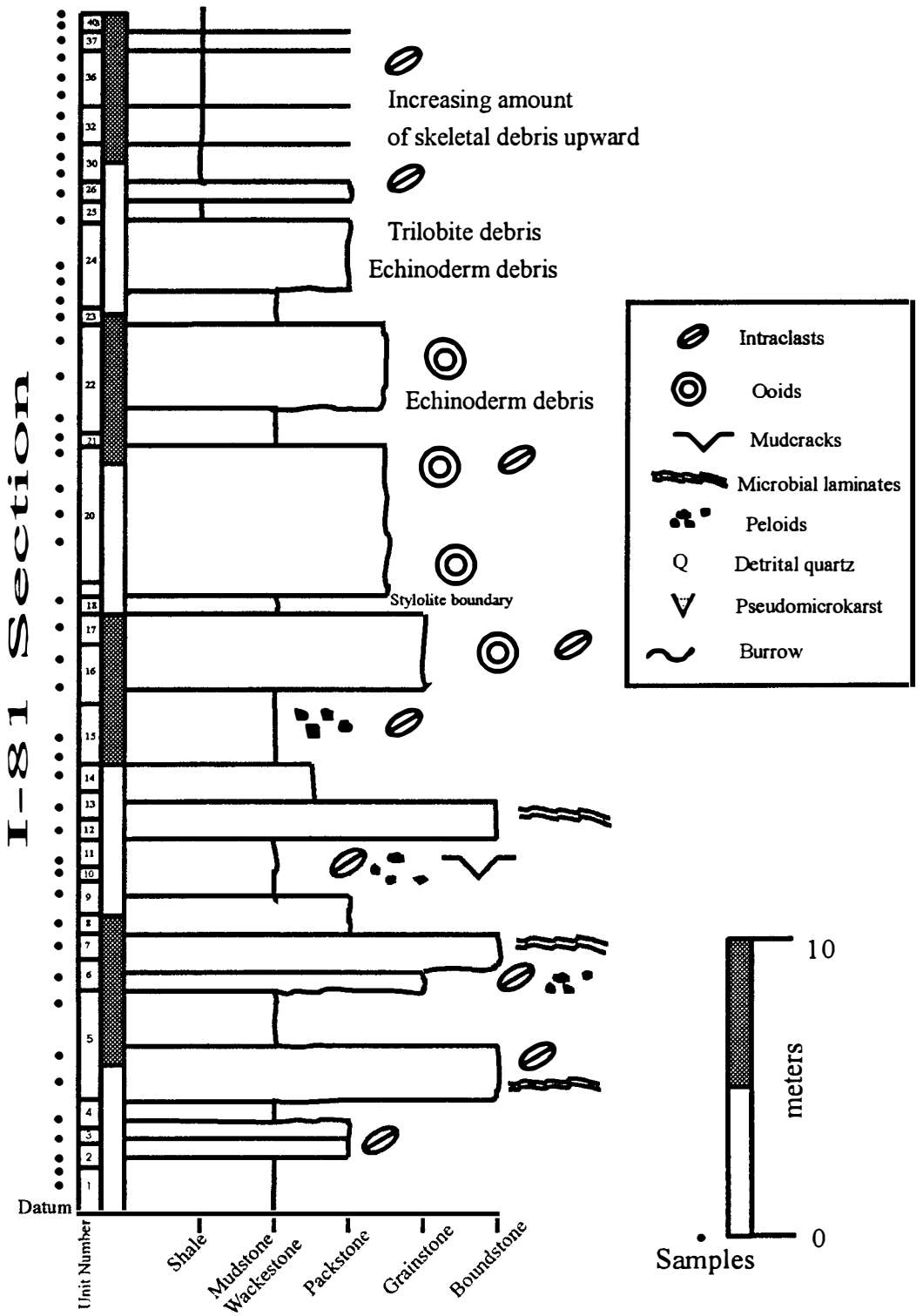
I-81 Section
Increasing amount
of skeletal debris upward
Trilobite debris
Echinoderm debris
Echinoderm debris
Stylolite boundary
Intraclasts
Ooids
Mudcracks
Microbial laminates
Peloids
Q Detrital quartz
Pseudomicrokarst
Burrow
10
meters
0
Samples
Datum
Unit Number
Shale
Mudstone
Wackestone
Packstone
Grainstone
Boundstone

I-81 Section

The I-81 section is one of the better Honaker/Nolichucky exposures in northeastern Tennessee. It serves as the "reference outcrop" to which the other exposures are compared and correlated. The outcrop is located on the eastern side of I-81 just north of the Fall Branch exit and south of the I-81/I-181 interchange in Sullivan County, Tennessee.

Unit Number	Cumulative Thickness (meters)	Description
		-Base of Honaker not exposed-
1a	.72	Dolomitized mudstone/algal mudstone. Sample has "clotted" texture similar to thrombolites. Porosity is intergranular for the most part with non-ferroan non-baroque dolomite infilling. Sample contains rare fractures and opaques. Sample 0.72.
1b	1.3	Dolomitized mudstone with rare peloids and/or intraclasts. Two distinct lithologies on either side of a bed parallel stylolite. Upper lithology is darker in color (more organic material) and contains less porosity. The dolomicrite is coarser compared to the lower lithology. The lower lithology is mud-rich as well but contains more porosity (vuggy, fenestral). These pores are predominantly filled with coarse crystalline dolomite. Hematite is also present in the lower lithology. The lower lithology has a more "clotted" texture similar to that of algal-rich lithologies. Sample 1.3.
2	1.8	Dolomitized intraclast packstone. Clasts vary in size, shape and color but are typically ~10 mm, subrounded, and brown. Also contains some peloids as well. Porosity in sample 1.8 includes fenestral, fractures, and vugs with turbid, yellowish non-ferroan non-baroque dolomite infilling. Hematite and opaques also occur. Appears to also possess laminations. Bed parallel stylolites also occur. Sample 1.8.

3	2.6	Dolomitized intraclast packstone. Clasts vary in size and shape but are typically 2-10 mm and angular. Matrix is very muddy (dolomicrite). Sample also contains some clay minerals as well as opaques. Fractures are rare. Sample 2.6
4	3.4	Dolomitized intraclast wackestone with predominantly angular clasts. Sample contains both ferroan and non-ferroan non-baroque dolomite as well as non-ferroan equant calcite. Brecciated in nonferroan calcite groundmass. Fractures and opaques are somewhat rare. Contains the most calcite compared to any other sample. Sample 3.4.
5a	4.6	Dolomitized intraclast wackestone. Degree of dolomiti--zation varies. Pores in sample 5.2 contain both ferroan and non-ferroan non-baroque dolomite. Sample also contains some rare opaques, stylolites, and fractures. Sample 4.6.
5b	5.5	Dolomitized algal laminated boundstone. Contains abundant intraclasts and peloids. Crystal size of dolomite comparable to dolomicrite/microspar. Fenestral porosity common with some vugs. Also contains framboidal pyrite or other iron oxides (hematite). Fractures are common as well as bed parallel and bed normal stylolites. Sample 5.5.
5c	7.4	Dolomitized mudstone with varying degrees of dolomitization. Very porous lithology consisting of vugs and bird's eye structures. Bed parallel stylolitization also common, as well as some fractures. Sample 7.4.
6	8.4	Dolomitized intraclast packstone. Dolomitization is coarser at the top of sample 7.5 compared to the bottom of the thin section. Peloids common. Porosity ranges from intergranular to fenestral. Sample contains a lot of organic material as well, especially near the stylolites. Fractures also occur. Sample contains some calcite also. Sample 8.4.
7	9.09	Dolomitized stromatolite boundstone. Layers contain abundant peloids. Fenestral porosity very common and filled with replacive dolomite (calcite). Fractures

		also present and filled with dolomite. Abrupt change in lithology at top of sample 8.65. Becomes more mud dominated and less algal laminated. Iron oxides also occur in a few places. Medium to thick bedded. Sample 9.09.
8	9.39	Coarsely dolomitized mudstone to intraclast wackestone with some intraclasts showing different textures for dolomitization. Some void filling cements have opaque boundaries. Coarse non-baroque dolomite also present in voids. Intraclasts vary in size (up to 3 mm). Peloids may (may not) be present. Dolomitization makes it difficult to determine for sure. Possible algal-derived intraclasts ?? Medium to thick bedded. Sample 9.39.
9	10.79	Abrupt change in lithology but no hardground or stylolite, etc. present. Faintly laminated. Dolomitized intraclast packstone. Upper lithology coarser-grained than lower lithology. Lower lithology intraclast wackestone (dolomitized?). Medium to thick beds. Sample 10.79.
10	11.49	Dolomitized mudstone with possible stromatolitic features at the bottom. Clay seams present. Brecciated areas filled with non-baroque dolomite (Fe or non-Fe?) near the top. Textural layering within sample gives appearance of LLH stromatolites ?? Horizontal burrows may be present as well. Medium to thick bedded. Sample 11.49.
11a	11.9	Coarse-grained dolomitized mudstone with in-situ brecciation at the top. Degree of dolomitization varies depending on host lithology. Unbrecciated portion has "chaotic" texture.....looks like dolomitized burrows?? Sample 11.9.
11b	11.9b	Abrupt change in lithology at stylolite. Dolomitized algal boundstone with peloids and intraclasts on the bottom; dolomitized peloid/intraclast packstone on top. In situ brecciation evident by translucent calcite cement. Lower lithology has desiccation feature filled with overlying sediment type. Degree of dolomitization increases upward. Intraclasts in upper lithology show evidence of

		compaction. In voids, dolomite is pore central. Medium to thick beds.
12	12.9	Dolomitized algal boundstone with micritic clasts (up to 1 mm). Crinkly, wavy appearance. Pores filled with equant calcite. Medium to thick bedded. Sample 12.9.
13	13.8	Dolomitized algal boundstone without laminations (thrombolite). Fenestral porosity ?? filled with equant calcite. Medium grained. Sample 13.8.
14	14.47	Medium-grained intraclast wackestone/packstone. Brownish gray on fresh surfaces. Intraclasts of algal origin. Clasts up to 3 cm long by 1.5 cm. Abrupt change in lithology. Upper lithology finer grained (intraclast wackestone). Sample 14.47.
15a	15.06	Fine-grained dolomitized mudstone with peloids common. Fenestral porosity with some fractures and intergranular as well. Dolomite is nonferroan. Sample 15.06.
15b	15.56	Thick bedded dolomitized peloid intraclast wackestone. Dolomite is very fine to fine grained. Dolomite is nonferroan. Some fractures and opaques present. Additional sample: 16.3. Stylolite contact between 16.3 and 17.8.
16a	17.86	Dolomitized burrow-mottled mudstone with peloids and intraclasts and/or ooids ?? Calcite-filled voids present. Medium-coarse grained dolomite – burrows are coarser grained. Bed-normal stylolite also present. Thick beds. Sample 17.86.
16b	18.5	Dolomitized mudstone / peloid ooid (?) intraclast wackestone. "Chaotic" texture and colors – burrow mottled ?? Dark shades of gray. Fractures very prominent and filled with equant calcite. Coarseness of dolomite changes depending on host lithology. Stylolites also common. Medium bedded. Samples: 18.5, 19.1..
17	19.6	Dolomitized intraclast ooid packstone/grainstone. Intraclasts vary in size (up to 5 mm long) but mostly smaller. Clasts also show micritic coatings on the

		outside edge. Medium to coarse grained dolomite. Dark gray in color. Medium bedded. Sample 19.6.
18	20.5	Dolomitized algal mudstone/boundstone. Abundant fenestrae filled with equant blocky calcite. Dolomitized burrows may also be present? Stylolites present. Dolomite is fine grained. What appears to be dolomitized burrows contain a clear, equant calcite rind. Dolomite coarsens upward in the thin section. Thin beds present. Sample 20.5
		------Stylolite contact----------
19	20.6	Dolomitized burrow-mottled mudstone. Dolomitized intraclasts also occur (coarse crystalline dolomite). Dark gray in color. Fractures filled with non-ferroan equant calcite. Evidence of non-ferroan calcite being replaced by dolomite on stained portion of slide. Hackly weathering, medium bedded. Sample 20.6.
20a	22.3	Dolomitized ooid packstone/grainstone. Ooids less than 1 mm in size. Stylolites present. Hackly weathering. Ooids have been micritized. Intraclasts scattered throughout – but predominantly all ooids in terms of grain type. Echinoderm grain or two also observed. Medium bedded. Sample 22.3.
20b	23.4	Medium to coarse grained dolomitized ooid grainstone with few intraclasts. Intraclasts contain ooids. The ooids show "more and less" micritization – some ooids possess a dolomite (clear) rind, some are all brown in color from micritization. Algal (thrombolite) clast also observed. Hackly weathering, medium beds occur. Sample 23.4.
20c	24.1	Dolomitized intraclast ooid grainstone. Medium to coarse grained dolomite. Intraclasts show red color from oxidation. These clasts contain micritic coats and may contain ooids. Stylolitization also present. Some ooids show more micritization than others – like sample 23.4. Medium bedded and hackly weathering. Samples: 24.1, 25.1, 25.4.

20d	25.23	Dolomitized ooid grainstone. Ooids have been micritized. Dolomite is medium-grained to coarse-grained. Contains grayish brown grains (algal clasts?) also. Some ooids are more dolomitized than others. Nice compressional features along stylolite (elephantine structure). Porosity predominantly intergranular with dolomite infill. Medium beds. Hackly weathering. Sample 25.23.
21	25.9	Dolomitized burrow-mottled mudstone. Dolomite ranges from fine to coarse grained. Fenestrae or evaporative vugs common. Ooids(?) and intraclasts (?) are rare. Vugs are filled with drusy calcite as well as some dolomite. Amber colored stains locally present (iron oxides?). Medium bedded. Hackly weathering. Sample 25.9.
22a	26.2	Dolomitized fossil intraclast ooid packstone/grainstone. Some clasts are red in color and up to 1 cm in length. Rare echinoderm fragments locally present. Dolomite is medium to coarse grained. Some clasts are multi-generational. Clasts possess a light colored rind. Stylolites also present. Rare syntaxial cement replaced by dolomite. Sample 26.2.
22b	27.9	Partially dolomitized ooid/oncoid(?) skeletal intraclast packstone/grainstone. Abundant echinoderm fragments and maybe a trilobite or two. Some syntaxial cements. Clasts are multi-generational. Dolomite is fine to coarse grained. Most of the skeletal grains have been dolomitized. Clasts range in size up to 1.5 cm long. Echinoderm grains have a dolomitized (and micritized) rind. Most skeletal grains have been micritized. Prominent bed parallel stylolite also occurs. Samples: 27.9, 28.5.
22c	29.2	Similar to previous samples (27.9, 28.5) except dolomite is fine to very coarse grained. Ferroan cements present. Dolomitization appears to be complete. The previous two samples showed more selective dolomitization. Bed parallel stylolites present. Skeletal grains have been micritized and dolomitized. Ooids appear to be less abundant then previous two samples. Medium bedded.

23	30	Dolomitized mudstone. Rare skeletal grains at the bottom of the thin section. Vugs within mudstone (evaporative in origin?). Ferroan cement phases occur. Opaques common. Vugs lie in a row across the bedding plane. Stylolites also present. Still medium beds but becoming less hackly weathering. Sample 30.
24a	30.6	Dolomitized skeletal intraclast packstone. Dolomite is medium to coarse grained. Some (rare) echinoderm fragments and trilobites. Pyrite present. Bed parallel stylolitization and fractures common. Clay seam at the top of the thin section. Ferroan cement phases, notably calcite present. Clay seam may be a finer grained (shaly) layer above one of the bed parallel stylolites. Occasional syntaxial cements. Thin to medium beds; less hackly weathering. Sample 30.6.
24b	31.0	Dolomitized skeletal intraclast packstone (echinoderms and trilobites). Stylolitization and clay seams common. Dolomite is fine to very coarse grained. Rare syntaxial cements . Calcite filled voids (clear). Cements are tan, yellow (amber) and clear – both appear to be calcite (?). This may simply be from micritization. Very fine grained at the top of the thin section. May be a lithologic change or simply a clay seam. Thin to medium beds. Sample 31.
24c	31.6	Dolomitized skeletal wackestone. Dolomite is fine to very coarse grained with different colors (clear to amber). Amber colored areas may be dolomitized peloids/intraclasts (?). Clay seams very common as well as fractures. Light green mineral also observed but rare (glauconite). Ferroan and non-ferroan cements. Upper most clay-rich part of the thin section shows laminations (interbedded shale(?) or just a clay seam). Opaque minerals also present.
	Nolichucky Formation ----------	
25	34.2	Dark greenish gray calcareous shale with thin, laminated limestone stringers. Stringers are discontinuous and seem to cross-cut bedding in places.

26	34.3	Intraclast packstone with skeletal fragments (trilobites, echinoderms, and brachiopods) and peloids. Clasts are tabular shaped (4 mm x 14mm average size). Contains a lot of dolomicrite (ferroan) and some non-baroque (ferroan) dolomite. Also contains non-ferroan and ferroan calcite and rare turbid syntaxial cements. Very rare specks of glauconite. Opaques are rare. Sample N2.
27	34.5	Greenish gray, platy shale with more continuous and thicker carbonate stringers. Shale layer is capped by wavy bedded limestone (N3)
28	34.6	Intraclast skeletal packstone. Similar fauna as N2 but appears to contain more skeletal allochems. Also contains ostracodes. Similar cement phases as in N2. Fractures present as well. Sample N3.
29	35.4	Greenish calcareous shale with carbonate stringers.
30	35.7	Intraclast skeletal packstone. Peloids common. Skeletal allochems consist of same fauna (trilobite, echinoderm, brachiopod, and ostracodes). Similar cement phases as N2 but also contains fibrous ferroan calcite and ferroan syntaxial cements. Dolomite is more ferroan. Clay seams also occur. Amber colored dolomite along fractures possibly from iron oxide leaching. Sample N4.
31	37.2	Greenish gray calcareous shale with intermittent carbonate stringers.
32	37.6	Thinly bedded greenish gray calcareous shale
33	37.7	Intraclast skeletal packstone consisting of echinoderm, trilobite, bryozoans, brachiopods, and ostracodes. Some intraclasts show sweeping laminations. Similar diagenetic phases as previous Nolichucky samples. Dolomite is ferroan (non-baroque). Amber colored dolomite common as well. Clay seam and fractures present as well. Sample N5.
34	37.82	Dark grayish green shale with few carbonate stringers. Capped by sample N6.

35	37.85	Intraclast skeletal packstone. Similar to N5 but contains framboidal pyrite and stylolitization is more prominent. Sample N6.
36	38.3	Dark grayish green calcareous shale with occasional carbonate stringers. Platy appearance.
37	38.7	Intraclast skeletal packstone. Similar to N6 but ratio of skeletal allochems to intraclasts has increased. Sample N7.
38	40.2	Yellowish gray green calcareous shale with platy or laminated beds. Few carbonate stringers are present in this interval. Capped by 15-20 cm gray limestone (sample N8).
39	41.7	Intraclast skeletal packstone. Similar to description for N7. Sample N8.
40	42.0	Calcareous shale with laminated bedding. Very few carbonate stringers occur here. Showing more and more evidence of deep water sedimentation from the change in dominant sediment type (carbonate to shale).

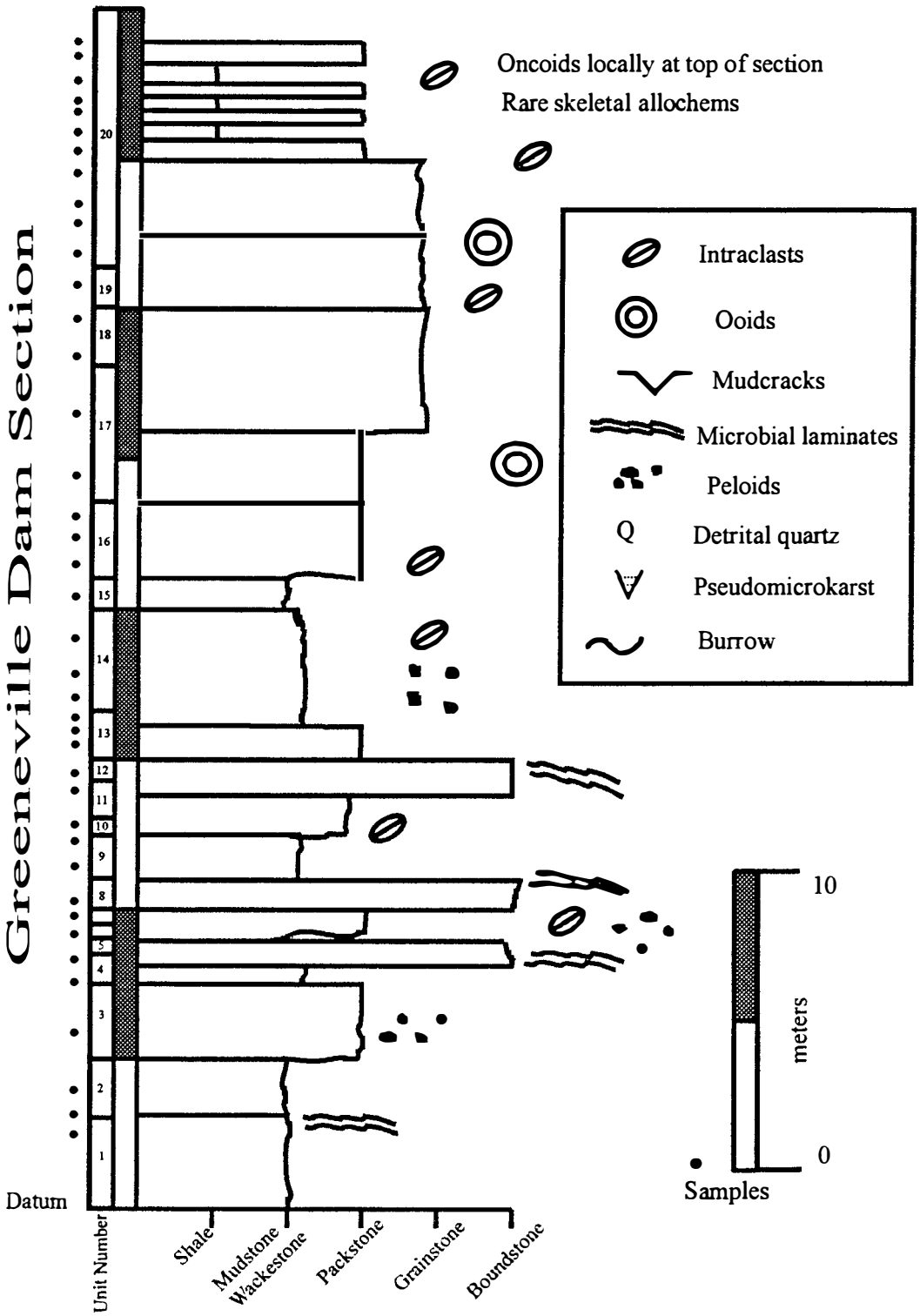
Greeneville Dam Section
Oncoids locally at top of section
Rare skeletal allochems
Intraclasts
Ooids
Mudcracks
Microbial laminates
Peloids
Q Detrital quartz
Pseudomicrokarst
Burrow
10
meters
0
Samples
Datum
Unit Number
Shale
Mudstone
Wackestone
Packstone
Grainstone
Boundstone

Greeneville Dam section

The Greeneville Dam section is another well exposed outcrop of the upper Honaker Dolomite. It only has indirect evidence of the overlying Nolichucky Formation, location of which is based solely on geomorphic expressions. The Upper Cambrian Maynardville Limestone occurs farther up section and is exposed fairly well. The outcrop is at the base of the Greeneville Dam on the Nolichucky River in Greene County, Tennessee along state road 70. Bedding at this locality is subvertical and outcrops occur along both sides of the river. The unexposed Nolichucky Formation has likely been eroded by the flowing water.

Bed Number	Cumulative Thickness	Description
		-Base of Honaker Dolomite not exposed at this locality. A significant interval of the upper Honaker is submerged at this locality. Measurements begin stratigraphically above the submerged area.
1	2.5	Dolomitized mudstone/stromatolitic boundstone to peloid wacke/packstone. Dark gray fine-grained dolostone. Variegated fresh surface with light colored patches in a darker groundmass. Light-dark areas occur bed parallel with an area at the top and bottom of sample. This color pattern has a stromatolitic texture. Abundant peloids. Medium bedded but thinly bedded in places. Sample 2.5.
2a	3.0	Dolomitized mudstone. Buff to medium gray fine grained dolostone. No bedding features present. Irregular array of buff patches with dark mineral(s) in center of patches. Fractures present as well. Medium bedded. Sample 3.0.
2b	4.0	Dolomitized algal (?) laminated mudstone. Dark gray fine grained dolostone. Faint laminations with darker gray 'stringers'. A zone of bed parallel geopetal structures also present. May be dissolved out intraclasts that have been partially infilled (?) or evaporitic vugs (?).

		Burrows may be present. Platy (barite?) mineral pore central. Medium bedded. Sample 4.0.
3	6.0	Dolomitized mudstone to peloid wacke/packstone. Dark gray, highly fractured fine grained dolostone. No bedding features observed. Clasts occur more in the top of sample. Peloids common. Medium bedded. Sample 6.0
4a	7.5	Dolomitized mudstone (algal boundstone?). Variegated medium-dark gray fine grained dolostone. Not as fractured as 6.0. Faint wavy laminations present. Also, bed parallel stylolites present. Occasional circular birdseye structure. Medium to thick bedded. Sample 7.5.
4b	8.3	Dolomitized laminated intraclast wackestone/algal boundstone. Medium gray fine grained dolostone with crinkly laminations. Even less fractures than 7.5. Laminations become deformed stratigraphically upward. Bed parallel stylolites also present. Stylolitization may have mimicked original laminations. Opaque minerals common. Medium to thick bedded. Sample 8.3.
5	8.7	Dolomitized boundstone. Tan to medium gray fine grained dolostone. Highly fractured unit. Numerous bed parallel stylolites. Sample contains a 'center' of fresh gray dolostone with large halo of light brown altered dolostone. Faint laminations are present (wavy form). Also contains dark specks which may be organic material. Medium bedded. Sample 8.7.
6	9.0	Dolomitized mudstone. Medium gray fine grained dolostone with less fractures than 8.7. Unit also appears to be not as altered as 8.7 as well. Sample contains wavy laminae with bed parallel stylolites. Laminae near the top appear sweeping and semi-circular. One large vug (1 cm) also present with coarse non-ferroan non-baroque fill. Intraclasts occur within one of the fractures. Desiccation at top of sample. The coarser grained muds within this sample may be dolomitized burrows (?). Thinly bedded. Sample 9.0.
7	9.8	Change in lithology. Dolomitized intraclast

		wackestone/packstone and mudstone to intraclast peloid packstone. Medium gray on fresh surfaces. Minimal fractures. Lower lithology is alternating light (tan) and dark beds with concentrated areas of intraclasts. Change occurs at bed parallel stylolite. Upper lithology is coarser with no observable bedding features. Intraclasts present as well. Opaque minerals and bed normal stylolites are rare. Thin to medium beds present. Sample 9.8.
8	10.1	Dolomitized algal boundstone. Variegated light brown to gray fine grained lithology with wavy laminations. Laminae are bed parallel for the most part except below a bed parallel stylolite where laminae appear imbricated and inclined. Large intraclasts (approximately 4mm) are also observed. Peloids common within laminae. Clay seams and fractures also occur. Thin to medium bedded. Sample 10.1.
9a	11.6	Dolomitized mudstone. Buff to light gray colored fine grained dolostone. Minimal bedding features within sample. Bed parallel stylolite or clay seam present. Opaque mineral within one of the voids. Sample 11.6.
9b	12.5	Dolomitized mudstone. Medium to dark gray medium grained dolostone. Fenestrae present as well as patchy zones of different gray dolomite (dolomitized burrows?). Intraclasts occur in lighter colored areas. Clasts may be *Renalcis* grains or just different micrite-rich grains. Bed parallel stylolites also occur within sample. The patchy areas of different gray hues may be large clasts? Thin to medium bedded. Sample 12.5.
10	12.7	Dolomitized algal boundstone. Buff to light gray fine grained dolostone. Very similar to 10.1. Wavy laminae with speckled texture. Peloids and/or intraclasts present between the laminae. Fractures as well as iron oxides present. Additional sample: 12.8; similar to 12.7 except for the occurrence of some bed parallel stylolites. Medium bedded. Sample 12.7.
11	14.0	Dolomitized mudstone to intraclast wackestone at the top. Light to dark gray and tan in color. Fractured fine grained dolostone. Tan portions rimmed by dark gray

		areas. Occasional tan zone crosscuts normal to the darker gray rim into another tan zone. Opaques also present within tan areas. Fractures common. Clay seams and bed normal stylolites present also. Vuggy porosity. Hackly weathered, medium bedded. Sample 14.
12	14.5	Dolomitized algal boundstone. Light gray crinkly (wavy) laminated fine grained dolostone. Both bed parallel and bed normal stylolites present. Fenestral fabric with zones of dark specks also occur. Fractures and iron oxides common. Thin to medium bedded. Sample 14.5.
13a	15.4	Burrowed intraclast peloid packstone/wackestone. Medium gray dolostone. Approximately 1 cm intraclasts at base of sample extend up to a bed parallel stylolite. Intraclasts occur above the stylolite but are smaller. Large patches of calcite fill within dolomitized medium-coarse grained rock. Karst cavity also present above lower stylolite. Burrows may also occur in areas where dolomite is coarser grained. Medium bedded. Stylolites common. Sample 15.4.
13b	16.1	Dolomitized intraclast wackestone. Light gray fine grained dolostone with intraclasts in the upper part of sample. Fractures present. No other bedding features. Medium bedded. Sample 16.1.
13c	16.4	Dolomitized intraclast packstone. Light to medium gray coarsening upward fine to medium grained dolostone. Distinct lithologic change at the top of sample. One mud-rich layer present showing desiccation. Baroque dolomite present as well as iron oxides. Vuggy porosity in lower part of sample. Quartz silt dispersed throughout. Medium bedded. Sample 16.4.
14a	16.9	Dolomitized intraclast wackestone. Medium gray fine to medium grained dolostone with no observable bedding features. Dark intraclasts common as well as circular dolomitic vugs. Fractures and stylolites present. Also contains a platy, high birefringent mineral (barite?). Thin to medium bedded. Sample 16.9.
14b	17.8	Dolomitized intraclast wackestone. Medium gray fine to

		coarse grained dolostone with vuggy texture. Color is somewhat variegated and irregular (tan to medium gray). Intraclasts present. These may account for the irregular color zones. The sample may also contain framboidal pyrite. Thin to medium bedded. Sample 17.8.
14c	19.0	Dolomitized intraclast wackestone/packstone. Light to medium gray fine to medium grained dolostone with no observable bedding features. Fractured lithology with ferroan and non-ferroan equant calcite around clasts. Stylolites common as well. Clasts show some compressional features. Thin to medium bedded. Sample 19.
15	20.5	Dolomitized burrow-mottled mudstone. Medium to dark gray medium to coarse grained dolostone with no observable bedding features. Sample shows calcite infilled fractures. Variegated color also (like 17.8). Dark peloids/intraclasts also present locally. Coarse dolomite infills the burrows. Bed normal stylolites and fractures also present. Thick bedded. Sample 20.5.
16a	21.4	Ooid (?) intraclast packstone. Similar to 20.5. Medium to coarse grained dolostone with more observable intraclasts than 20.5. Intraclasts concentrated in patches. Fractures present. Dominant grain type may not be exclusively intraclasts: ooids may also be present. Dolomitization makes this distinction difficult. Thick bedded. Sample 21.4.
16b	22.7	Dolomitized intraclast packstone. Medium to dark gray medium to coarse grained dolostone with no observable bedding features. Intraclasts very common and range in size. Calcite-infilled fractures with some karst vugs also occur. *Renalcis*(?) grains rare. Thick bedded. Sample 22.7.
16c	23.3	Dolomitized ooid packstone. Light to medium gray medium - coarse grained dolostone. Dolomitization is so pervasive that grain identification is difficult. Bed parallel stylolites are rare. Rare opaque minerals/grains. Fractures common and filled with non-baroque and sparse baroque dolomite. Thick bedded. Sample 23.3.

17a	24.1	Dolomitized ooid (?) packstone. Light to medium gray medium to coarse grained dolostone. Same problem as 23.3 with pervasive dolomitization. Dominant grain type appears to be ooids. Size, shape, and color of the circular grains differ. Fractures also present with calcite infill; some portions dissolved out. Bed parallel stylolites present. Above stylolite, dolomite is coarser grained; below stylolite, dolomite is finer grained. Thickly bedded and pitted in the field. Samples: 24.1,24.8, 25.4.
17b	26.3	Dolomitized intraclast ooid packstone. Medium to thick bedded. Light to medium gray medium to coarse grained dolostone. Sample vuggy in appearance. Coarsest dolomite crystals occur in patchy array – possibly burrows (?). In vugs, dolomite is very turbid (tan) pore central with a translucent rim along the pore wall. Clasts are multi-generational. Rare skeletal grains (echinoderms). Samples: 26.3, 26.7.
18a	27.4	Dolomitized ooid intraclast wackestone. Light to medium gray medium-coarse grained dolostone with no observable bedding features. Fractures and stylolites present. Intraclasts are the dominant grain type however ooids also occur but in random patches. Sample has vuggy texture but more prevalent compared to 26.7. Dolomite infill more prominent as well. Coarser dolomite areas may be burrows? Sample 27.4.
18b	30.3	Dolomitized ooid intraclast packstone. Light medium gray medium grained dolostone with ooids and intraclasts. Intraclasts differ in size, shape, and color. Bed normal stylolitization present. Clasts are multigenerational and poorly sorted. No other bedding features observed. Sample 30.3.
18c	30.7	Dolomitized intraclast ooid packstone/grainstone. Light to medium gray medium grained dolostone with no observable bedding features on fresh surfaces. Differing texture fabrics on weathered surfaces. Areas of positive relief are dark, fine grained patches with coarser material around them. Some intraclasts but predominantly ooids. Bed parallel stylolites present as well. Sample 30.7.
19	31.0	Dolomitized intraclast wackestone/packstone. Light to

		medium gray medium grained dolostone with limited observable bedding features. Weathered texture similar to 30.7. A thin layer of buff material is present near the bottom of the sample. Quartz grains. Sample coarsens upward. Medium bedded. Some grains show compressional features. Rare opaque minerals/grains. Fractures present. Sample 31.
20a	32.3	Dolomitized intraclast ooid packstone. Medium gray medium to coarse grained dolostone with mottled or variegated colors on fresh cuts. Lumpy weathered fabric similar to 30.7 also. Circular grains present (ooids(?), intraclasts). Fractures and bed normal stylolites also present. Beds becoming more hackly weathered, thicker bedded. Sample 32.3.
20b	32.9	Dolomitized intraclast packstone. Light to medium gray medium to coarse grained dolostone with circular grains (ooids and/or intraclasts?). Fractures present. Fenestral or cement filled voids also present. Medium bedded. Sample 32.9.
20c	33.5	Dolomitized intraclast ooid packstone. Medium gray medium grained dolostone with no observable bedding features. Intraclasts and/or ooids present. Fractures also occur. Sample also contains mineral with metallic luster (pyrite?). Bed parallel and bed normal stylolitization also evidenced. Sample 33.5.
20d	34.4	Dolomitized intraclast/ooid packstone. Light to medium gray coarse grained dolostone with vast intraclasts/ooids. Clasts visible without hand lens, are well rounded, and poorly sorted. The sample contains areas where clasts are more visible (crystalline matrix versus mud-rich matrix). Clasts are multi-generational. Medium bedded. Sample 34.4
20e	35.2	Dolomitized ooid/intraclast packstone/grainstone. Medium dark gray medium to coarse grained dolostone with 2 distinct lithologies. Lower type is variable grained with wavy laminations (clay seams) and coarser (silty?) material together. It is typically darker than overriding lithology. Lower lithology contains both intraclasts and ooids. Contact between both lithologies is sharp. Upper

		lithology is fractured, cement void-filled, and contains intraclasts/ooids. Color is somewhat mottled in upper lithology. Fractures present. Some grains show compressional features as well. Sample 35.2.
20f	35.8	Dolomitized intraclast peloid packstone. Light to medium gray medium grained dolostone with large polymictic intraclasts. Fractures also present. Amber to reddish dolomite areas also appear. At the top of the sample, "teepee" structures occur within bedding. Both bed normal and bed parallel stylolites occur as well as compressed grains. Sample also contains fractures. Thin to medium bedded. Sample 35.8.
20g	36.0	Dolomitized intraclast ooid packstone. Medium to dark gray medium grained dolostone with ooids and intraclasts. Clasts easily visible on fresh and weathered surfaces. Large clasts appear scattered throughout sample. Clasts are dark with black rind on weathered surface. Sample contains both bed normal and bed parallel stylolites as well as fractures. Thick bedded. Sample 36.
20h	36.4, 36.6	Dolomitized intraclast packstone interbedded with shale. Light to medium gray and brown medium grained dolostone with increasing percentage of shale stratigraphically upward. Clasts differ in size, shape, and color. Smaller clasts infill around larger clasts. Compressional sutures also present (bed parallel and bed normal). Medium bedded with thin interbeds. Intraclasts are up to 2 cm in length. Clay seam separates samples 36.4, 36.6.
20i	37.0	Dolomitized intraclast packstone interbedded with shale. Medium gray medium grained dolostone with wavy appearance. Intraclasts are abundant with size, shape, and color varying. Sample contains patches of cement-filled voids. Bed parallel compressional sutures also present. Pitted on weathered surface. Clay seams are common within sample. Barite(?) may also occur as a pore central filler. Thick bedded. Sample 37.
20j	38.3	Dolomitized intraclast packstone. Light gray to buff fine

to medium grained dolostone with variegated color on fresh cut. Intraclasts vary in size, shape, and color. Shaly interbeds are rare. Fractures and compressional sutures (mostly bed parallel) are present. Contains a central zone of concentrated intraclasts. Barite (?) may also occur. Few skeletal grains are present. Sample also contains opaque minerals along substrates. Medium bedded. Sample 38.3.

20k 38.7 Dolomitized intraclast packstone interbedded with shale. Light gray, buff, medium gray coarse grained dolostone with wavy appearance. Intraclasts are abundant with differing size, shape, and color. The sample contains reddish oxidized minerals as well. Oncoids seen in the field, however none appear in the sample. Rare echinoderm fragments also present. Fractured lithology. Medium bedded. Sample 38.7.

Contact with the Nolichucky Formation not directly observed at this locality. Evidenced only by a geomorphic expression along the river bank. This is characterized by a significant cut-back into the landscape. This area is now the site of a parking lot for boaters and visitors to the dam. The flow of water from the dam likely contributed to erosion of the Nolichucky at this locality. Carbonate beds of the Upper Cambrian Maynardville Formation can be seen adjacent to the dam just up-section from the parking lot.

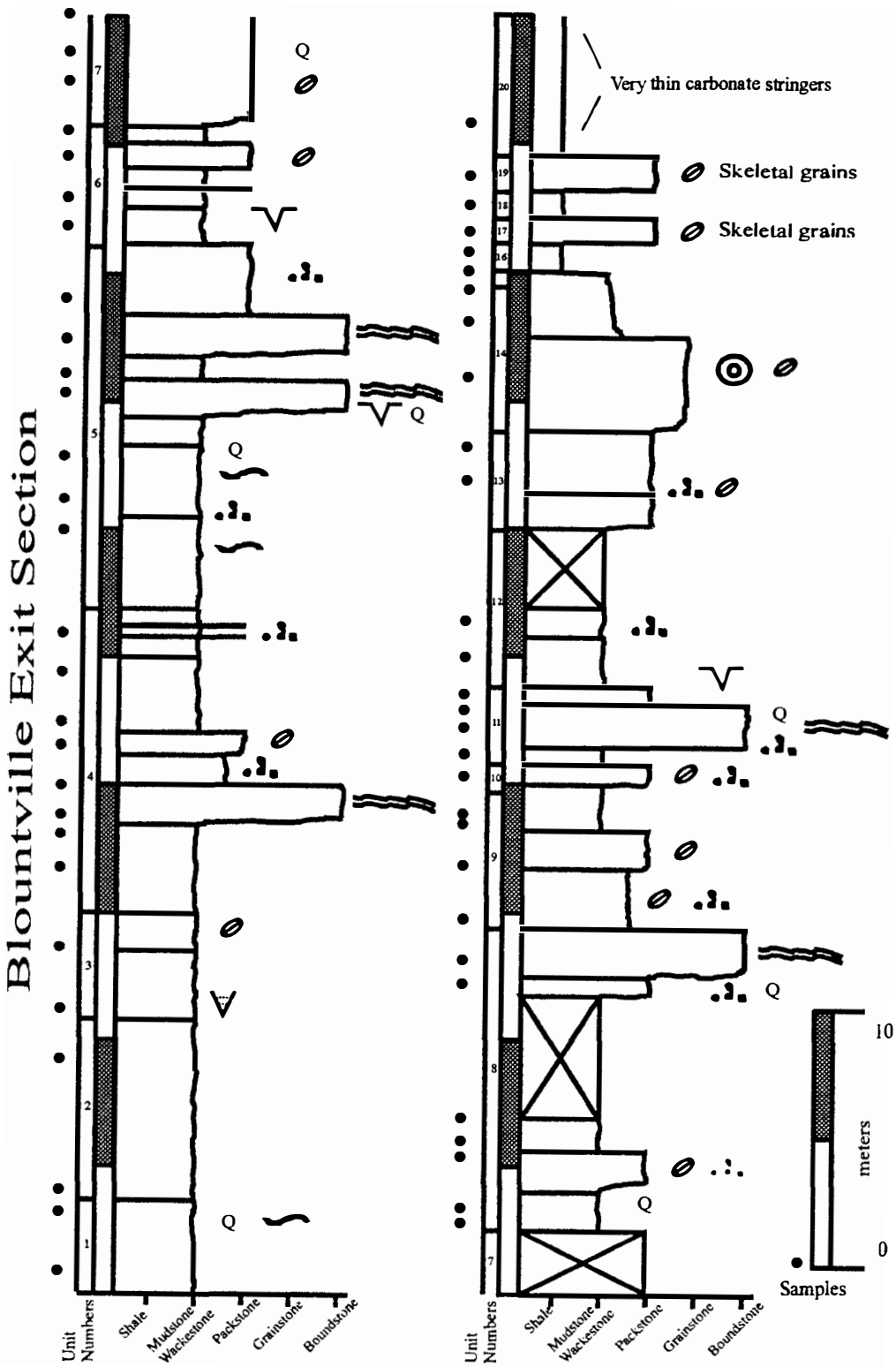
Blountville Exit Section
Very thin carbonate stringers
Skeletal grains
Skeletal grains
Q
meters
10
0
Samples
Unit Numbers
Shale
Mudstone
Wackestone
Packstone
Grainstone
Boundstone

Blountville Exit section

This outcrop was probably deposited farthest on-platform compared to the other two sections. Lower portions of the Honaker Dolomite as well as the overlying Nolichucky Formation are exposed at this locality. The outcrop is well exposed on the southbound side of I-81 along the exit ramp. Strata at this locality are oriented subvertically.

Bed Number	Cumulative Thickness	Description
1a	1.0	Buff to medium gray very fine grained mudstone to peloid packstone. Lenticular bedded limestone composed of non-ferroan calcite. Medium to thick bedded. Late fractures filled with non-ferroan baroque dolomite and some non-ferroan calcite. Darker portions are mudstone and lighter areas are peloid-rich. Sample 1.
1b	4.0	Medium to dark gray very fine grained dolomitized mudstone with layer detrital quartz. Laminated. Escape burrows present. Dolomite is nonferroan to weakly ferroan. Rare fenestral porosity. Bed parallel stylolites common. Some intraclasts also. Very organic-rich sample. Sample 4
2a	4.3	Medium gray very fine grained dolomitized mudstone. Laminated. Rare fenestral porosity but quite vuggy. Vugs filled with weakly ferroan calcite. Fractures common as well as bed parallel stylolites. Opaques speckled throughout sample. Rare intraclasts at base of sample. Sample: Base 2 (4.3).
2b	9.1	Medium to dark gray very fine grained dolomitized mudstone. Brown zones around porous areas of sample. Dolomite is non-ferroan. Sample shows some soft sediment deformation. Opaque mineral/grains common. Organic material (?) common as well parallel to bedding. Sample 9.1.
3a	11.3	Buff to medium gray coarse grained dolomitized

		mudstone (?). No observable allochems but dolomite crystal size may have obliterated any present. Non-ferroan dolomite is planar to non-planar and turbid. Hand sample looks like pseudomicrokarst based on morphology of fill. Abundant clays (?) along crystal boundaries Thick, hackly weathered beds. Sample 11.3.
3b	13.9	Buff to medium gray dolomitized intraclast wackestone and mudstone. Fractures very common as well as vugs. Fractures contain both calcite and dolomite whereas vugs are strictly dolomite. Abrupt lithologic change from intraclast wackestone to mudstone. Thick, hackly weathered beds. Sample 13.9
4a	16.8	Buff to light gray coarse grained dolostone. Any allochems are indistinguishable. Dolomite is predominantly non-ferroan baroque and very turbid. Some crystals are bladed to equant in morphology – possibly replaced calcite. Clay residue is common around crystal boundaries but not as much as BL 11.3. Thick, hackly weathered beds. Sample 16.8.
4b	17.9	Buff to light gray dolomitized mudstone. Non-ferroan non-baroque dolomite ranges from very fine to coarse grained. Bed parallel stylolites very common as well as fractures. Turbid dolomite. Also contains a few intraclasts. Thickly bedded.
4c	18.8	Alternating buff and light gray dolomitized microbial laminated boundstone. Very fine to coarse grained. Very wavy, crinkly laminations. Dolomite is non-ferroan and non-baroque. Fractures common with iron oxides and clay lining them. Distinct late fractures possess non-ferroan equant calcite. Opaque mineral/grains rare. Thick bedded. Sample 18.8.
4d	20	Medium to dark gray dolomitized peloid/intraclast wackestone/packstone. Dolomite is very fine to coarse grained and both non-ferroan planar and saddle morphologies are present. Fractures and stylolites common. Opaque mineral/grains rare. The predominant allochems occur in zones rather than evenly spread throughout the sample. Thick, hackly weathered beds. Sample 20.

4e	21.8	Medium to dark gray dolomitized intraclast packstone. Dolomite is very fine to coarse grained (non-ferroan). Fractures common and infilled with calcite. Clasts appear to be algal in origin. Thick bedded. Sample 21.8.
4f	22.5	Buff to medium gray dolomitized mudstone (?). Fractures and stylolites common. Dolomite is non-ferroan. Opaque minerals/grains rare (framboidal pyrite). Thick bedded. Sample 22.5.
4g	24.7	Light to medium gray dolomitized mudstone with faint sweeping laminations. Early fractures rare and filled with peloids and intraclasts. Dolomite is non-ferroan and very fine grained. Stylolites and late fractures common. Thick bedded. Sample 24.7.
4h	26	Similar to 24.7 but coarser and no laminations. Thick bedded, light to medium gray dolomitized alternating mudstone and peloid packstone. More porous than 24.7 as well with fenestral being the dominant type. Dolomite is very fine grained (non-ferroan, non-baroque). Stylolites and fractures common. Opaque minerals/grains rare. Non-ferroan calcite in fractures is being replaced by dolomite. Medium to thick bedded. Sample 26.
		Siliceous (?) nodules in field between 26 and 30.
5a	30	Medium to dark gray dolomitized mudstone with cross laminations. Quartz silt sparse. Escape burrow with soft sediment deformation in sample. Fracturing along stylolites common in sample. Numerous events of truncation present. Dolomite is very fine grained and non-ferroan. Medium to thick bedded. Sample 30.
5b	31.3	Medium to dark gray dolomitized mudstone with peloid/intraclast packstone intervals. Evidence of soft sediment deformation (escape burrow?) infilled with quartz silt and peloids/intraclasts. Relative percentage of quartz has increased from samples 30 to 31.3. Late fractures contain equant non-ferroan calcite being replaced by ferroan calcite and dolomite. Opaque

		minerals/grains rare. Medium to thick beds. Sample 31.3.
5c	33	Similar to 31.3. Escape burrow more pronounced. Sample 33.
5d	35.3	Buff to light gray dolomitized mudstone and algal boundstone. Medium bedded. Mudstone shows desiccation with quartz silt infilling. Quartz silt in even greater amounts compared to previous samples. Quartz abundant in microbial laminations as well. Dolomite is very fine grained and non-ferroan. Some fenestral porosity with non-baroque dolomite. Opaque minerals/grains common. Sample 35.3.
5e	36.2	Buff to tan dolomitized mudstone. Thin to medium bedded. Mudstone possesses onlapping layers which indicate previous scour and later infill. Dolomite is very fine grained and non-ferroan. Opaque minerals/grains rare. Sample 36.2.
5f	37.7	Very similar to 26. Light to medium gray algal laminated boundstone with fenestral porosity common. Medium bedded. Stylolites and fractures present. Quartz silt is minimal but peloids are quite prevalent. Dolomite is very fine grained and non-ferroan. Opaque minerals/grains rare. Sample 37.7.
5g	38.3	Medium gray dolomitized peloid packstone. Thin bedded. Dolomite is fine to medium grained. Opaque minerals/grains common. Fractures. Dolomite is non-ferroan and non-baroque. Sample 38.3.
6a	42	Light to medium gray dolomitized mudstone. Thick bedded. Vuggy. Varying degrees of coloration in random patterns. Looks similar to enterolithic structure (?). Sample 42.
6b	42.9	Light to medium gray dolomitized mudstone and intraclast packstone. Thin bedded. Mudstone shows persistent and severe desiccation. Some of the overlying intraclasts look similar to this lithotype. Very rare detrital quartz grains. Clasts vary in size, shape, and morphology – poorly sorted. Dolomite is non-ferroan,

		non-baroque and porosity is either fracture of intergranular. Iron oxides along fractures. Opaque minerals/grains rare. Sample 42.9.
6c	44.5	Buff to light gray dolomitized mudstone/intraclast wackestone. Thin bedded. Dolomite is fine to medium grained and non-ferroan. Fractures common with iron oxide stains. Opaque minerals/grains rare. Clasts vary in size and shape – poorly sorted. Sample 44.5.
6d	46	Very similar to 44.5 but strictly dolomitized mudstone. Sample 46.
7a	47.5	Buff to medium gray dolomitized intraclast packstone. Thick bedded. Dolomite is very fine grained, non-ferroan, with both planar and saddle morphologies. Stylolites common between intraclasts. Opaques rare. Fractures rare. Clasts average 15 mm in size.
7b	48.7	Medium gray dolomitized intraclast packstone. Medium bedded. Abundant quartz detritus, poorly sorted. Some quartz grains are too large to be wind blown - likely storm deposits. Dolomite is very fine grained (non-ferroan). Framboidal pyrite present. Stylolites and fractures rather common. Fractures filled with non-ferroan planar non-baroque dolomite. Sample 48.7.
7c	50.2	Buff to light gray dolomitized microbial boundstone. Thin bedded. Fenestrae common. Wavy texture. Dolomite is very fine to medium grained and non-ferroan, non-baroque. Some layers show desiccation. Bed parallel stylolites and fractures common. Sample 50.2.
		Covered interval from 50.2 – 52.3.
8a	52.3	Medium gray dolomitized mudstone with faint current-generated laminations. Some quartz silt (very rare). Stylolites occur with fractures cross-cutting. Dolomite is very fine grained. Opaque minerals/grains rare. Thick, hackly weathered beds. Sample 52.3.
8b	53.8	Medium gray dolomitized mudstone with faint

		laminations but more obvious than previous sample. Quartz detritus occurs in bands or layers that are normally graded (storms?). Evidence of soft sediment deformation. Dolomite is very fine grained and non-ferroan. Bed parallel stylolites and fractures present. Opaque minerals/grains rare. Thick, hackly weathered beds. Sample 53.8.
8c	55.2	Buff to light gray dolomitized peloid/intraclast packstone. Thick bedded. Dolomite is coarse grained, turbid, and non-ferroan. Bed parallel stylolites and fractures common. Rare framboidal pyrite. Both baroque and non-baroque morphologies present. Mostly intergranular porosity. Sample 55.2.
8d	56	Light to medium gray dolomitized mudstone. Thick bedded. Bed parallel layers of opaques present (pyrite?). Some fenestral porosity filled with non-ferroan, non-baroque dolomite. Fractures common. Sample 56.
8e	57	Medium gray dolomitized mudstone. Thin to medium bedded. Dolomite is very fine grained and non-ferroan. Fractures (at least 2 generations) and bed parallel stylolites present. Sample 57.
		Covered interval from 58.7- 62.
8f	62.7	Medium to dark gray dolomitized peloid/intraclast packstone. Thick bedded. Quartz silt dispersed throughout (rare) and relative percentage decreases upward in the sample. Dolomite is non-ferroan and fine to medium grained. Stylolites and fractures present as well. Sample 62.7.
8g	63.8	Light gray dolomitized algal boundstone. Medium bedded. Fenestrae very common as well as some evaporitic vugs. Peloids common. Dolomite is non-ferroan and very fine grained. Stylolites and fractures common. Opaques very rare.
9a	64.9	Light to medium gray dolomitized peloid/intraclast wackestone-packstone. Thin to medium bedded. Dolomite is fine grained and non-ferroan. Opaque minerals/grains rare. Fractures sparse. Sample 64.9.

9b	67	Light to medium gray dolomitized intraclast packstone. Thin to medium bedded. Dolomite is medium to coarse grained and non-ferroan. Peloids common. Poorly sorted. Pyrite present. Bed parallel stylolites and fractures also. Sample coarsens upward. Sample 67.
9c	68	Dark gray dolomitized mudstone. Medium bedded. Faint current generated laminations. Clay seams present. Dolomite is medium to coarse grained and non-ferroan. Fenestral porosity and fractures both filled with dolomite. Opaque grains/minerals common. Porosity and laminations increase upward in the sample. Sample 68.
9d	68.5	Tan, brown dolomitized mudstone. Medium bedded. Very fine grained. Patches of opaque minerals/grains dispersed throughout. Fractures common. Highly weathered. Sample 68.5.
10	69.7	Brecciated layer in field. Extraction of sample impossible.
	70.2	Light to medium gray dolomitized peloid/intraclast packstone. Thin to medium bedded. Microbial clasts at top of sample with detrital quartz between laminations. Opaque minerals/grains sparse. Dolomite is non-ferroan and fine grained except for fenestral pores (non-ferroan, non-baroque). Bed parallel stylolites and fractures common with iron oxides lining them.
11a	71.6	Buff to light gray dolomitized mudstone. Thin to medium bedded. Fenestral porosity with fine to medium grained non-ferroan, non-baroque dolomite. Opaque grains/minerals lie in rows parallel to bedding and show leaching into surrounding lithology. Very faint laminations. Fractures present also. Sample 71.6.
11b	72.2	Light to medium gray dolomitized microbial boundstone. Thin bedded. Fenestral porosity. Quartz silt and peloids/intraclasts distributed throughout sample. Opaque minerals/grains sparse. Stylolites cross-cut by fractures. Sample 72.2.

11c	73.2	Similar to 72.2 but sample is darker and the detrital quartz is coarser grained. Horizontal fractures at top of sample and filled with non-ferroan, baroque dolomite. Thin to medium bedded. Sample 73.2.
11d	74	Medium to dark gray dolomitized intraclast packstone. Medium bedded. Peloids common. Dolomite is coarse grained at the bottom of the sample below stylolite. Above stylolite, sample fines upward. Desiccation in hand sample (at least 2 different episodes). Bed parallel stylolites common and at least 2 generations of fractures. Sample 74.
12a	74.6	Light to medium gray dolomitized mudstone. Medium bedded. Mechanical induced laminations. Some soft sediment deformation present. Patches of pyrite dispersed throughout sample. Dolomite is very fine grained and non-ferroan. Sample 74.6.
12b	76.4	Light gray dolomitized peloidal wackestone/mudstone. Highly fractured. Dolomite is fine to medium grained. Sample 76.4.
		Covered interval from 76.4-80.
13a	82.5	Medium gray dolomitized peloid intraclast packstone. Thin to medium bedded. Porosity is predominantly intergranular with some fenestrae. Dolomite in sample is non-ferroan and both non-baroque and baroque morphologies occur. Bed parallel stylolites rare. Clasts are moderate to well sorted. Sample 82.5.
13b	84.2	Similar to 82.5 but not as well sorted.
14a	86.6	Medium gray dolomitized ooid intraclast packstone/grainstone. Dolomite is intergranular pore filler (non-ferroan). Medium bedded. Stylolites present with compressed grains. Very rare quartz grains at top of sample. Some rare non-planar dolomite. Sample 86.6.
14b	87.4	Medium to dark gray dolomitized ooid intraclast packstone. Very similar to 86.6. Medium bedded. Sample 87.4.

15a	89	**Starting to become more shaly. Medium gray dolomitized mudstone. Medium bedded. Fenestral porosity with slightly clear to turbid non-ferroan dolomite (wall to pore central). Selective dolomitization in sample. Enterolithic structure (?) - circular discolorations. Zone of intraclasts in mudstone. Highly fractured and numerous bed parallel stylolites. MVT mineralization (barite?) present. Sample 89.
15b	90.7	Medium gray dolomitized mudstone with peloid packstone intervals between stylolites. Fenestral porosity common with non-ferroan, non-baroque dolomite. Fractures contain turbid non-ferroan baroque dolomite. Bedding is thin to medium. Clay seams common and stylolites contain some quartz. Very rare mouldic porosity occluded with non-ferroan, non-baroque dolomite. Dolomite in sample is fine to medium grained. Framboidal pyrite common. Sample 90.7.
16	91	From prominent shale unit. -----**Nolichucky Formation**.
17	92.7	Light to medium gray dolomitized intraclast skeletal packstone interbedded with shale. Thin bedded. Mudstone ribbon at base of sample. Echinoderm and trilobite hash common. Peloids common as well; ooids very rare. Cements are turbid (amber colored) and ferroan. Late ferroan non-planar dolomite. Bed parallel stylolites present. Stylolite at contact between mudstone and packstone. Sample has speckled texture (secondary in origin) OR peloids (?), opaque minerals/grains (?). Sample 92.7.
18	93	Brown calcareous shale. Thin bedded with very thin carbonate stringers. Sample 93.
19	94.4	Light to medium gray partially dolomitized intraclast skeletal packstone interbedded with shale. Thin bedded and calcite-rich. Relative percentage of intraclasts decreased and skeletal grains increased compared to sample 92.7. Echinoderm, trilobite, and brachiopod fragments common. Some peloids. Turbid ferroan calcite cements with patches of ferroan dolomite. Rare

		syntaxial cement phases. Skeletal grains decrease upwards in sample. Fractures filled with ferroan calcite. Ferroan, turbid non-planar dolomite also present. Sample 94.4.
20	95	Calcareous shale. Thin bedded with very thin carbonate stringers. Extraction of carbonate samples difficult. Sample: 95.

Appendix B

Stable Isotopic Compositions

DOLOMITE PHASES (All are in standard permil notation relative to PDB)

Sample	Description	$\delta^{13}C$	2σ	$\delta^{18}O$	2σ
GD 9.8 m	Dolomicrite	-0.97	*0.014*	-8.87	*0.023*
GD 3.0 m	Dolomicrite	-0.90	*0.013*	-7.78	*0.029*
I-81 H8/10 m	Dolomicrite	-0.97	*0.012*	-8.26	*0.021*
	Dolomicrite	-0.99	*0.015*	-7.98	*0.024*
GD 9.0 m	Dolomicrite	-0.83	*0.012*	-8.64	*0.018*
I-81 25.9 m	Dolomicrite	-0.29	*0.002*	-9.08	*0.015*
BL 36.2 m	Dolomicrite	-1.15	*0.013*	-8.46	*0.023*
BL 52.3	Dolomicrite	-1.21	*0.010*	-8.11	*0.015*
BL 92.7 m	Dolomicrite (altered)	-6.54	*0.017*	-11.2	*0.011*
		-13.85		-78.38	
Total (n): 9	**Average**	**-1.54**		**-8.71**	

Sample	Description	$\delta^{13}C$	2σ	$\delta^{18}O$	2σ
GD 27.4 m	Vuggy, turbid dolomite	-0.98	*0.007*	-10.26	*0.029*
GD 37 m	Vuggy, turbid dolomite	-1.08	*0.003*	-10.75	*0.046*
		-2.06		-21.01	
Total (n): 2	**Average**	**-1.03**		**-10.51**	

Sample	Description	$\delta^{13}C$	2σ	$\delta^{18}O$	2σ
GD 16.9 m	Fenestral dolomite	-0.90	*0.007*	-10.7	*0.026*
Total (n): 1	**Average**	**-0.90**		**-10.7**	

Sample	Description	$\delta^{13}C$	2σ	$\delta^{18}O$	2σ
I-81 10.79 m	Dolomite (Non-descriptive)	-1.21	*0.016*	-9.25	*0.030*
Total (n): 1	**Average**	**-1.21**		**-10.7**	

Sample	Description	$\delta^{13}C$	2σ	$\delta^{18}O$	2σ
I-81 18.5 m	Replacive dolomite	-1.13	*0.008*	-9.37	*0.041*
Total (n): 1	**Average**	**-1.13**		**-9.37**	

Sample	Description	$\delta^{13}C$	2σ	$\delta^{18}O$	2σ
BL 11.3 m	Turbid baroque dolomite (matrix material)	-1.65	*0.015*	-8.32	*0.021*
	Turbid baroque dolomite (fracture fill)	-1.69	*0.009*	-9.43	*0.017*
		-3.34		-17.75	
Total (n): 2	**Average**	**-1.67**		**-8.875**	

CALCITE PHASES (All are in standard permil notation relative to PDB)

Sample	Description	$\delta^{13}C$	2σ	$\delta^{18}O$	2σ
I-81 11.9 m	Clear, equant, intergranular calcite	-8.84	*0.009*	-15.6	*0.015*
I-81 H4/3.4 m	Clear, equant, intergranular calcite	-9.29	*0.006*	-6.64	*0.021*
		-18.13		-22.24	
Total (n): 2	**Average**	**-9.07**		**-11.12**	

Sample	Description	$\delta^{13}C$	2σ	$\delta^{18}O$	2σ
GD 15.4 m	Clear, equant, vuggy calcite	-9.54	*0.020*	-8.99	*0.050*
BL Base 2 m	Clear, equant, vuggy calcite	-9.88	*0.013*	-10.15	*0.022*
		-19.42		-19.14	
Total (n): 2	**Average**	**-9.71**		**-9.57**	

Sample	Description	$\delta^{13}C$	2σ	$\delta^{18}O$	2σ
BL 18.8 m	Clear, equant, fracture calcite	-8.91	*0.013*	-8.75	*0.027*
Total (n): 1	**Average**	**-8.91**		**-8.75**	

STANDARDS (All are in standard permil notation relative to PDB)

Sample	$\delta^{13}C$	2σ	$\delta^{18}O$	2σ
ANU - M2	3.03	*0.005*	-7.21	*0.015*
ANU - M2	2.87	*0.009*	-7.38	*0.015*
ANU - M2	2.90	*0.01*	-7.29	*0.031*
	8.8	*0.024*	-21.88	*0.061*
Average	**2.933**	***0.008***	**-7.293**	***0.0203***
Expected lab values for ANU-M2 standard	**2.76**		**-7.22**	

CHCC	-10.54	*0.015*	-9.51	*0.029*
CHCC	-10.61	*0.013*	-9.22	*0.012*
	-21.15	*0.028*	-18.73	*0.041*
Average	**-10.575**	***0.014***	**-9.365**	***0.021***
Expected lab values for CHCC standard	**-10.6**		**-9.28**	

VITA

Gary Alan Ottinger was born one snowy morning, January 5, 1972 in Knoxville, Tennessee. He attended Powell schools where he gained many friends and learned the importance of an education. Thanks to his wonderful science teachers throughout primary and secondary schools, Gary decided to pursue biology, pharmacy, or engineering as a career choice following graduation in May 1990. He enrolled at the University of Tennessee in August 1990 with an undecided major, hoping classes would confine his career interests. He discovered a passion for earth science after taking a geology course as an elective Due to its integration of scientific disciplines, he later declared geology as his major.

A summer field course in the balmy Florida Keys focused Gary's geologic emphasis on carbonate sedimentology. Following graduation in August 1995, Gary contemplated graduate school while working as a nurseryman at Thress Nursery in Knoxville, Tennessee, a part-time job he had held since the age of sixteen.

He was accepted into graduate school at the University of Tennessee and began his studies in January of 1996. He was offered a teaching assistantship which gave him the opportunity to teach historical geology labs at the university and help undergraduates at the West Virginia field camp. He also aided in organizing geologic talks for area youth who visited UT's McClung Museum hoping to learn about fossils, minerals, and geologic history of Tennessee. Gary received the "Best Graduate Teaching Assistant" award in the spring of 1998, an honor of which he is still proud.

Gary was fortunate enough to be offered a summer internship with Exxon Exploration Company in Houston, Texas during the summer of 1998. He worked with the Gulf of Mexico Prospect Evaluation Team searching for potential deepwater petroleum reservoirs before returning to UT to finish his thesis. Gary served another internship with Exxon's New Orleans Production Organization after completing his thesis.